

**PHYTOPLANKTON AND NUTRIENT DYNAMICS
IN IRON GATE AND COPCO RESERVOIRS
2005-2010**



**PREPARED FOR THE
KLAMATH BASIN TRIBAL WATER QUALITY WORK GROUP**

BY

**ELI ASARIAN
KIER ASSOCIATES
EUREKA, CALIFORNIA**

**JACOB KANN, PH.D.
AQUATIC ECOSYSTEM SCIENCES LLC
ASHLAND, OREGON**

**PHYTOPLANKTON AND NUTRIENT DYNAMICS
IN IRON GATE AND COPCO RESERVOIRS
2005-2010**

THIS REPORT WAS PREPARED FOR THE

KLAMATH BASIN TRIBAL WATER QUALITY WORK GROUP

BY

ELI ASARIAN
KIER ASSOCIATES
EUREKA, CALIFORNIA
WWW.KIERASSOCIATES.NET

JACOB KANN, PH.D.
AQUATIC ECOSYSTEM SCIENCES LLC
ASHLAND, OREGON
WWW.AQUATIC-ECOSCIENCES.COM

DECEMBER 2011

Citation:

Asarian, E. and J. Kann. 2011. Phytoplankton and Nutrient Dynamics in Iron Gate and Copco Reservoirs 2005-2010. Prepared by Kier Associates and Aquatic Ecosystem Sciences for the Klamath Basin Tribal Water Quality Work Group. 60p + appendices.

EXECUTIVE SUMMARY

Copco and Iron Gate reservoirs are mainstem reservoirs on the Klamath River in northern California, one of the major salmon rivers of the western United States. The overall goals of the study described herein were to 1) compile the detailed water quality, nutrient, and phytoplankton data for Copco and Iron Gate reservoirs and the Klamath River stations directly above and below the reservoirs for the years 2005-2010, 2) analyze the longitudinal, temporal, and depth dynamics of these data, and 3) provide a limited and preliminary assessment of nutrient controlling factors on phytoplankton species composition and biomass. Samples were collected above, within, and below Copco and Iron Gate reservoirs by the Karuk Tribe and PacifiCorp. It is important to note that the goal of this report is not to comprehensively analyze and interpret all data collected during the study period, but rather to provide an overview of the seasonal and inter-annual dynamics, as well as provide a baseline database for future analyses and efforts to understand Klamath River water quality dynamics.

Both reservoirs thermally stratified during the warm summer months, and the upper water column layers (epilimnion) in both reservoirs hosted large blooms of phytoplankton. Concentrations of total nitrogen (TN) were consistently lower at Klamath River below Iron Gate than Klamath River above Copco for the July through October period. Relative to the Klamath River above Copco, total phosphorus (TP) concentrations at the Klamath River below Iron Gate were generally equal or lower from January through August or September (varies by year), but then exhibit an opposite pattern until approximately December.

The longitudinal effects of reservoirs on phytoplankton at Iron Gate Dam (i.e. relative to above Copco) is higher chlorophyll and total phytoplankton biovolume from June-October (blue green blooms), due to in-reservoir blooms of blue-green algae. Conversely, chlorophyll and algal biovolume were lower below Iron Gate than above Copco from November through April, reflecting the settling of diatoms from upstream; however, there were relatively few samples collected in November-April, so additional data should be collected to confirm this apparent trend. Both relative and absolute biovolume of blue-green algae, predominantly *Aphanizomenon flos-aquae* and *Microcystis aeruginosa* were substantially higher below each of the reservoirs than they were in the Klamath River above the reservoirs, clearly indicating the role of the reservoirs in serving as a source of these species to the downstream river environment.

Prolific blue-green algal blooms occurred in Iron Gate and Copco reservoirs each summer, primarily composed of *Aphanizomenon flos-aquae* and *Microcystis aeruginosa*. A seasonal progression to the blooms was evident, with *Aphanizomenon* blooms beginning sooner, followed by *Microcystis*. One apparent contributor to the seasonal dynamics was that SRP increased earlier in the spring than nitrate, favoring early season blooms of N-fixing species (*Aphanizomenon*). Later in the season there is a transition to non-N-fixing *Microcystis*. With variation, *Microcystis* was generally higher at surface (0.1m), while *Aphanizomenon* higher at 0.5-1m depth. Peak blooms (as measured by either chlorophyll or total algal biovolume) were generally larger in Copco than Iron Gate (with exceptions). *Microcystis* was generally lower in Iron Gate than in Copco (for both open-water and shoreline stations).

Time-series graphs and scatter plots between inflowing and in-reservoir nutrient concentrations and phytoplankton parameters indicate that both NO_3 and SRP are important drivers of *Microcystis* dominance in Copco and Iron Gate reservoirs. Both higher NO_3 and higher SRP were associated with increased July dominance of *Microcystis* in Copco Reservoir, indicating that not only was NO_3 necessary for the non-nitrogen fixing *Microcystis* to increase in importance but that increased SRP was further associated with increased *Microcystis* dominance. Relationships with inflow SRP also indicate that relative supply of SRP to the reservoirs may explain year-to-year dominance patterns of *Microcystis* and N-fixing algae.

For *Aphanizomenon*, the ratio of heterocysts to vegetative cells was higher in Iron Gate than in Copco, consistent with lower nitrate concentrations at depths <10m; however, heterocyst ratios did not correspond to differences in nitrogen concentrations or N:P ratios between years.

TABLE OF CONTENTS

1	INTRODUCTION.....	1
1.1	Description of Study Area	1
1.2	Background	1
1.3	Previous reservoir Studies	1
1.4	Study Goals	2
2	METHODS.....	3
2.1	Sampling locations and parameters	3
2.2	Meteorological data.....	8
3	RESULTS AND DISCUSSION.....	8
3.1	Meteorological Data.....	8
3.2	Longitudinal Nutrient Concentrations	10
3.2.1	Nitrogen.....	10
3.2.2	Phosphorus	11
3.3	Vertical Distribution of temperature, dissolved oxygen, pH, nutrients within the reservoirs	15
3.4	Phytoplankton.....	23
3.4.1	Longitudinal Comparison at Seasonal and Annual Time Scales.....	23
3.4.1.1	Total Biovolume and Chlorophyll a.....	23
3.4.1.2	Major Taxonomic Groups and Species Composition	30
3.4.2	Seasonal Trends.....	30
3.4.2.1	Reservoir Stations: Major Taxonomic Groups and Species/Generic Composition.....	30
3.4.2.2	River Stations: Major Taxonomic Groups and Species/Generic Composition	39
3.4.3	Toxic Species and a Comparison of Shoreline Stations and Open-Water Stations.....	42
3.4.4	Seasonal Cyanophyta Dynamics and Relationships to Other Variables.....	44
3.4.5	Nitrogen Fixing Species and Heterocyst Ratios.....	52
3.4.6	Chlorophyll to Algal Biovolume Relationship.....	55
4	CONCLUSIONS	57
5	LITERATURE CITED.....	58

APPENDICES

Appendix A:	Depth-time isopleths of dissolved oxygen and pH.....	A-1
Appendix B:	Depth profiles of temperature, dissolved oxygen, and pH for each sampled date at IR01 and CR01.....	B-1
Appendix C:	Time Series for Nutrient Parameters at CR01 and IR01, by Depth.....	C-1
Appendix D:	Time Series for Nutrient Parameters at River Stations.....	D-1
Appendix E:	Time series of biovolume and percent biovolume for major taxonomic groups and dominant phytoplankton species at shoreline stations	E-1
Appendix F:	Time Series of Seasonal Cyanophyta Dynamics for 0.5-1m Depth, for Each Year	F-1
Appendix G:	Annual Time Series of Biovolume and Nitrate Concentration for 0.5-1m Depth	G-1

LIST OF FIGURES

Figure 1. Regional location of Copco and Iron Gate reservoirs.	2
Figure 2. Location of nutrient and phytoplankton sample sites.	3
Figure 3. Timing of January 2005 – December 2010 nutrient samples collected in Copco and Iron Gate reservoirs and the Klamath River. Note: 2008 TN data are missing except for KRAC and KRBI; 2009 TN data are missing except for KRBI.	5
Figure 4. Timing of January 2005 – December 2010 phytoplankton samples collected in Copco and Iron Gate reservoirs and adjacent Klamath River sites. Sites are listed in longitudinal (i.e. upstream to downstream) order.	5
Figure 5. Timing, depth, and type of January 2005 – December 2010 nutrient and chlorophyll samples collected in Copco (CR01) and Iron Gate (IR01) reservoirs. Note: TN data for 2008-2009 are missing for the reservoir sites.....	6
Figure 6. Timing, depth, and type of January 2005 – December 2010 phytoplankton samples collected in Copco (CR01) and Iron Gate reservoirs (IR01).	7
Figure 7. 14-day moving average of daily average (14DAMean) for air temperature and wind speed at the Montague Airport.	9
Figure 8. Monthly box plots of nitrogen concentrations above and below Copco and Iron Gate reservoirs, January 2005 – December 2010 (some 2008-2009 data missing for TN and ORGN).....	12
Figure 9. Monthly box plots of phosphorus concentrations and nitrogen:phosphorus ratios above and below Copco and Iron Gate reservoirs, January 2005 – December 2010.	13
Figure 10. Monthly box plots of percent composition of nitrogen and phosphorus species above and below Copco and Iron Gate reservoirs, January 2005 – December 2010.	14
Figure 11. Depth-time distributions of isopleths of temperature at station CR01 in Copco Reservoir and IR01 in Iron Gate Reservoir, January 2005-December 2010.....	17
Figure 12. Depth-time distributions of isopleths of dissolved oxygen concentration at station CR01 in Copco Reservoir and IR01 in Iron Gate Reservoir, January 2005-December 2010.	18
Figure 13. Monthly box of nitrogen concentrations for various depths at Copco Reservoir sampling station CR01, January 2005 – December 2010.	19
Figure 14. Monthly box plots of phosphorus concentrations and nitrogen:phosphorus mass ratios for various depths at Copco Reservoir sampling station CR01, January 2005 – December 2010.	20
Figure 15. Monthly box plots of nitrogen concentrations for various depths at Iron Gate Reservoir sampling station IR01, January 2005 – December 2010. Samples sizes are very low (1 to 3) in January-April.....	21
Figure 16. Monthly box plots of phosphorus concentrations and nitrogen:phosphorus mass ratios for various depths at Iron Gate Reservoir sampling station IR01, Jan. 2005 – Dec. 2010. Samples sizes are very low (1 to 3) in January-April. TNTP is mass ratio of TN to TP, and TINSRP is mass ratio of TIN to SRP.	22
Figure 17. Total phytoplankton biovolume, and total and percent biovolume of the Cyanophyta, Diatoms, Cryptophyta, Chlorophyta, Euglenophyta, Pyrrophyta, and Chrysophyta for surface to 0.5-1.0 m samples for all sample dates 2005-2010.....	24
Figure 18. Total phytoplankton biovolume, and total and percent biovolume of the Cyanophyta, Diatoms, Cryptophyta, Chlorophyta, Euglenophyta, Pyrrophyta, and Chrysophyta for surface to 0.5-1.0 m samples for all June-October 2005-2010.....	25
Figure 19. Total algal biovolume by month at river stations KRAC, KRAI, and KRBI for 2005-2010.....	27
Figure 20. Total algal biovolume, diatom biovolume, and chlorophyll-a concentrations for January-May at river stations KRAC, KRAI, and KRBI.	27
Figure 21. Longitudinal chlorophyll <i>a</i> concentrations for 0-8m depth-integrated samples (a) and a range of discrete depths: all depths (b), depth 0-1m (c) , depth 5m (d), and depths 8-10m (e), June-October, 2005-2010.	28
Figure 22. Biweekly time series of chlorophyll- <i>a</i> concentrations at Klamath River above Copco (KRAC), Klamath River above Iron Gate (KRAI), and Klamath River below Iron Gate (KRBI), January 2005 - December 2010.	29
Figure 23. Boxplot of chlorophyll- <i>a</i> concentrations at Klamath River above Copco (KRAC), Klamath River above Iron Gate (KRAI), and Klamath River below Iron Gate (KRBI), January 2005 - December 2010.	29
Figure 24. Biovolume and percent biovolume of major phytoplankton taxonomic groups at measured depths for reservoir station CR01, 2005-2010.....	33
Figure 25. Biovolume and percent biovolume of major phytoplankton taxonomic groups at measured depths for reservoir station IR01, 2005-2010.	34
Figure 26. Chlorophyll <i>a</i> at measured depths for reservoir stations CR01 and IR01, 2005-2010. To reduce y-axis and improve legibility, all values less than 0.5 are set to 0.5.	35

Figure 27. Biovolume and percent biovolume of dominant species of phytoplankton at measured depths for reservoir station CR01, 2005-2010.	37
Figure 28. Biovolume and percent biovolume of dominant species of phytoplankton at measured depths for reservoir station IR01, 2005-2010.	38
Figure 29. Biovolume and percent biovolume of major phytoplankton taxonomic groups at Klamath River stations KRAC, KRAI, and KRBI, 2005-2010.	40
Figure 30. Biovolume and percent biovolume of dominant species of phytoplankton at Klamath River stations KRAC, KRAI, and KRBI, 2005-2010.	41
Figure 31. Median percent biovolume of <i>Microcystis</i> (MSAE), <i>Aphanizomenon</i> (APFA), diatoms, other Cyanophyta, and other taxonomic groups for August and September 2005-2010 surface (0.1 m depth)(left panel) samples at shoreline stations (CRMC, CRCC, IRCC, and IRJW) and open water stations (CR01 and IR01), as well as the 0.5-1m depth for open-water stations (right panel).	43
Figure 32. Total biovolume, <i>Microcystis aeruginosa</i> (MSAE) biovolume, and <i>Aphanizomenon flos-aquae</i> (APFA) biovolume for August and September 2005-2010 surface (0.1 m depth)(left panel) samples at shoreline stations (CRMC, CRCC, IRCC, and IRJW) and open water stations (CR01 and IR01), as well as the 0.5-1m depth for open-water stations (right panel).	44
Figure 33. Biovolume and percent composition of <i>Microcystis aeruginosa</i> (MSAE), 0-1m samples, June-Sept. 2005-2010.	44
Figure 34. Seasonal trends for nutrient and phytoplankton parameters in the inflow and surface of Copco Reservoir 2005-2010.	45
Figure 35. Seasonal trends for nutrient and phytoplankton parameters in the inflow and surface of Iron Gate Reservoir 2005-2010.	46
Figure 36. Relationships between TP concentration and algal response variables for Copco (red) and Iron Gate Reservoirs (blue), arranged in rows (months July-Sept) and columns (response variables).	49
Figure 37. Relationships between SRP concentration and algal response variables for Copco (red) and Iron Gate Reservoirs (blue), arranged in rows (months July-Sept) and columns (response variables).	50
Figure 38. Relationships between NO ₃ concentration and algal response variables for Copco (red) and Iron Gate Reservoirs (blue), arranged in rows (months July-Sept) and columns (response variables).	51
Figure 39. Summary by station of the ratio of number of heterocysts to vegetative cells for <i>Aphanizomenon flos-aquae</i> (APFA) and <i>Anabaena flos-aquae</i> (ABFA) at Klamath River and reservoir stations KRAC, CR01, KRAI, IR01, and KRBI, 2005-2008.	53
Figure 40. Summary by year of the ratio of number of heterocysts to vegetative cells for <i>Aphanizomenon flos-aquae</i> (APFA) and <i>Anabaena flos-aquae</i> (ABFA) at Klamath River and reservoir stations KRAC, CR01, KRAI, IR01, and KRBI, 2005-2008.	53
Figure 41. Time series of the ratio of number of heterocysts to vegetative cells for <i>Aphanizomenon flos-aquae</i> (APFA) and <i>Anabaena flos-aquae</i> (ABFA) at Klamath River and reservoir stations KRAC, CR01, KRAI, IR01, and KRBI, 2005-2008.	54
Figure 42. Biovolume and percent composition of the Cyanophyta (top panel) and nitrogen-fixing species (bottom panel) for 0-1m samples, June-September 2005-2010.	55
Figure 43. Chlorophyll- <i>a</i> vs. total algal biovolume for individual samples (or daily averages if there was more than one sample per day) for all dates, stations, depths, 2005-2010.	56

LIST OF TABLES

Table 1. Key and description for sampling locations shown in Figure 2, listed in longitudinal (i.e. upstream to downstream) order.	4
Table 2. Summary of biovolume data by station for river stations and 0.5-1m discrete and 0-8m depth-integrated samples at reservoir stations during the period June-October, 2005-2010.	26
Table 3. Top ten species (ranked by mean biovolume) for samples in the June – Oct. period of 2005-2010 for each site and depth.	31
Table 4. Key to four-letter species coded used in Table 3.	32

1 INTRODUCTION

1.1 DESCRIPTION OF STUDY AREA

The Klamath River is one of the major salmon rivers of the western United States. Its uppermost tributaries originate in southern Oregon, which then drain into large, shallow Upper Klamath Lake, and after a short stretch of river known as the Link River (followed by Lake Ewauna), the Klamath River proper begins. From this point the River continues through a series of impoundments, including Keno, J.C. Boyle, Copco, and Iron Gate Reservoirs, below which the river flows freely 190 miles to the Pacific Ocean.

This study focuses specifically on Copco and Iron Gate reservoirs (Figure 1) located near the town of Yreka in northern California's Siskiyou County. PacifiCorp Energy (PacifiCorp) operates these reservoirs as part of the Klamath Hydroelectric Project (KHP) to regulate flows and generate electricity.

1.2 BACKGROUND

Due to human activities, the concentrations of nitrogen and phosphorus in the Klamath River are significantly higher than natural background, resulting in water quality impairments including large seasonal blooms of blue-green algae in KHP reservoirs (NCRWQCB 2010). The Klamath River in California is listed as an impaired water body on the Clean Water Act (CWA) section 303(d) list for temperature, nutrients, microcystin, sediment, and dissolved oxygen. Copco and Iron Gate reservoirs have been the subject of North Coast Regional Water Quality Control Board Total Maximum Daily Load (TMDL) development (NCRWQCB 2010), PacifiCorp relicensing the KHP with the Federal Energy Regulatory Commission, and State Water Board section 401 of the Clean Water Act water quality certification. The TMDL has been completed but the other two processes have been put on hold pending potential implementation of two linked agreements: Klamath Hydrologic Settlement Agreement (KBRA) and Klamath Basin Restoration Agreement (KBRA). The KBRA is an agreement between Klamath Basin Tribes, irrigators, fishermen, environmental groups, counties, states, and federal agencies that aims to restore Klamath Basin fisheries and provide stability to local economies. The KHSA is a multi-party agreement to remove J.C. Boyle, Copco and Iron Gate reservoirs.

Because water quality management of the reservoirs is an ongoing need (even if the KBRA and KHSA are implemented the dams would not be removed until 2020), water quality data continues to be collected by various Klamath River Tribes and PacifiCorp. Thus, it is the intent of this report to provide a compilation of these continuing data collection efforts, as well as provide a preliminary summary of the water quality dynamics between 2005 and 2010.

The analysis was completed using funds provided to the Quartz Valley Indian Community and Klamath Basin Tribal Water Quality Work Group by the U.S. Environmental Protection Agency.

1.3 PREVIOUS RESERVOIR STUDIES

Previous analyses of Iron Gate and Copco reservoir data focused on phytoplankton with respect to public health threshold values for toxigenic species (Kann and Corum 2006, 2007, 2009; Kann et al. 2010), and nutrient data with respect to formulation of nutrient budgets and estimates of nutrient

retention (Kann and Asarian 2007; Asarian et al. 2009, 2010). To date there have only been limited analyses of the remainder of the detailed database that exists for the reservoir system. As opposed to analysis of toxigenic algal species only, this report is intended to provide detailed seasonal and inter-annual trends for the entire phytoplankton community (i.e., not only toxigenic species such as *Microcystis aeruginosa*, but also diatoms and other pertinent species), as well as major controlling factors such as nutrients and water temperature. Because the reservoirs will remain in place for at least the next 10 years, results from the studies could be used to advise interim management measures intended to improve water quality conditions.

1.4 STUDY GOALS

The overall goals of this study were to 1) compile the detailed water quality, nutrient, and phytoplankton data for Copco and Iron Gate reservoirs and the Klamath River stations directly above and below the reservoirs for the years 2005-2010, 2) analyze the longitudinal, temporal, and depth dynamics of these data, and 3) provide a limited and preliminary assessment of nutrient controlling factors on phytoplankton species composition and biomass.

It is important to note that the goal of this report is not to comprehensively analyze and interpret all the data during the study period, but rather to provide an overview of the seasonal and inter-annual dynamics, as well as provide a baseline database for future analyses and efforts to understand Klamath River water quality dynamics.

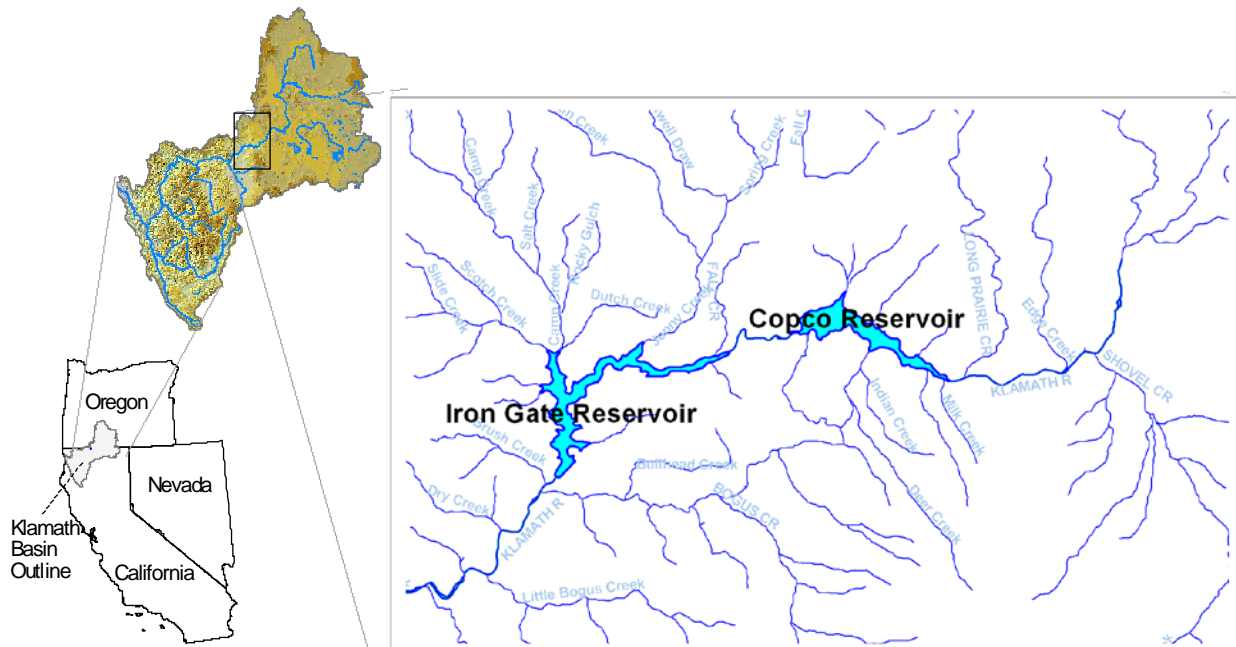


Figure 1. Regional location of Copco and Iron Gate reservoirs.

2 METHODS

This report utilizes data from a variety of sources, as described below.

2.1 SAMPLING LOCATIONS AND PARAMETERS

Samples were collected above, within, and below Copco and Iron Gate reservoirs. Sampling stations and station codes used for this study are shown in and Table 1 and Figure 2 will be used throughout this report. The primary sampling station in each reservoir (CR01 and IR01; Figure 2 and Table 1) was located near the deepest portion of the reservoir, with two shoreline phytoplankton sampling stations located in each reservoir¹. Data were collected by a variety of entities, with methodology and results described in the following reports: Karuk Tribe (2007, 2008), Armstrong and Ward (2005), ARFO (2005), Raymond (2008a, 2008b, 2009a, 2009b, 2010a, 2010b), Deas (2008), Kann and Asarian (2007), Asarian et al. (2009), Watercourse Engineering (2011), Kann et al. (2010), and Kann and Corum (2006, 2007, 2009).

Sampling frequency varied by station and year, but generally occurred at monthly to weekly frequencies (Figure 3 and Figure 4). Samples were collected less frequently during December-April, with gaps of three to five months occurring in 2007, 2008, and 2009. Sampling frequency was highest during 2005 and 2007 when both Karuk Tribe and PacifiCorp were sampling, and was lowest in 2009-2010 when PacifiCorp was primarily sampling most stations. Data collected during high-frequency, short-duration special studies² were excluded from this report in order to maintain a relatively even spatial and temporal data distribution for analysis of long-term patterns. Sample depth resolution also varies by parameter, agency and year (Figure 5 and Figure 6), and thus comparisons were generally performed on standardized subsets of the various depths.

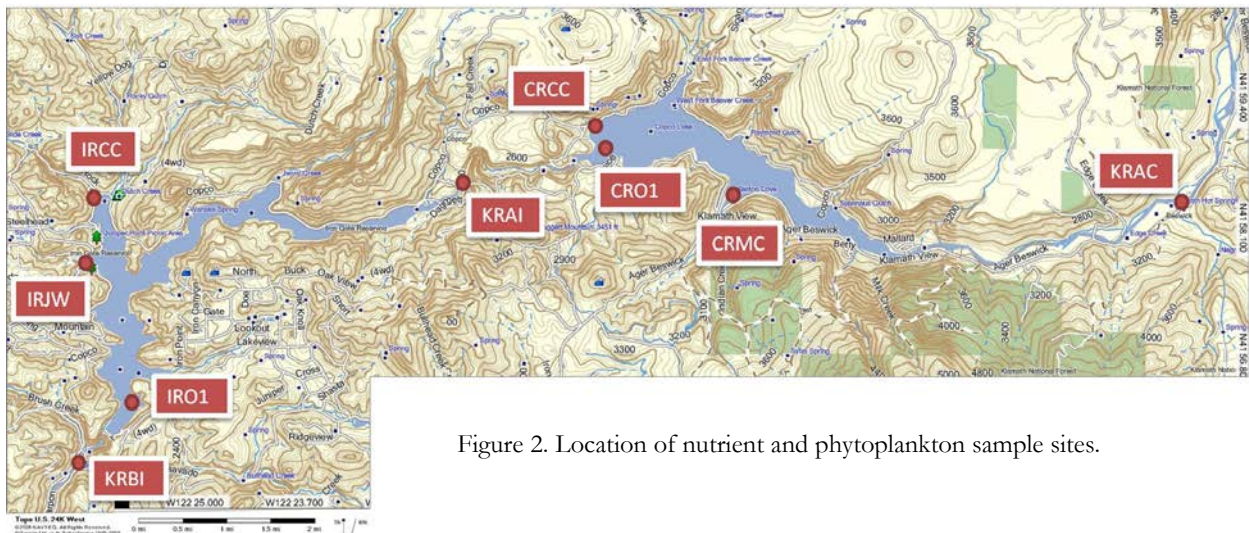


Figure 2. Location of nutrient and phytoplankton sample sites.

¹ The Karuk Tribe also collected data at two additional stations (CR02 for 2005 and IRO3 for 2005-2006 but these were not included in this report due to the lack of long-term data. Those data are presented in Kann and Asarian (2007).

² Examples include PacifiCorp's Klamath River Fate and Transport Study (Deas 2008) at KRBI in 2007 and the Karuk Tribe's multiple samples per day at KRAC in 2006 and KRBI in 2008.

Table 1. Key and description for sampling locations shown in Figure 2, listed in longitudinal (i.e. upstream to downstream) order.

Station Code	Station Description	River Mile	Station Type	Latitude (decimal degrees)	Longitude (decimal degrees)	Phyto. Data Source/Years³	Nutrient Data Source/Years
KRAC	Klamath River Above Copco Reservoir	206.42	River	41.97242	-122.20168	Karuk 2005-08, PC 2005/2007-10	Karuk 2005-08, PC 2005/2007-10
CRMC	Copco Reservoir at Mallard Cove ramp	201.50	Reservoir Shoreline	41.97402	-122.29782	Karuk 2005-08, PC 2008-09	-
CRCC	Copco Reservoir at Copco Cove ramp	200.00	Reservoir Shoreline	41.98392	-122.33003	Karuk 2005-08, PC 2008-09	-
CR01	Copco Reservoir Near Dam	198.74	Reservoir Open-Water	41.98220	-122.32823	Karuk 2005-08, PC 2005/2007-10	Karuk 2005-07, PC 2005/2007-10
KRAI	Klamath River Above Iron Gate Res.	196.45	River	41.97289	-122.98106	Karuk 2005-07, PC 2005/2007-10	Karuk 2005-07, PC 2008-2009
IRCC	Iron Gate Reservoir at Camp Creek area	192.80	Reservoir Shoreline	41.97280	-122.43523	Karuk 2005-08, PC 2008-09	-
IRJW	Iron Gate Reservoir at Williams boat ramp	192.40	Reservoir Shoreline	41.96202	-122.44042	Karuk 2005-08, PC 2008-09	-
IR01	Iron Gate Reservoir near dam	190.19	Reservoir Open-Water	41.93883	-122.43217	Karuk 2005-08, PC 2005/2007-10	Karuk 2005-07, PC 2005/2007-10
KRBI	Klamath River below Iron Gate Reservoir		River	41.93108	-122.44220	Karuk 2005-10, PC 2005/2007-10	Karuk 2005-09, PC 2005/2007-10

³ PC=PacifiCorp

Nutrient Sampling at Reservoir and River Stations

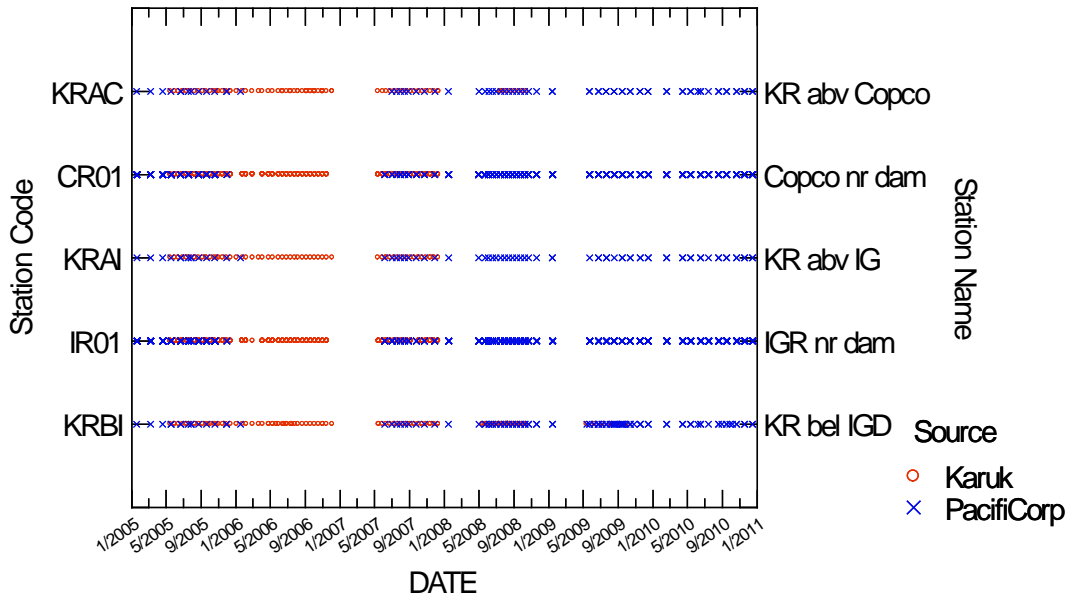


Figure 3. Timing of January 2005 – December 2010 nutrient samples collected in Copco and Iron Gate reservoirs and the Klamath River. Note: 2008 TN data are missing except for KRAC and KRBI; 2009 TN data are missing except for KRBI.

Phytoplankton Sampling at River and Reservoir Stations

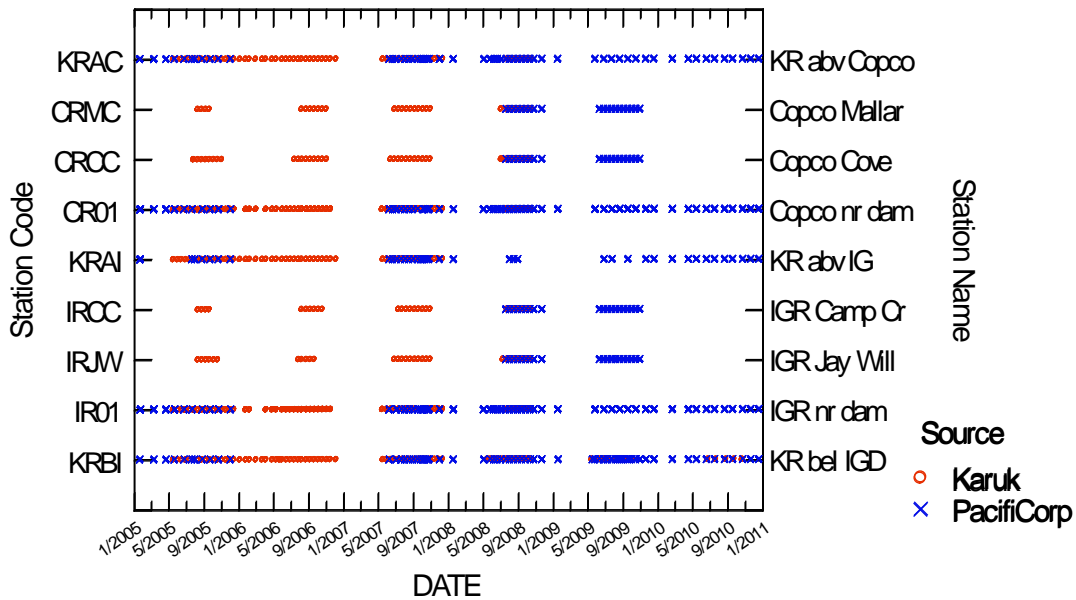


Figure 4. Timing of January 2005 – December 2010 phytoplankton samples collected in Copco and Iron Gate reservoirs and adjacent Klamath River sites. Sites are listed in longitudinal (i.e. upstream to downstream) order.

CR01 and IR01 Nutrient and Chlorophyll Samples: Dates, Depths, Types

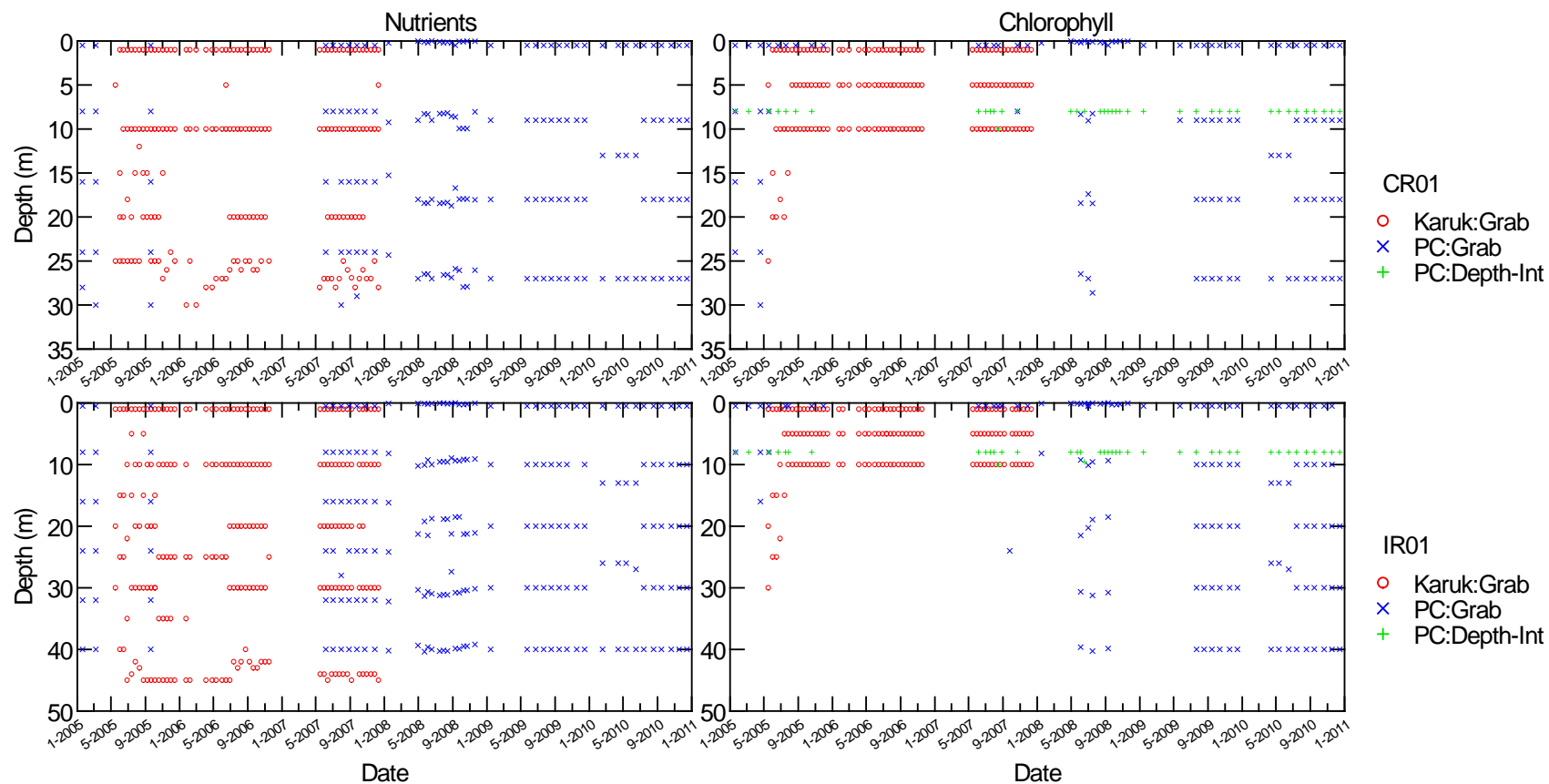


Figure 5. Timing, depth, and type of January 2005 – December 2010 nutrient and chlorophyll samples collected in Copco (CR01) and Iron Gate (IR01) reservoirs. Note: TN data for 2008-2009 are missing for the reservoir sites.

CR01 and IR01 Phytoplankton Samples: Dates, Depths, Types

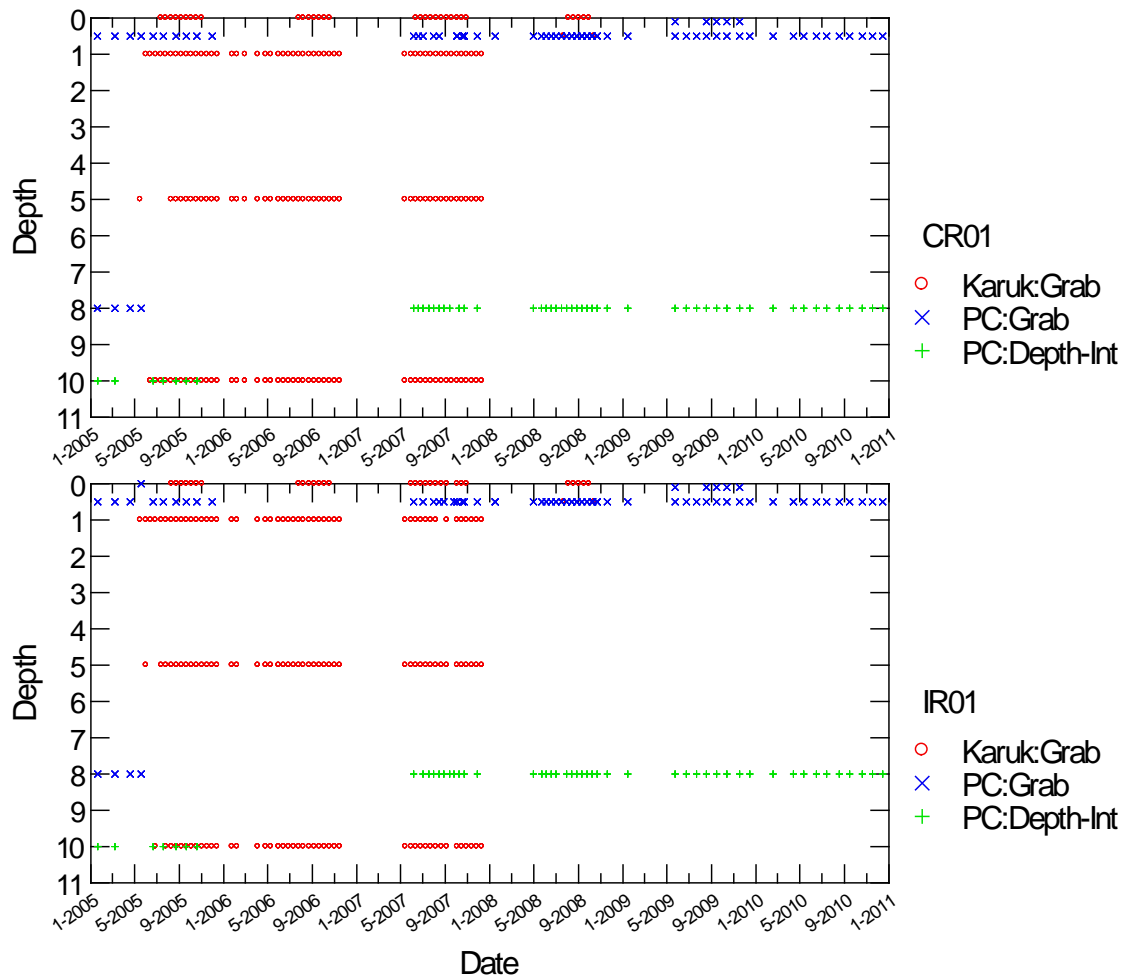


Figure 6. Timing, depth, and type of January 2005 – December 2010 phytoplankton samples collected in Copco (CR01) and Iron Gate reservoirs (IR01).

Parameters analyzed included ammonia (NH_3), nitrate-plus-nitrite ($\text{NO}_3\text{-NO}_2$), total nitrogen (TN), soluble reactive phosphorus (SRP), total phosphorus (TP), total organic carbon (TOC) chlorophyll-a (CHLA), and phaeophytin (PHEO). Total inorganic nitrogen (TIN) was computed as NH_3 plus $\text{NO}_3\text{-NO}_2$, organic nitrogen (ORGN) was computed as TN minus NH_3 minus $\text{NO}_3\text{-NO}_2$, particulate phosphorus (PP) was calculated as TP minus SRP. Additional parameters collected only by PacifiCorp include volatile suspended solids (VSS), total suspended solids (TSS), and total Kjeldahl nitrogen (TKN: for those samples TN was calculated as TKN plus $\text{NO}_3\text{-NO}_2$). Beginning in 2009, PacifiCorp also began analyzing samples from particulate nitrogen and particulate phosphorus.

The CH2M Hill Applied Sciences Laboratory utilized by PacifiCorp produced unreliable results for TN in 2008-2009 (Raymond 2010b) and therefore we did not include those data in this report. In addition, CH2M Hill Applied Sciences Laboratory's reporting limit for the NH_3 was 0.1 mg/L, un-

acceptably high for some purposes in this report; therefore, PacifiCorp's ammonia data was not utilized for analyses (though it is shown in time series plots).

2.2 METEOROLOGICAL DATA

Daily air temperature and wind speed records were obtained for the Montague Airport, located approximately 11 miles south of Iron Gate Dam, from the National Oceanic and Atmospheric Administration National Weather Service⁴.

3 RESULTS AND DISCUSSION

3.1 METEOROLOGICAL DATA

Meteorological data at Montague Airport show seasonal and year-to-year variation in air temperature and wind speed (Figure 7). For example, 2008 was cooler in general mid-July to mid-August and windier during the latter half of August; 2005 was generally windier from mid-July to mid-August period. In 2007 and 2009, air temperatures were high in mid/late May. Although beyond the scope of this data report, such climatic data could be utilized in future assessments of reservoir and river phytoplankton and nutrient dynamics. For example, the observed cooler and windier conditions during the typical period of *Microcystis* dominance in 2008 may explain the decreased dominance and lower overall biomass observed in that year.

⁴ Available online at:

http://www.wunderground.com/history/airport/KSIY/2006/1/11/DailyHistory.html?req_city=NA&req_state=NA&req_statename=NA

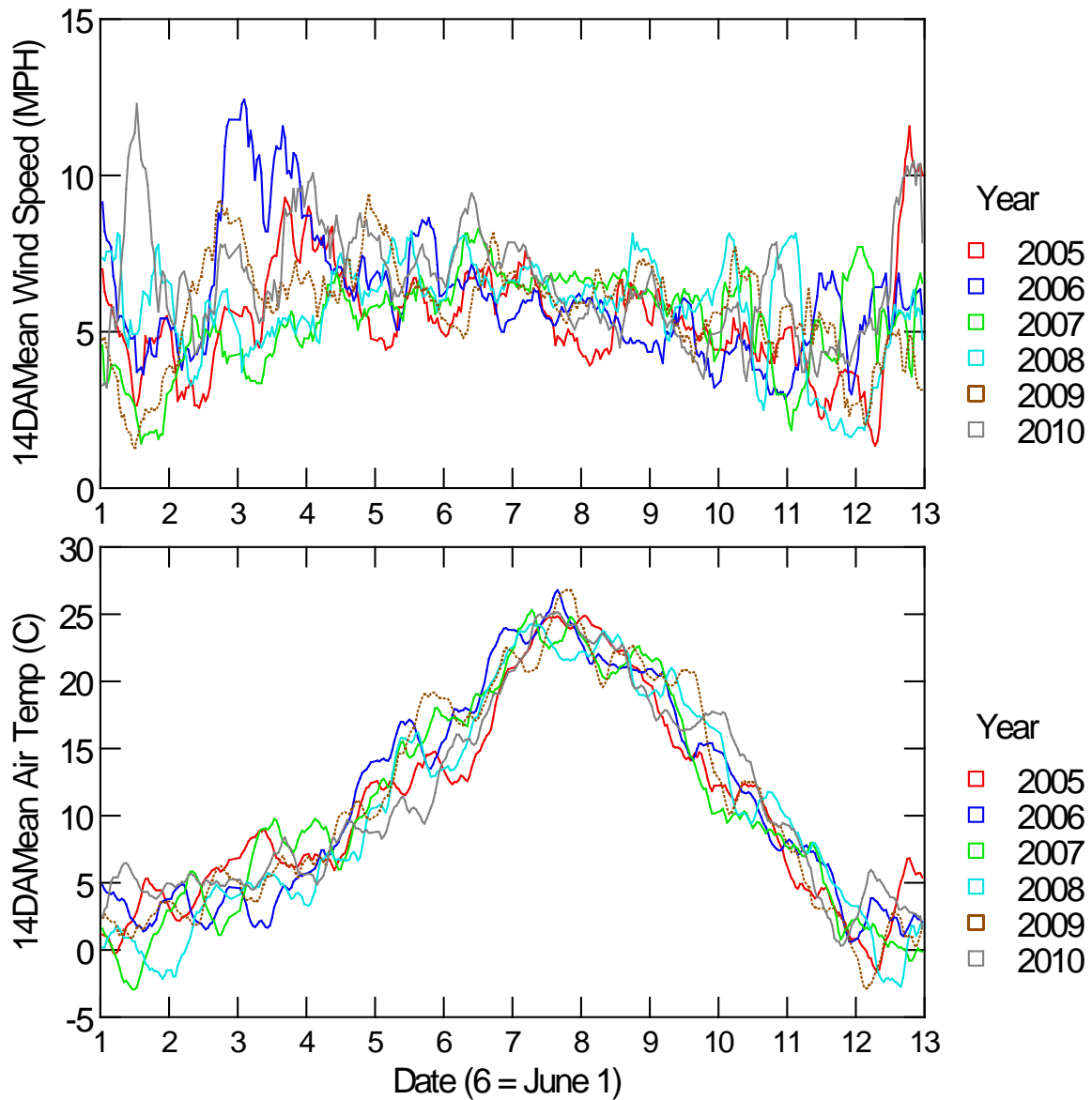


Figure 7. 14-day moving average of daily average (14DAMean) for air temperature and wind speed at the Montague Airport.

3.2 LONGITUDINAL NUTRIENT CONCENTRATIONS

Monthly summaries of nutrient parameters for Klamath River stations⁵ for January 2005-December 2010 are shown in Figure 8 through Figure 10. In addition, the graphs of the full time series of individual samples are available in Appendix D.

3.2.1 Nitrogen

From May-September, NH₃ concentrations were often lowest at KRAC or KRBI, with the highest concentrations in Copco Reservoir (Figure 8). The likely cause of these low NH₃ concentrations at KRAC is that during warm months, high concentrations of ammonia released from Keno Reservoir are rapidly nitrified⁶ in the turbulent oxygen-rich river reach between Keno Dam and Copco Reservoir (Deas 2008). Compared with the May-September period, the October-December period exhibited higher NH₃ at KRAI and KRBI (and to a lesser extent at KRAC) likely due to senescing algal blooms and reservoir turnover (Figure 8). At KRBI, the highest NH₃ levels of 2005-2010 occurred in late October and early November of 2008 (Appendix D). The limited number of January-April samples show ammonia declining through the period. Incomplete nitrification (caused by low water temperatures slowing down nitrification rates), potentially exacerbated by non-point sources of NH₃ from upstream, are likely causes of high winter ammonia levels.

During the thermally stratified period from June through November, NO₃-NO₂ concentrations at KRAC were substantially higher than at reservoir outlets KRAI and KRBI (Figure 8). This difference was generally not present during isothermal periods. During stratification, NO₃-NO₂ concentrations at KRBI were consistently lower than or equal to the other locations. For every sample at all river stations, NO₃-NO₂ concentration was greater than NH₃ and thus TIN is largely composed of NO₃-NO₂ (Appendix D).

Concentrations of organic N were typically lower at KRAC than downstream at KRAI and KRBI (Figure 8), but there were times during peak phytoplankton blooms such as mid-August to mid-September 2007 and mid-September 2010 when organic N was substantially higher at KRBI and KRAI (2006 was too difficult to judge due to timing of sample collection at KRAC)(Appendix D). Organic N generally comprised ≥50% (up to 90%) of the TN at all locations, with the percentage following a seasonal pattern of being highest in May-September and lowest in November-December (Figure 10). High May-September organic N composition corresponds with algal blooms in the study area (see chlorophyll-*a* data in Figure 22) and upstream. During June-October, KRAC had the lowest percent composition of organic N (Figure 10), due to high concentrations of NO₃-NO₂ resulting from the decomposition of organic matter from upstream sources (Figure 8).

Overall TN concentrations showed a longitudinal decrease, with concentrations being most often highest at KRAC, intermediate at KRAI, and lowest at KRBI (Figure 8). This is likely due to 1) nutrient storage in the water column and sediments of the reservoirs, 2) penstock intakes that draw water from intermediate depths where concentrations are lower, and 3) possible atmospheric losses through denitrification.

⁵ KRAC data are affected by hydropower peaking (see Asarian and Kann 2009), and so nutrient concentrations can vary dramatically depending upon when along the daily hydrograph samples are collected. Sufficient data were available for TN and TP only to adjust values to approximate the daily flow-weighted average. Due to time/budget constraints, these adjustments were applied only to the 2005-2008 Karuk data and the 2005-2007 PacifiCorp data. Comparison of adjusted and unadjusted TN (or TP) for a sample can be used to approximate the effect of adjustment on other parameters.

⁶ Nitrification is the conversion of NH₃ to NO₃-NO₂

There is some evidence of a longitudinal time lag in TN concentrations. For example, TN concentrations at KRAC begin to rise rapidly each year in late June or early July, but this rise does not appear at KRBI for approximately one month (Appendix D).

3.2.2 Phosphorus

TP concentrations follow a seasonal cycle, with highest concentrations typically occurring in July-October and lowest concentrations occurring in December-May, although in 2006 there were high TP concentrations during peak winter/spring flows particularly at KRAC (Figure 9 and Appendix D).

Longitudinally, TP concentrations generally showed a decreasing pattern at river stations (highest at KRAC, intermediate at KRAI, lowest at KRBI) from January through May and from July through August/September (varies by year), but then exhibit an opposite pattern until approximately December. This reversal is likely the result of the combination of internally-driven reservoir nutrient dynamics, P associated with reservoir algal blooms, and a temporal lag as nutrients move through the reservoirs resulting from hydraulic residence time. This apparent temporal lag varies from approximately one to two months. The longitudinal attenuation of annual maximum concentrations was not nearly as large for TP as it was for TN and occurred primarily only in 2005 (Appendix D).

In May-December, SRP accounted for a substantial majority (~50-90%, Figure 10) of the TP, and exhibited similar temporal and longitudinal dynamics as TP (Figure 9) (Appendix D). Inversely, PP generally was only a small portion of the TP during the May-December period, but comprised a majority of TP during the January-April period and was particularly high during peak flow events.

The mass ratios of total nitrogen to total phosphorus (TN:TP) and total inorganic nitrogen to SRP (TIN:SRP) were generally higher in Copco inflow KRAC than in KRAI, indicating that conditions are potentially more nitrogen-limiting below Copco than above (Figure 9), but in January through May TN:TP and TIN:SRP ratios sometimes showed an opposite pattern. The ratios of TN:TP and TIN:SRP were further reduced at KRBI, especially during the August through mid-fall period (Figure 9). Reduction in these ratios increases potential for N limitation and has the potential to promote the growth of nitrogen fixing blue-green algae.

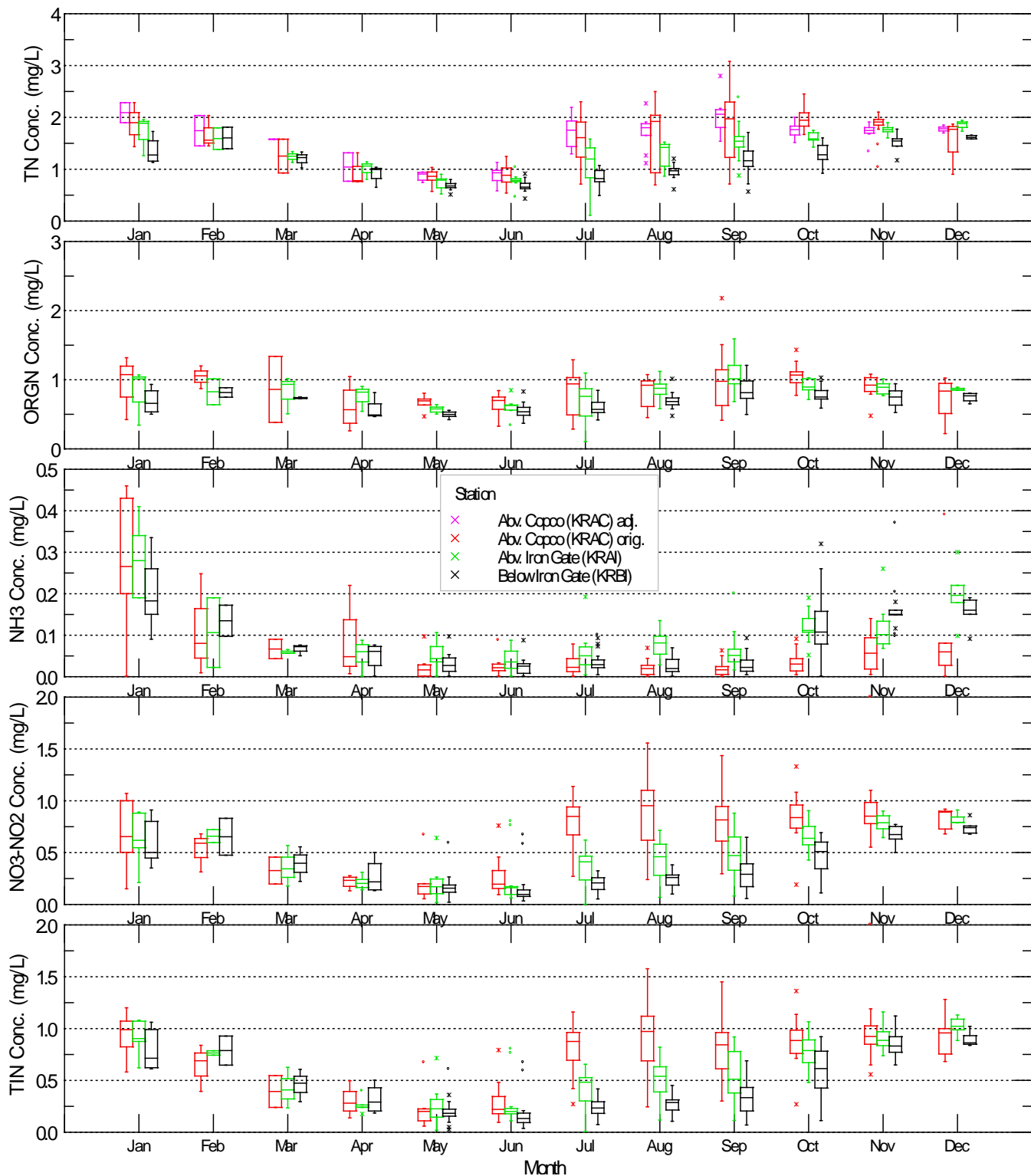


Figure 8. Monthly box plots of nitrogen concentrations above and below Copco and Iron Gate reservoirs, January 2005 – December 2010 (some 2008-2009 data missing for TN and ORGN)KRAC data are affected by hydropower peaking (see footnote 5 above). Note: to reduce the y-axis scale, an outlier value for TIN and NO₃+NO₂ was reduced at KRAC in November.

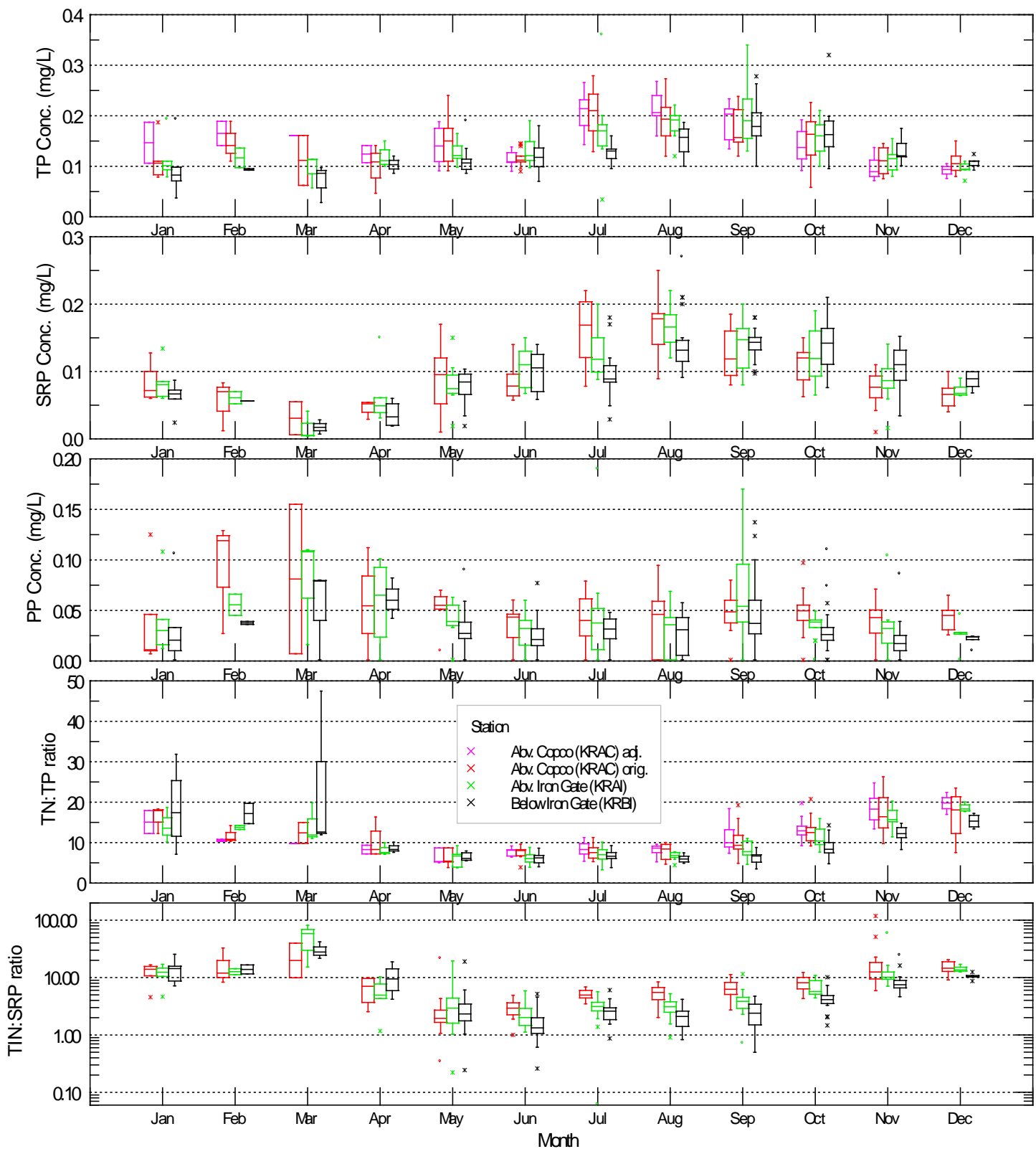


Figure 9. Monthly box plots of phosphorus concentrations and nitrogen:phosphorus ratios above and below Copco and Iron Gate reservoirs, January 2005 – December 2010. KRAC data are affected by hydropower peaking (see footnote 5 above).

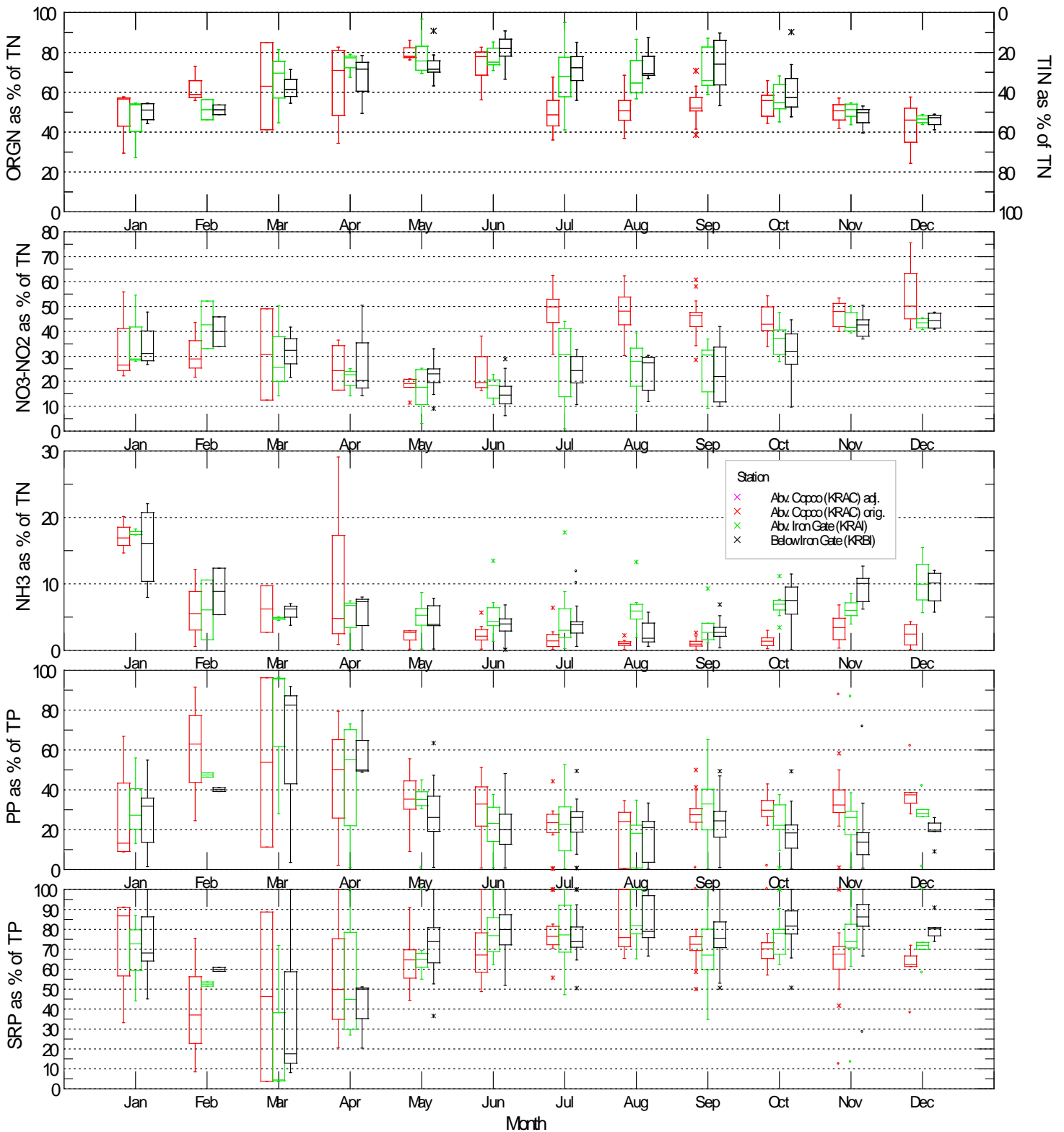


Figure 10. Monthly box plots of percent composition of nitrogen and phosphorus species above and below Copco and Iron Gate reservoirs, January 2005 – December 2010. KRAC data are affected by hydropower peaking (see footnote 5 above).

3.3 VERTICAL DISTRIBUTION OF TEMPERATURE, DISSOLVED OXYGEN, PH, NUTRIENTS WITHIN THE RESERVOIRS

Depth distribution of temperature, dissolved oxygen (DO), and pH is an important aspect of water quality dynamics and fish habitat, and depth-time plots of isotherms and isopleths for these parameters allows both seasonal and depth distribution to be evaluated simultaneously (Figure 11, Figure 12, Appendix A). For the purposes of this report they were mainly utilized to determine stratification and mixing patterns with respect to understanding nutrient and phytoplankton dynamics.

Temperature isotherms show that stratification begins around April in the deeper Iron Gate Reservoir and during May in shallower Copco Reservoir (Figure 12). Copco also showed earlier fall mixing than did Iron Gate, with complete mixing occurring approximately a month later in Iron Gate (early December) than it did in Copco (mid-October to early November). Likewise, low dissolved oxygen ($< 3\text{mg/L}$) extended further up in the water column and longer in the season in Iron Gate (Figure 12). In 2007 and 2009, near-surface waters heated up earlier than in other years (Figure 12) reaching temperatures $>20^{\circ}\text{C}$ by mid/late May, likely due to high air temperatures during the same period (Figure 7). Coinciding with the period of elevated upper water column temperatures during summer months, pH and dissolved oxygen also showed elevated levels during this same period (Figure 12, Appendix A). Supersaturated dissolved oxygen and high pH near the surface during the stratified period are the likely reflection of higher algal biomass and productivity from buoyant cyanobacteria concentrating near the reservoir surface (see below for description of chlorophyll dynamics)

Figure 13 through Figure 16 summarize seasonal differences in nitrogen and phosphorus concentrations at various depths over time in Copco and Iron Gate reservoirs, and the time series of individual measurements is displayed in Appendix C. In both reservoirs, the deepest depths generally had the highest TN concentrations, except on some July-September dates when organic N was very high during phytoplankton blooms (Figure 13, Figure 15, and Appendix C).

During the period of deeper reservoir anoxia, NH_3 increased in the bottom layer, reaching a seasonal maximum in late August/early October in Copco (Figure 13 and Appendix C) and October/November in Iron Gate (Figure 15). Coincident with the period of maximum stratification and low dissolved oxygen, $\text{NO}_3\text{-NO}_2$ at the deepest depths followed a generally decreasing pattern from May through August/September at Copco and November in Iron Gate prior to reservoir mixing (Figure 13, Figure 15). Minimum late summer/early fall $\text{NO}_3\text{-NO}_2$ concentrations at the deepest depths were lower in Copco than in Iron Gate, with Copco nearing zero (e.g. $<0.05\text{ mg/L}$) in all three years compared to Iron Gate which only approached zero in 2006 and 2010 (Appendix C).

$\text{NO}_3\text{-NO}_2$ and TIN concentrations in the upper layers (0-1m and 5-10m) in Copco Reservoir were typically at annual lows (with some variation but minimum values near zero) in April-June (Figure 13) and exhibited an overall rise through December/January; however, in some years low concentrations did also occur in mid/late summer (Appendix C) coincident with phytoplankton blooms. $\text{NO}_3\text{-NO}_2$ and TIN concentrations at the 0-1m depth in Iron Gate (Figure 15) were much lower than in Copco, approaching zero for extended periods each summer (Appendix C); however, $\text{NO}_3\text{-NO}_2$ was substantially higher at the 5-10m depth than at the 0-1m depth, potentially providing a nitrogen supply for algal species that can migrate vertically in the water column (i.e. blue-green

algae such as *Aphanizomenon flos-aquae* and *Microcystis aeruginosa*). The seasonal patterns of $\text{NO}_3\text{-NO}_2$ and TIN are likely the result of phytoplankton growth in the upper reservoir layers, as organic N and chlorophyll were often high during this period. The concentration of all forms of nitrogen at specific depths then tended to converge during water column mixing in the fall months.

During the stratified period, TP and SRP increased in the bottom layer through October in Copco (Figure 14) and October or November in Iron Gate (Figure 16). Similar to ammonia increases, SRP increases generally coincided with the development of an anoxic hypolimnion, and are possibly reflective of internal P loading due to release of iron-bound P. As noted by Moisander (2008, 2009) the observed anoxic layer and associated increased concentrations of NH_3 and SRP appears to provide a nutrient source for vertically migrating *Microcystis aeruginosa* colonies. SRP in the surface layer of Copco followed an overall increasing pattern from May through August or September (Figure 14), before declining into December. SRP in the surface layer of Iron Gate followed a similar overall pattern, but also declined in July of each year and did not peak until later (October) (Figure 16).

There was also a seasonal increase in particulate P (PP) in the surface (1 m) of both reservoirs (Figure 14 and Figure 16) that likely stems from phytoplankton concentrating near the surface during the stratified period. This trend was consistent with the trend in organic nitrogen. Particulate P was also often elevated in the deepest samples at both reservoirs during the stratified period. As with nitrogen, the concentration of all forms of phosphorus at specific depths then tended to converge during water column mixing in the fall months.

During the stratified period TIN:SRP mass ratios tended to be lower in the upper water column layers and showed an increasing trend with depth in Iron Gate (Figure 16), but were quite variable in Copco (Figure 14). In the upper layers during the stratified period, for both reservoirs the TIN:SRP mass ratios were relatively low (approximately <5 in Iron Gate and <7 in Copco) and TN:TP ratios were variable (range $\sim 3\text{-}12$ in Iron Gate and $\sim 3\text{-}10$ in Copco).

CR01 Temperature 2005-2010

IR01 Temperature 2005-2010

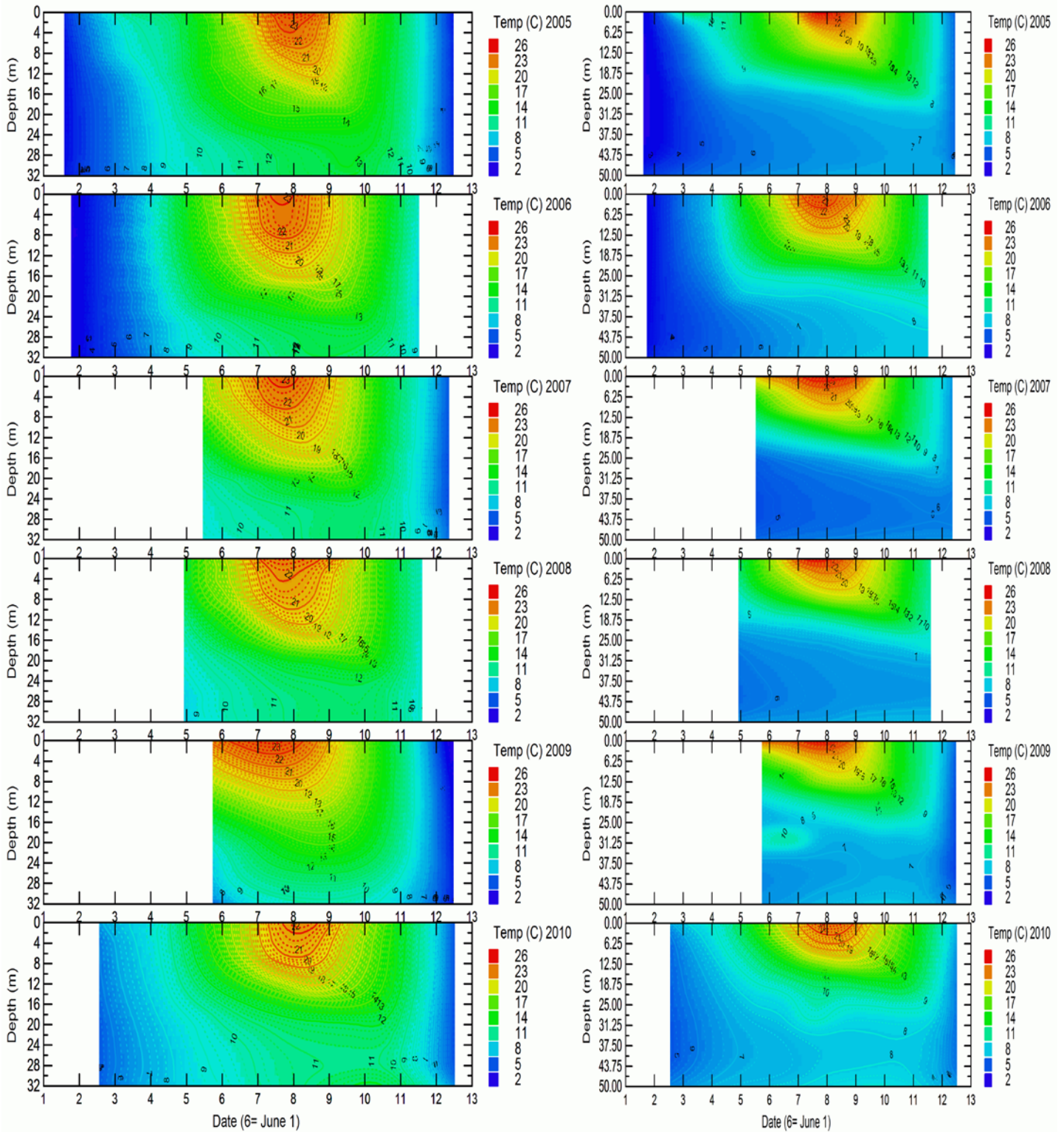


Figure 11. Depth-time distributions of isopleths of temperature at station CR01 in Copco Reservoir and IR01 in Iron Gate Reservoir, January 2005-December 2010.

CR01 Dissolved Oxygen 2005-2010

IR01 Dissolved Oxygen 2005-2010

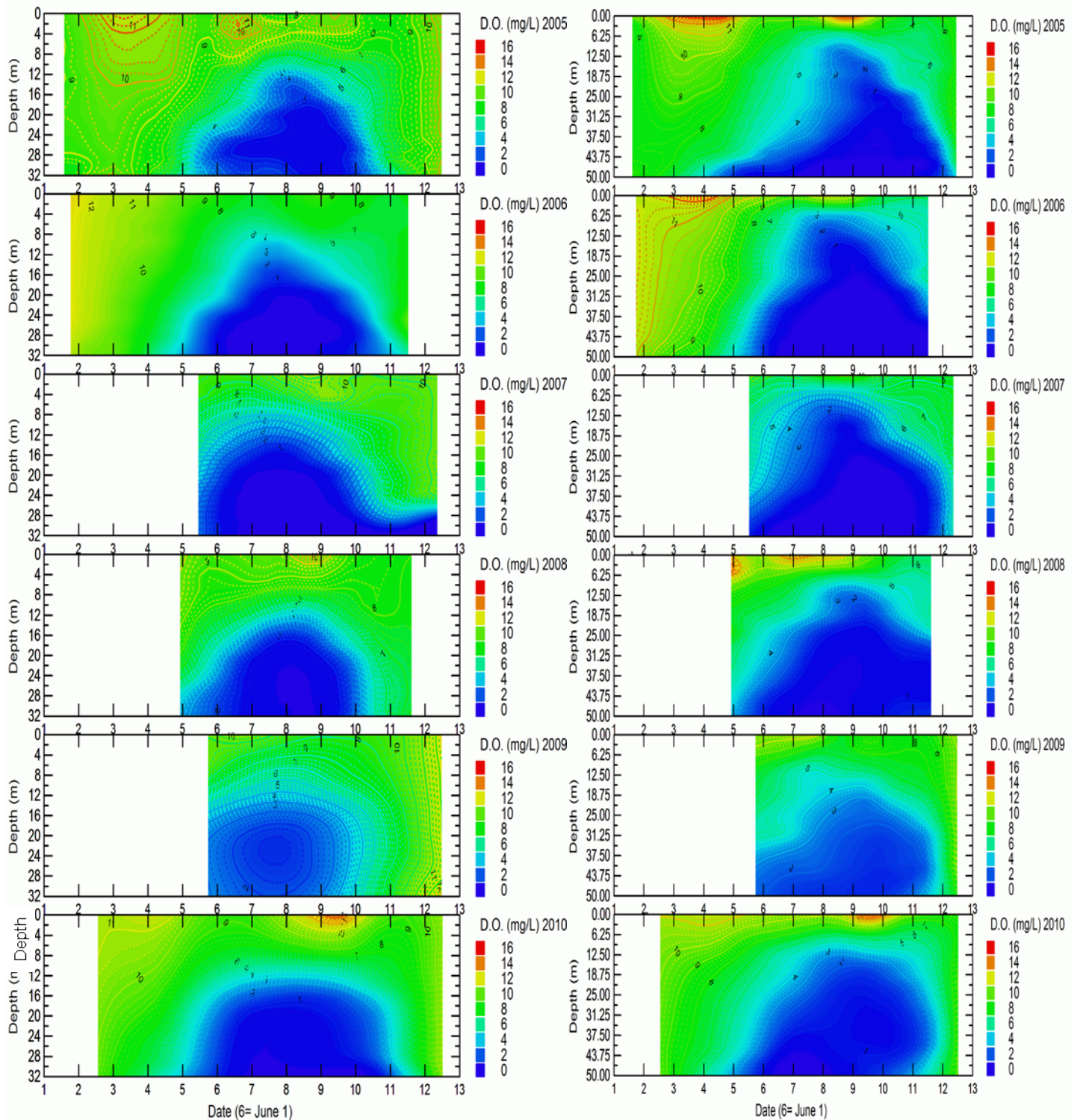


Figure 12. Depth-time distributions of isopleths of dissolved oxygen concentration at station CR01 in Copco Reservoir and IR01 in Iron Gate Reservoir, January 2005-December 2010.

Copco (CR01)

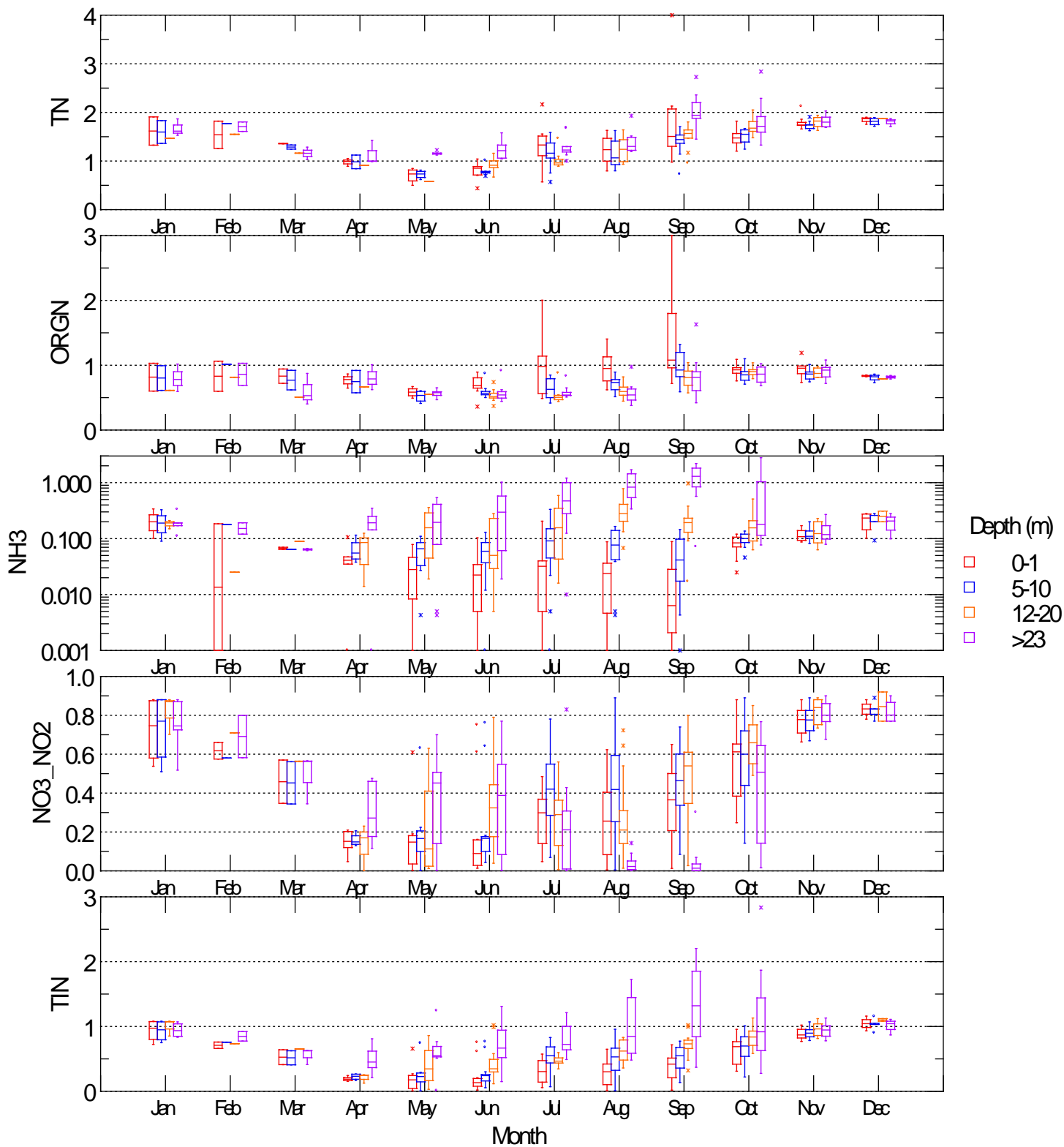


Figure 13. Monthly box of nitrogen concentrations for various depths at Copco Reservoir sampling station CR01, January 2005 – December 2010. Samples sizes are very low (1 to 3) in January-April. Note: to reduce the y-axis scale, an outlier value for TN and ORGN was reduced at 0-1m depth in September 2007.

Copco (CR01)

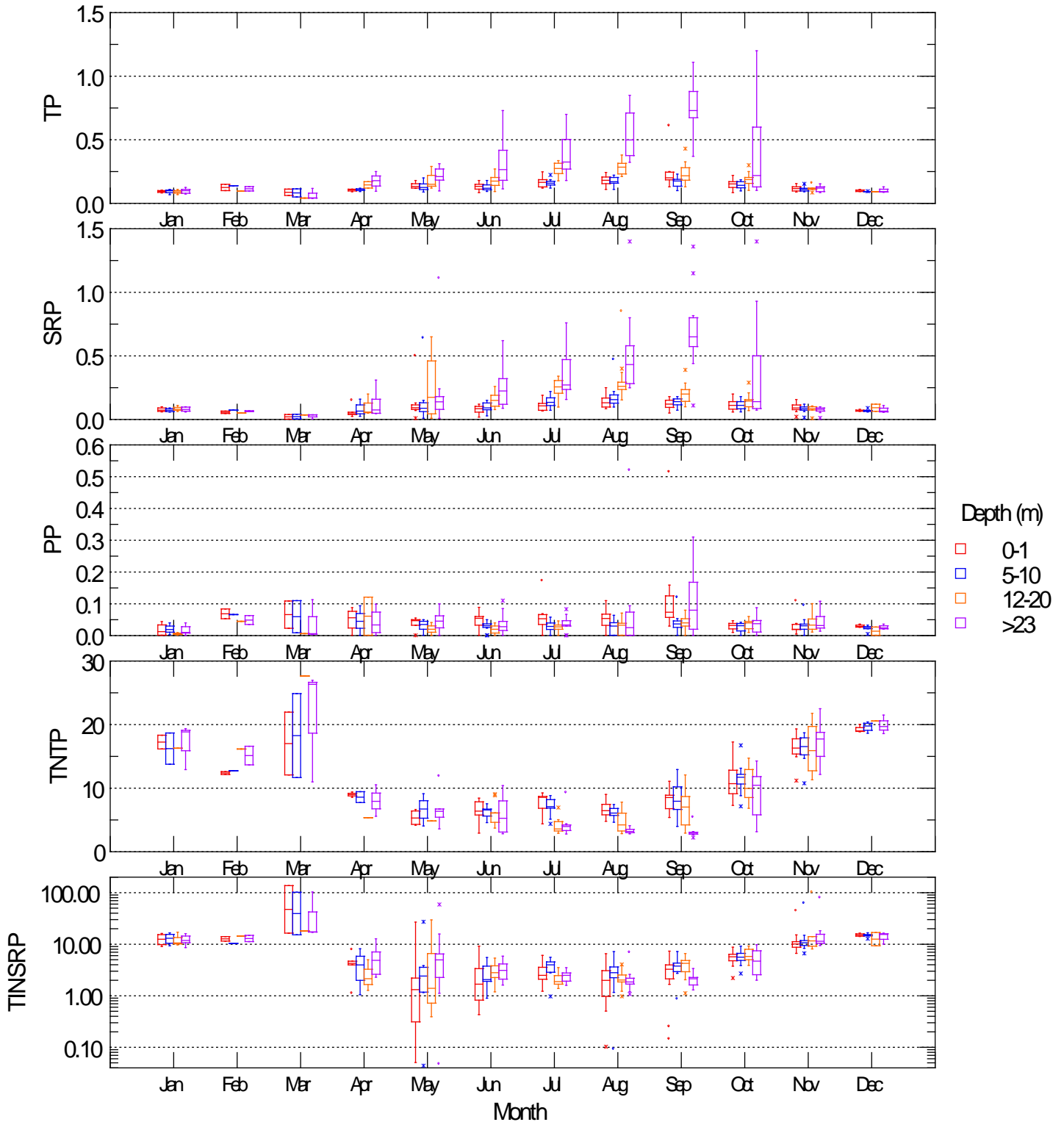


Figure 14. Monthly box plots of phosphorus concentrations and nitrogen:phosphorus mass ratios for various depths at Copco Reservoir sampling station CR01, January 2005 – December 2010. Samples sizes are very low (1 to 3) in January-April. TNTP is mass ratio of TN to TP, and TINSRP is mass ratio of TIN to SRP.

Iron Gate (IR01)

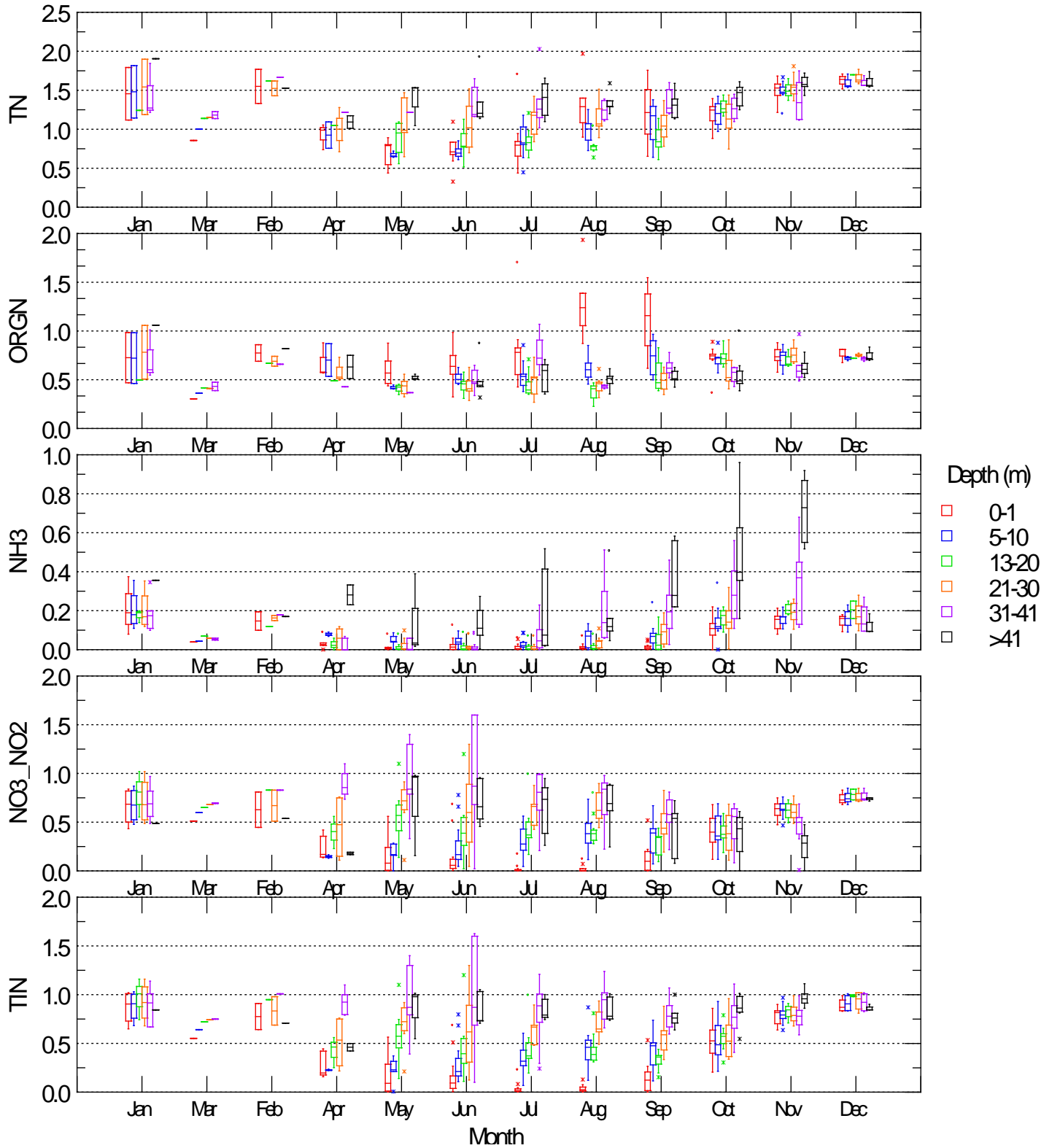


Figure 15. Monthly box plots of nitrogen concentrations for various depths at Iron Gate Reservoir sampling station IR01, January 2005 – December 2010. Samples sizes are very low (1 to 3) in January-April.

Iron Gate (IR01)

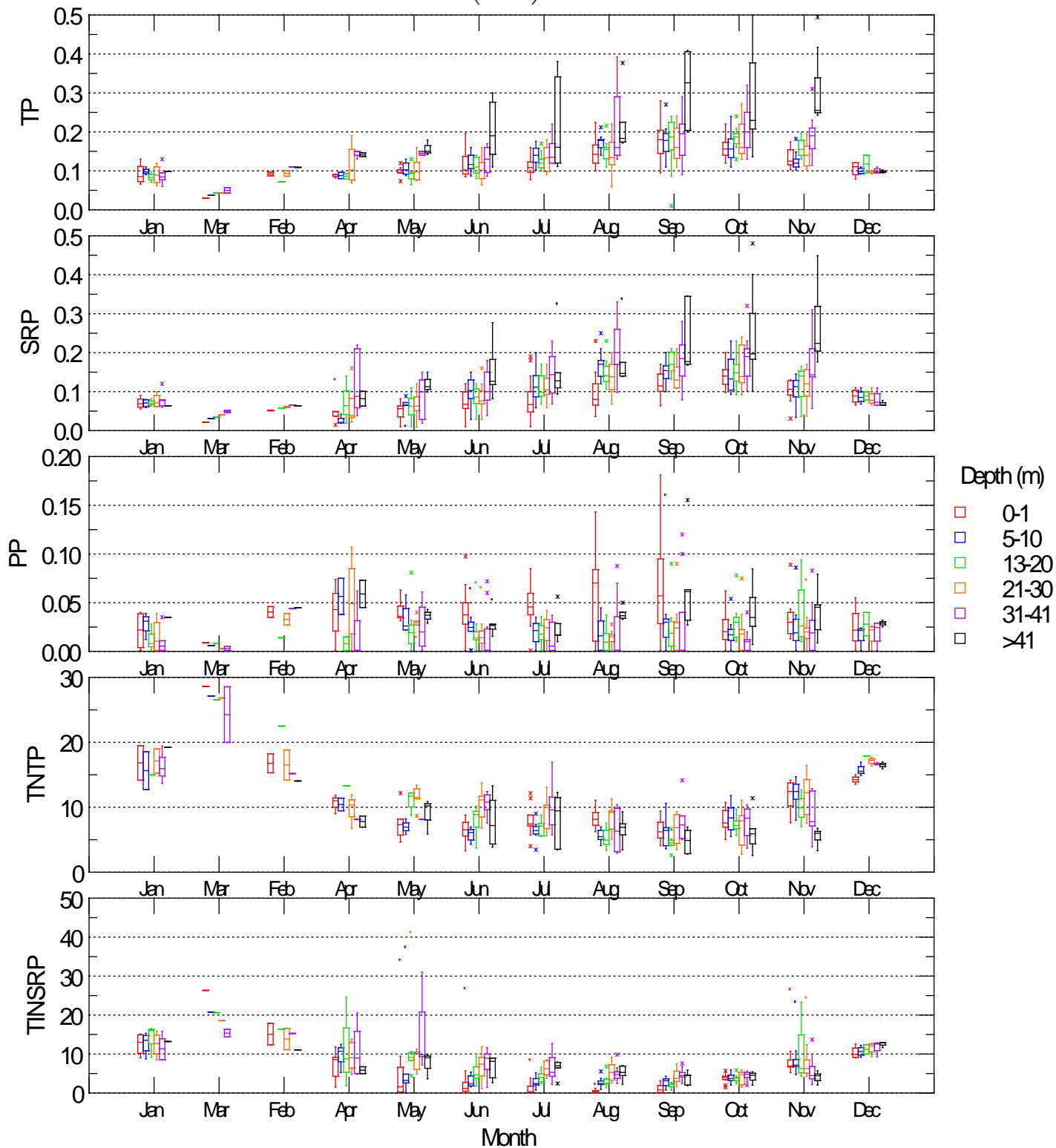


Figure 16. Monthly box plots of phosphorus concentrations and nitrogen:phosphorus mass ratios for various depths at Iron Gate Reservoir sampling station IR01, Jan. 2005 – Dec. 2010. Samples sizes are very low (1 to 3) in January-April. TNTP is mass ratio of TN to TP, and TINSRP is mass ratio of TIN to SRP.

3.4 Phytoplankton

Phytoplankton dynamics are an important aspect of understanding reservoir nutrient dynamics as well as overall water quality patterns, particularly in such systems as Copco and Iron Gate that have extensive blooms of both toxic and non-toxic cyanobacteria (Kann 2006, Kann and Corum 2009, Kann et al. 2010).

3.4.1 Longitudinal Comparison at Seasonal and Annual Time Scales

3.4.1.1 *Total Biovolume and Chlorophyll a*

Box plots of total phytoplankton biovolume for all sample dates and June-October 2005-2010 dates show that total biovolume was higher at the reservoir stations CR01 and IR01 than at the river stations above (KRAC) and below (KRAI, KRBI) the reservoirs, and that CR01 had higher biovolume than IR01 (top panel; Figure 17 and Figure 18). There is also an increasing trend in biovolume between KRAC and the river stations downstream of the reservoirs (KRAI and KRBI). This trend was particularly strong in the Jun-Oct period when the KRAI station directly below Copco had higher upper quartile (1.4x) values than did KRAC, KRBI station below Iron Gate had higher median (2.1x higher) and upper quartile (3.4x) values than KRAC (Figure 17, Table 2). Due to water withdrawal depths (7 to 9.8 m in Copco and 4 – 6.4 m in Iron Gate⁷) generally low in the photic zone, total biovolume below the reservoirs was not as high as within the reservoirs. Total biovolume at KRAC was less variable (i.e. upper quartile is lower, and lower quartile is higher) than the other stations for both the Jun-Oct period and all sample dates (Figure 17 and Figure 18). The longitudinal trend in total biovolume for November-April was the reverse of the June-October pattern, with total biovolume being lower at KRBI than KRAC (Figure 19, Figure 20).

Chlorophyll *a* (another indicator of algal biomass) showed similar directionality of longitudinal trends to those of total biovolume, but with a somewhat larger magnitude. Of the three river stations, chlorophyll-*a* concentrations were typically substantially higher in June-October at KRAI and KRBI than at KRAC, indicating an increase through the reservoir complex (Figure 21, Figure 23). For example, the median and upper quartile values for chlorophyll at KRBI were substantially elevated (2.8x and 3.6x, respectively) compared to KRAC for June-October (Table 2, Figure 21). The pattern was consistent in all years, although overall values were higher in 2007 and 2008, particularly at KRBI (Figure 22). This trend of elevated chlorophyll through the reservoir complex and below was evident for all evaluated reservoir depths (with the exception the 8-10m depth in some years), and not only for the surface to 1 m layer (Figure 21).

⁷ According to PacifiCorp (2005b), the elevation of penstock intakes is 2575 ft in Copco and 2309 ft in Iron Gate. During May 2005 – February 2008 (the only part of the study period for which we have obtained elevation data, but is likely representative), water surface elevations in Copco ranged from 2598 to 2607 ft, thus release depths were 23 to 32 ft (7 to 9.8 m) below the water surface. In the same period, water surface elevations in Iron Gate ranged from 2322 to 2330 ft, thus release depths were 13 to 21 ft (4.0 to 6.4 m).

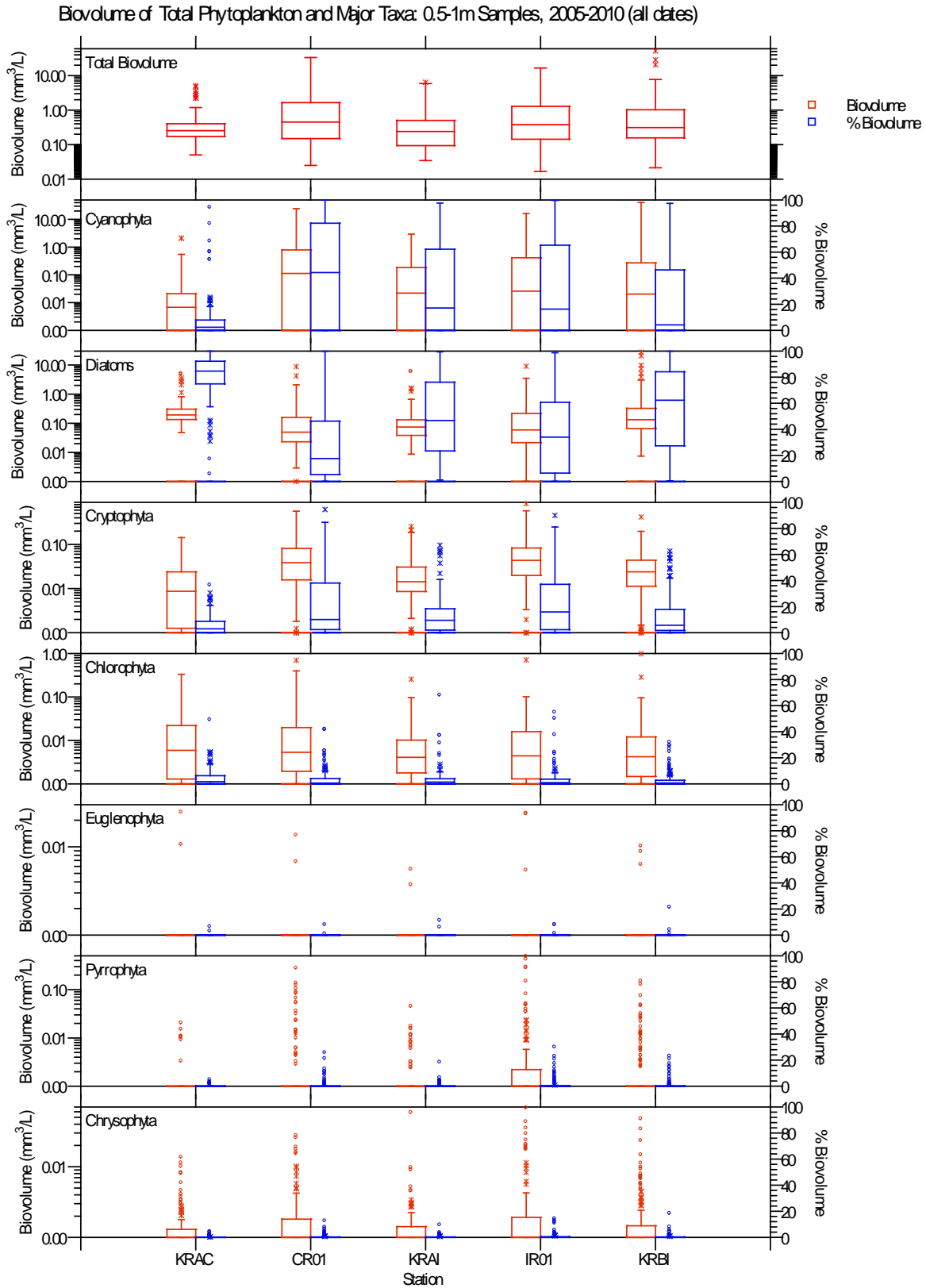


Figure 17. Total phytoplankton biovolume, and total and percent biovolume of the Cyanophyta, Diatoms, Cryptophyta, Chlorophyta, Euglenophyta, Pyrrophyta, and Chrysophyta for surface to 0.5-1.0 m samples for all sample dates 2005-2010. The line inside each box is the median and the edges of each box are the 25th and 75th percentiles. The whiskers represent data points beyond 1.5 times the interquartile (75th-25th) range.

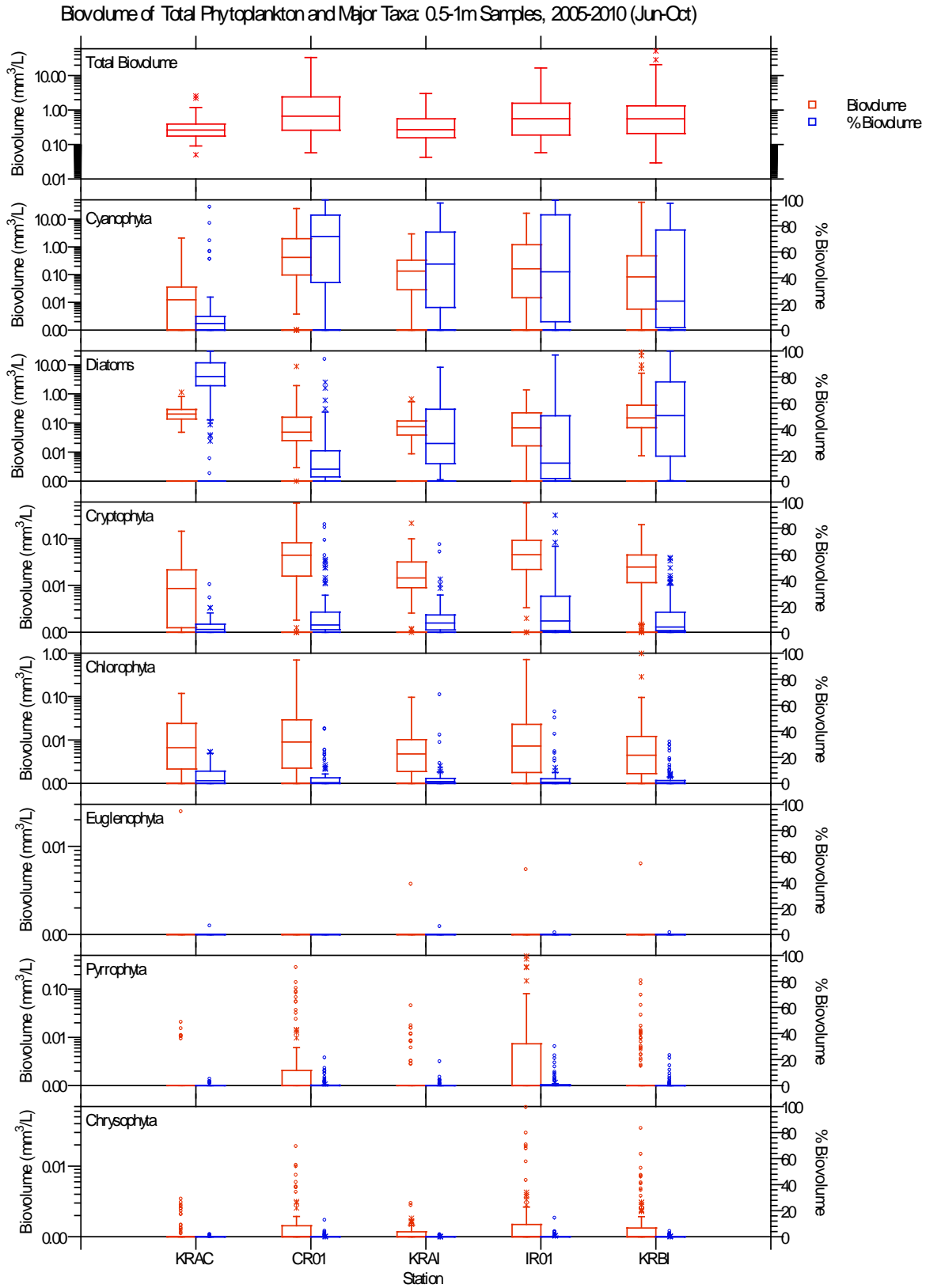


Figure 18. Total phytoplankton biovolume, and total and percent biovolume of the Cyanophyta, Diatoms, Cryptophyta, Chlorophyta, Euglenophyta, Pyrrophyta, and Chrysophyta for surface to 0.5-1.0 m samples for all June-October 2005-2010. The line inside each box is the median and the edges of each box are the 25th and 75th percentiles. The whiskers represent data points beyond 1.5 times the interquartile (75th-25th) range.

Table 2. Summary of biovolume data by station for river stations and 0.5-1m discrete and 0-8m depth-integrated samples at reservoir stations during the period June-October, 2005-2010. For each site and depth, statistics include the number of samples (N) and the lower quartile, median, and upper quartile biovolume for major taxonomic groups.

Station and Depth (m)	Parameter	Chlorophyll <i>a</i> (ug/L)	Biovolume (mm ³ /L)							
			Total	Cyano-phyta	Chloro-phyta	Diatoms	Crypto-phyta	Chryso-phyta	Eugleno-phyta	Pyrro-phyta
KRAC	N of cases	71	79	79	79	79	79	79	79	79
KRAC	Lower Quartile	1.9	0.173	0.000	0.001	0.135	0.000	0.000	0.000	0.000
KRAC	Median	2.9	0.262	0.011	0.006	0.202	0.008	0.000	0.000	0.000
KRAC	Upper Quartile	4.3	0.390	0.036	0.023	0.291	0.021	0.000	0.000	0.000
CR01 0.5-1m	N of cases	61	80	80	80	80	80	80	80	80
CR01 0.5-1m	Lower Quartile	5.5	0.259	0.096	0.001	0.024	0.015	0.000	0.000	0.000
CR01 0.5-1m	Median	16.6	0.665	0.419	0.008	0.047	0.043	0.000	0.000	0.000
CR01 0.5-1m	Upper Quartile	33.3	2.410	1.988	0.028	0.158	0.080	0.000	0.000	0.002
CR01 0-8m Int*	N of cases	26	36	36	36	36	36	36	36	36
CR01 0-8m Int*	Lower Quartile	3.2	0.247	0.094	0.001	0.024	0.017	0.000	0.000	0.000
CR01 0-8m Int*	Median	7.1	0.619	0.472	0.006	0.049	0.033	0.000	0.000	0.000
CR01 0-8m Int*	Upper Quartile	18.3	1.689	1.415	0.015	0.106	0.083	0.001	0.000	0.002
KRAI	N of cases	56	62	62	62	62	62	62	62	62
KRAI	Lower Quartile	2.7	0.156	0.027	0.001	0.037	0.008	0.000	0.000	0.000
KRAI	Median	8.2	0.267	0.133	0.004	0.074	0.013	0.000	0.000	0.000
KRAI	Upper Quartile	14.7	0.556	0.329	0.009	0.117	0.031	0.000	0.000	0.000
IR01 0.5-1m	N of cases	62	76	76	76	76	76	76	76	76
IR01 0.5-1m	Lower Quartile	4.4	0.187	0.014	0.001	0.015	0.021	0.000	0.000	0.000
IR01 0.5-1m	Median	14.7	0.558	0.162	0.006	0.067	0.044	0.000	0.000	0.000
IR01 0.5-1m	Upper Quartile	41.1	1.571	1.198	0.022	0.222	0.091	0.000	0.000	0.007
IR01 0-8m Int*	N of cases	27	35	35	35	35	35	35	35	35
IR01 0-8m Int*	Lower Quartile	2.5	0.161	0.007	0.002	0.015	0.014	0.000	0.000	0.000
IR01 0-8m Int*	Median	6.2	0.833	0.061	0.005	0.043	0.035	0.000	0.000	0.000
IR01 0-8m Int*	Upper Quartile	18.3	1.799	0.946	0.011	0.249	0.069	0.001	0.000	0.000
KRBI	N of cases	105	120	120	120	120	120	120	120	120
KRBI	Lower Quartile	3.5	0.207	0.005	0.001	0.068	0.010	0.000	0.000	0.000
KRBI	Median	8.0	0.557	0.082	0.003	0.149	0.024	0.000	0.000	0.000
KRBI	Upper Quartile	15.5	1.316	0.473	0.011	0.408	0.043	0.000	0.000	0.000

* No depth-integrated samples were collected at CR01 and IR01 in 2006 because PacifiCorp did not sample that year. 0-10m depth-integrated samples from 2005 are included with the "0-8m Int" data in the table.

In contrast to the June-October season, chlorophyll was often lower at KRBI than KRAC for November-April (Figure 21, Figure 23). This seasonal transposition of longitudinal chlorophyll *a* patterns is likely due to the settling of diatoms species washed downstream from Upper Klamath Lake (UKL)⁸. In addition, tributary dilution may also contribute to this pattern due to input of water with low chlorophyll concentrations⁹. As shown in Figure 20 the relatively large increase in chlorophyll tracked that of diatoms during March and April in the river above Copco Reservoir, with a progressive downstream decrease in both parameters. Peak chlorophyll values in March 2006

⁸ Substantial spring blooms of such diatom species as *Asterionella formosa* occur in UKL (Kann 2010). Such species are generally heavy compared to other algal species and are thus prone to settling in lacustrine environments.

⁹ Tributaries contribute approximately 5-20% of inflow to Iron Gate and Copco Reservoirs during high-flow periods in the winter/spring (Asarian and Kann 2009).

and April 2010 were similar to or higher than peaks in summer 2005, 2006, 2009, and 2010 (but lower than summer 2007 and 2008) (Figure 22), perhaps caused by outwash from Upper Klamath Lake during typical spring diatom blooms. It is important to note that there are relatively few November-April samples, so additional data should be collected to confirm trend for that time period.

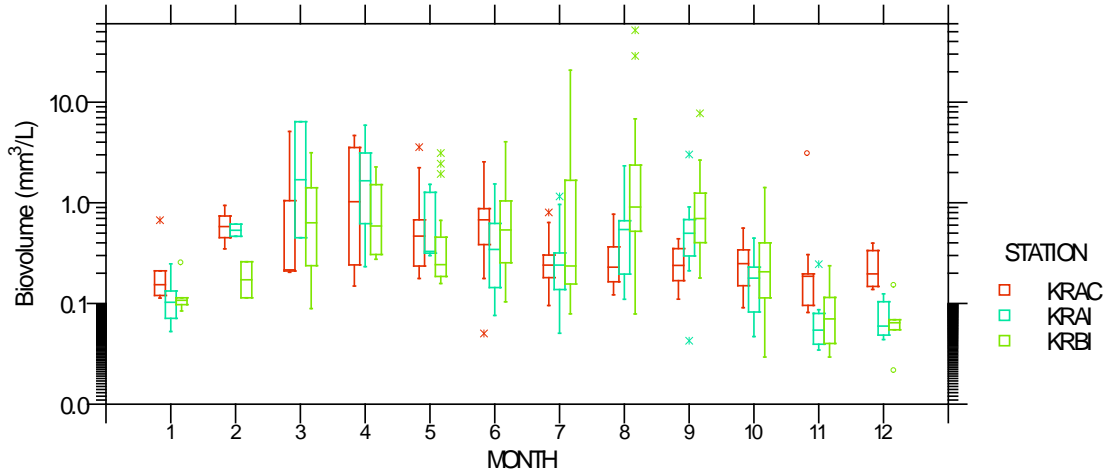


Figure 19. Total algal biovolume by month at river stations KRAC, KRAI, and KRBI for 2005-2010.

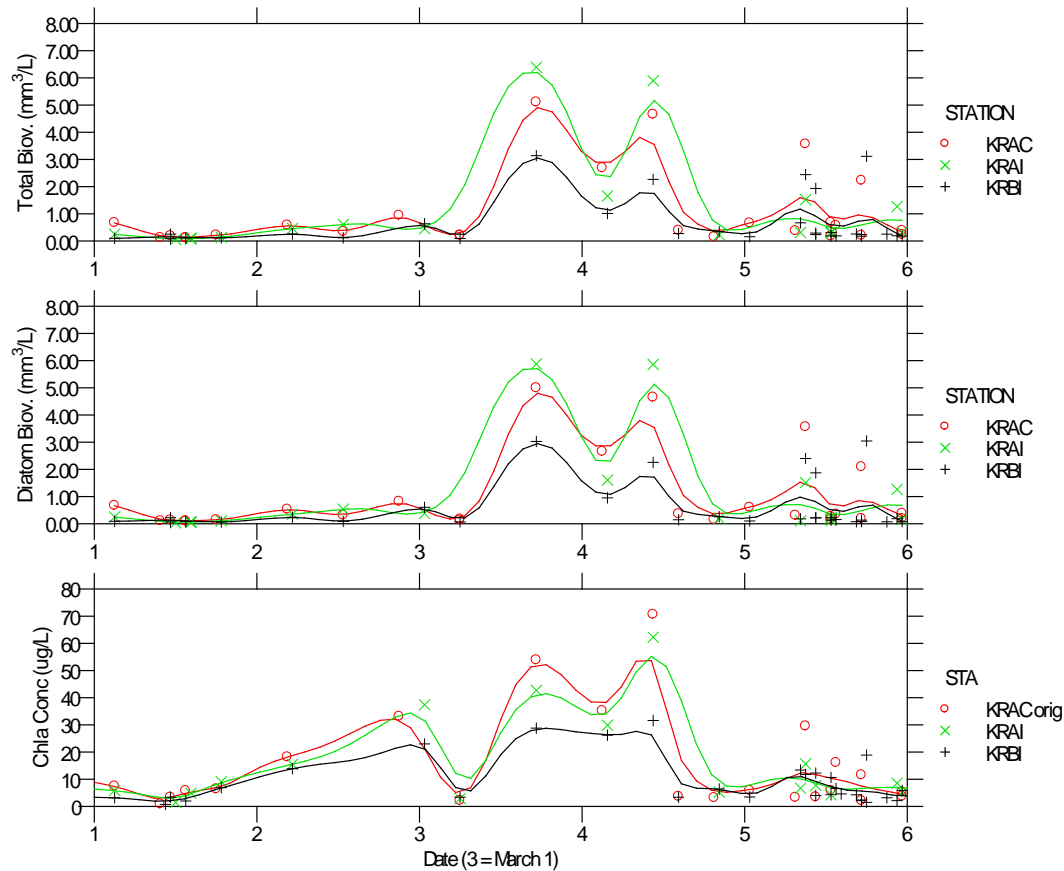


Figure 20. Total algal biovolume, diatom biovolume, and chlorophyll-a concentrations for January-May at river stations KRAC, KRAI, and KRBI. All years 2005-2010 are combined and a distance-weighted least squares (DWLS) smoother is displayed as a visual aid.

Chlorophyll a 2005-2010 June-October

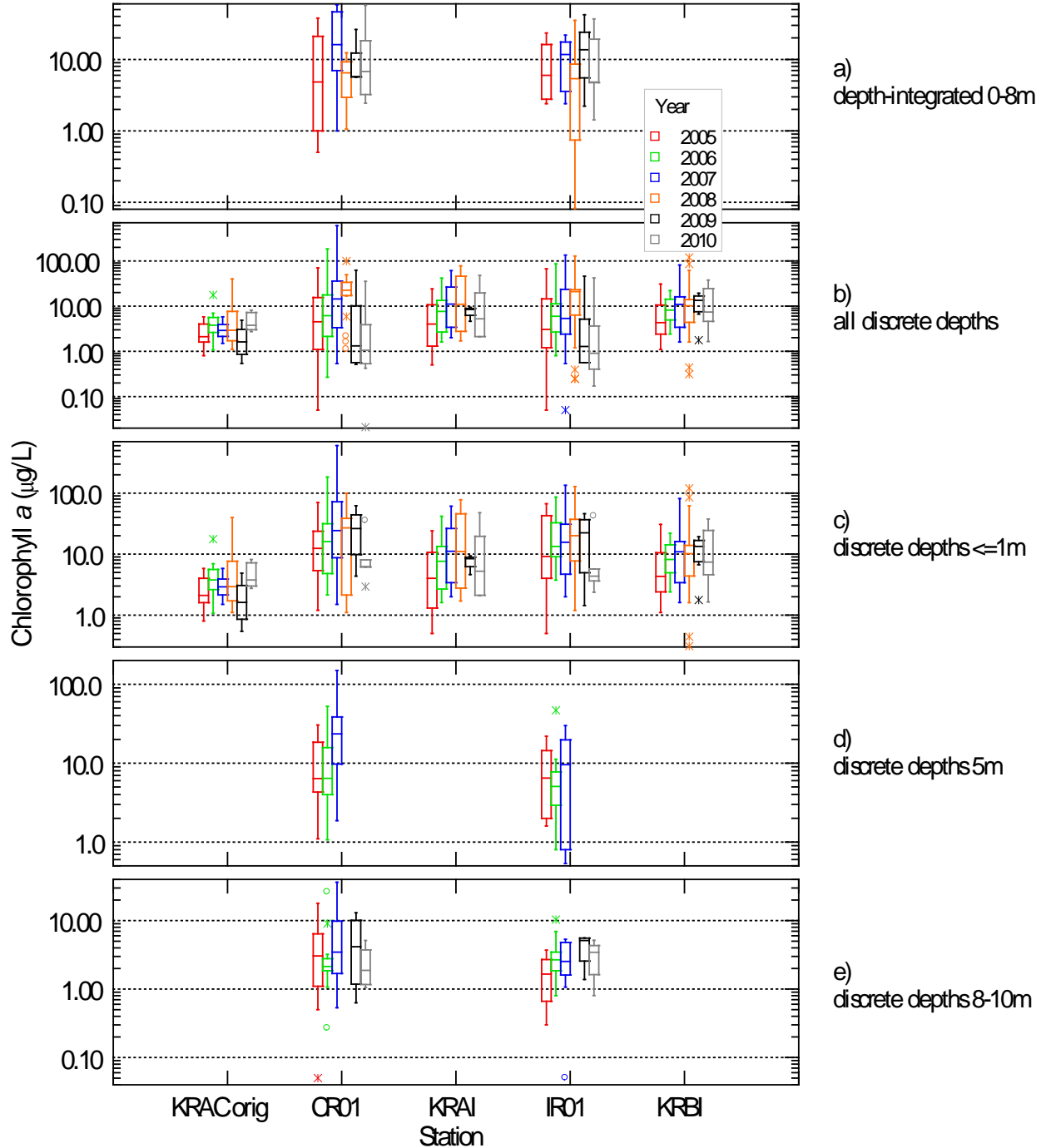


Figure 21. Longitudinal chlorophyll *a* concentrations for 0-8m¹⁰ depth-integrated samples (a) and a range of discrete depths: all depths (b), depth 0-1m (c), depth 5m (d), and depths 8-10m (e), June-October, 2005-2010. Note that values for river stations KRAC, KRAI, and KRBI are only for the 0-1 m layer which represents the entire mixed water column. As noted in Figure 22, KRAC samples were not adjusted to account for hydropower peaking effects.

¹⁰ Note: there are also a few 0-10m integrated samples included with the 0-8m samples.

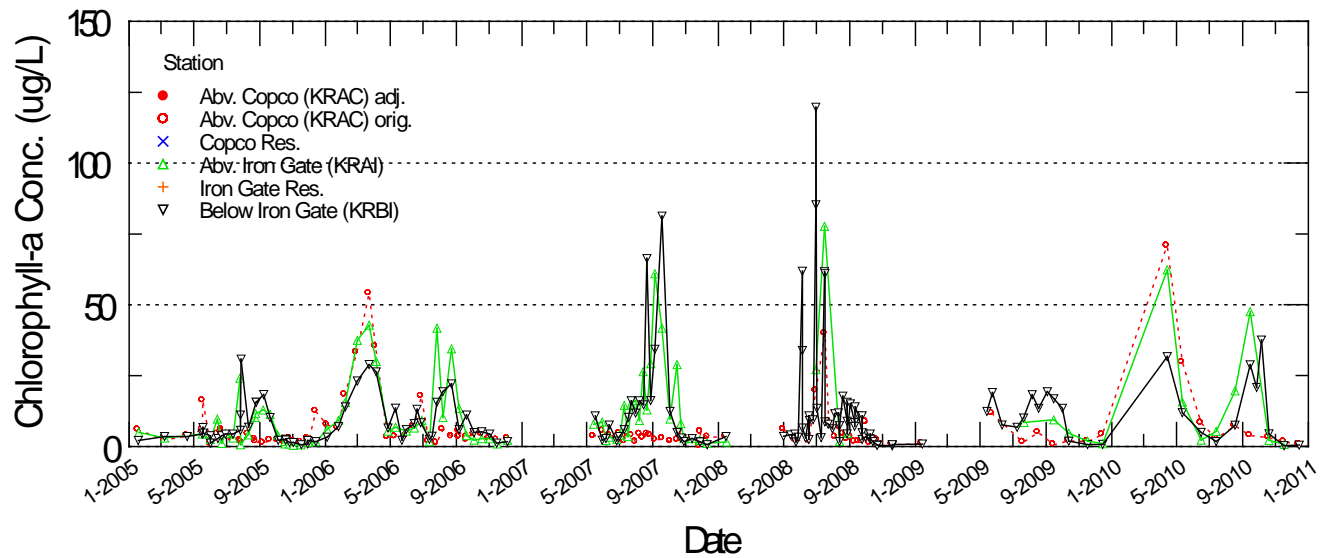


Figure 22. Biweekly time series of chlorophyll-*a* concentrations at Klamath River above Copco (KRAC), Klamath River above Iron Gate (KRAI), and Klamath River below Iron Gate (KRBI), January 2005 - December 2010. KRAC samples were not adjusted to account for hydropower peaking effects; however, based on time of day that samples were collected, the above chlorophyll values for summer 2005 and summer 2007 are likely somewhat higher than daily flow-weighted averages, and summer 2006 samples are likely somewhat lower than daily flow-weighted averages.

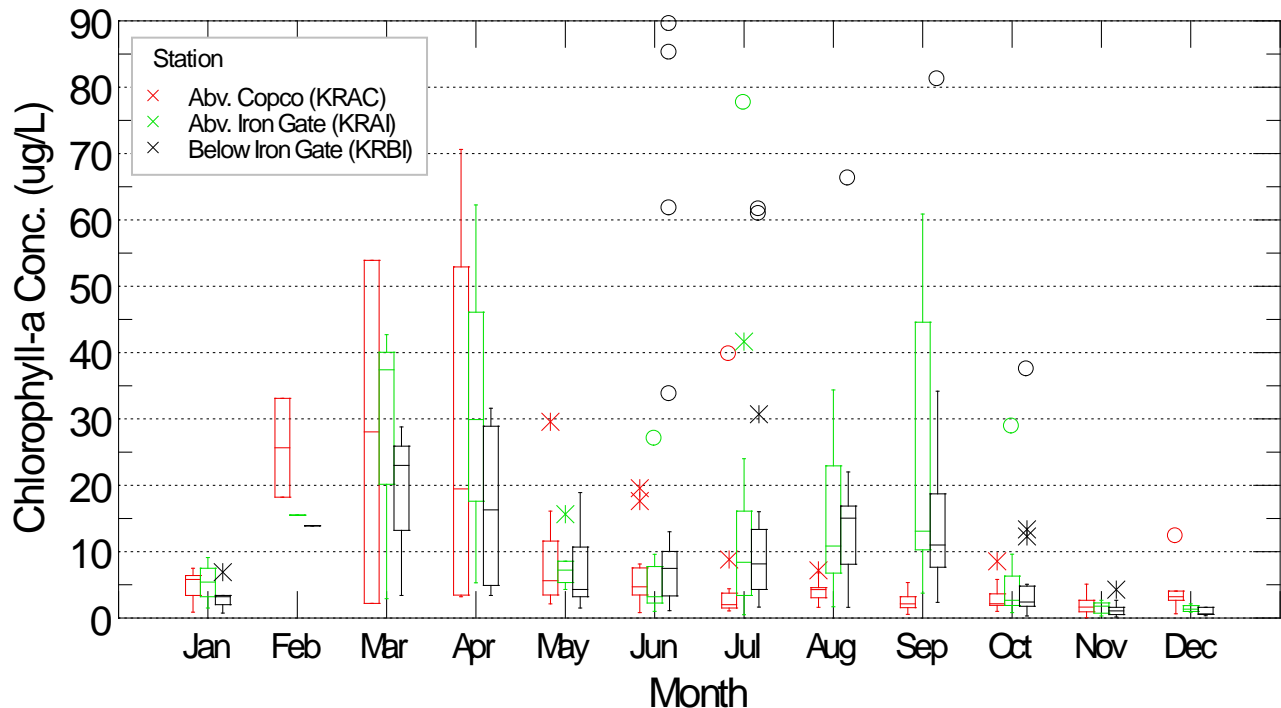


Figure 23. Boxplot of chlorophyll-*a* concentrations at Klamath River above Copco (KRAC), Klamath River above Iron Gate (KRAI), and Klamath River below Iron Gate (KRBI), January 2005 - December 2010. High KRAC samples were not adjusted to account for hydropower peaking effects. Note: to reduce the y-axis scale, a value of 120 on 6/30/2008 at KRAC was reduced to 90.

3.4.1.2 Major Taxonomic Groups and Species Composition

Cyanophyta

As expected based upon previous observations of large blue-green algal blooms in the reservoirs, the longitudinal trend in both total biovolume and percent biovolume of the Cyanophyta increased substantially through the reservoirs and below at KRBI (Figure 17 and Figure 18). For the June-October period median and upper quartile biovolume values were 10x to >50x higher at CR01 and IR01 than they were at KRAC, and were 7-13x higher at KRBI, below Iron Gate (Table 2). The trend in Cyanophyta percent composition was also pronounced through the reservoir complex, with upper quartile levels increasing from ~10% at KRAC to ~90% at CR01 and IR01 and >75% at KRBI (Figure 18). These trends in the upper distribution indicate that periodic high values of both biovolume and percent biovolume of Cyanophyta occurred in the reservoir complex and below relative to stations directly upstream. The dominant Cyanophyta species in the reservoirs were *Aphanizomenon flos-aquae* (APFA) and *Microcystis aeruginosa* (MSAE) (Table 3).

Other dominant groups

As expected as the system changed from the riverine environment of the Klamath River to the lacustrine environment of the reservoirs, a reverse trend to that noted for the Cyanophytes occurred for the Diatoms. Diatoms decreased in prevalence from KRAC to the in-reservoir stations and at KRBI (Figure 17, Figure 18, and Table 2). Diatoms comprised ~80% of the composition at KRAC in June-October, with median values decreasing substantially to ~50% at KRBI. Other major taxonomic groups that increased in prevalence in the reservoirs were the Cryptophyta (cryptophytes) and, to a lesser extent, Chlorophyta (green algae). As with the Cyanophyta, the species in these groups (e.g., *Cryptomonas erosa* and *Rhodomonas minuta*) tend to be more lacustrine. Relative to diatoms and the Cyanophyta, the Euglenophyta (euglena), Pyrrophyta (dinoflagellates), and Chrysophyta (golden algae) comprised a very minor portion of the overall biovolume at all stations.

3.4.2 Seasonal Trends

3.4.2.1 Reservoir Stations: Major Taxonomic Groups and Species/Generic Composition

Seasonal trends for major taxonomic groups at each measured depth at open water reservoir stations are shown in Figure 24 and Figure 25. As expected based on the above June-October analyses, Cyanophyta biomass and composition increased beginning in June and continued into October in both reservoirs. Peak cyanophyte biovolume and percent composition tended to occur between August and September, with early (January through May/June) and later season (October/November through-December) phytoplankton dominated by diatoms and cryptophytes, with some chlorophytes and chrysophytes.

As expected based on expected water column light attenuation, overall biovolume decreased with increasing depth. The biomass and percent composition of the cyanophytes was highest at surface (0-0.1m) samples, remained relatively high at 0.5-1m, and although the peak was more contracted there was continued prevalence even at depths of 5m and the 0-8m depth integrated samples. In general, diatoms and cryptophytes, and occasionally chlorophytes, showed increased dominance at depths of 5m, but there were significant periods during the season at CR01 and IR01 when cyanophyte dominance was >50% of the total biovolume those depths (Figure 24 and Figure 25).

Table 3. Top ten species (ranked by mean biovolume) for samples in the June – Oct. period of 2005-2010 for each site and depth. The table is intended intent of the table is to provide relative information on the dominant species, not to make precise quantitative comparisons between sites. Note that mean biovolume is strongly affected by occasional extremely high values (for example GTEC was only abundant at IR01, IRCC and IRJW in 2005, but high concentrations resulted in it being a top-10 species for the entire 2005-2010 period). See Table 4 for key to species codes.

Station and Depth	N Samples		Species ranked by mean biovolume (mm ³ /L) for samples June 1 - Oct. 31										
			Totals	1	2	3	4	5	6	7	8	9	10
KRAC	79	Species	TOTAL	APFA	COPC	DTVL	MLGR	NZDS	NVTP	CXER	NZFR	RHCU	CCMG
		Mean	0.373	0.093	0.033	0.027	0.027	0.021	0.021	0.013	0.013	0.009	0.008
		Percent	100.0%	25.0%	8.8%	7.1%	7.1%	5.5%	5.5%	3.5%	3.4%	2.5%	2.2%
CRMC 0-0.1m	47**	Species	TOTAL	APFA	MSAE	ABFA	GSHR	NZPL	FRCM	MLVR	GFSB	SNUL	CHXX
		Mean	131.802	73.314	45.083	5.821	1.713	1.469	1.028	0.762	0.467	0.352	0.300
		Percent	100.0%	55.6%	34.2%	4.4%	1.3%	1.1%	0.8%	0.6%	0.4%	0.3%	0.2%
CRCC 0-0.1m	55**	Species	TOTAL	MSAE	APFA	NZPL	CHXX	GTEC	ABFA	ABXX	MLVR	GSHR	AUGR
		Mean	251.190	143.339	89.592	13.045	1.557	1.394	0.265	0.243	0.209	0.208	0.187
		Percent	100.0%	57.1%	35.7%	5.2%	0.6%	0.6%	0.1%	0.1%	0.1%	0.1%	0.1%
CR01 0-0.1m	34	Species	TOTAL	MSAE	APFA	NZPL	CHXX	ABFA	FRCR	CXER	CUMC	NZFR	GSHR
		Mean	15.562	12.236	1.885	0.995	0.242	0.037	0.037	0.036	0.023	0.010	0.009
		Percent	100.0%	78.6%	12.1%	6.4%	1.6%	0.2%	0.2%	0.2%	0.1%	0.1%	0.1%
CR01 0.5-1m	80	Species	TOTAL	APFA	MSAE	NZPL	CXER	MLGR	CHXX	ABFA	STHN	STAM	RDMN
		Mean	2.550	1.716	0.436	0.160	0.061	0.023	0.022	0.017	0.016	0.012	0.010
		Percent	100.0%	67.3%	17.1%	6.3%	2.4%	0.9%	0.9%	0.7%	0.6%	0.5%	0.4%
CR01 8m-Int	36*	Species	TOTAL	APFA	MSAE	CXER	NZPL	MLGR	AUGR	CHXX	STAM	GDXX	ABFA
		Mean	1.032	0.720	0.117	0.045	0.039	0.034	0.009	0.009	0.006	0.005	0.005
		Percent	100.0%	69.8%	11.3%	4.4%	3.8%	3.3%	0.9%	0.9%	0.6%	0.5%	0.4%
KRAI	62	Species	TOTAL	APFA	MSAE	NZPL	CXER	MLGR	AUGR	COPC	FRCR	CHXX	GSHR
		Mean	0.446	0.215	0.078	0.030	0.023	0.019	0.012	0.010	0.006	0.004	0.004
		Percent	100.0%	48.2%	17.6%	6.7%	5.1%	4.4%	2.7%	2.3%	1.4%	1.0%	0.9%
IRCC 0-0.1m	45**	Species	TOTAL	MSAE	GTEC	APFA	SNUL	NZPL	COPC	FRCR	GFSB	SPXX	GSHR
		Mean	9.501	4.647	1.186	1.055	0.583	0.457	0.314	0.232	0.130	0.089	0.077
		Percent	100.0%	48.9%	12.5%	11.1%	6.1%	4.8%	3.3%	2.4%	1.4%	0.9%	0.8%
IRJW 0-0.1m	49**	Species	TOTAL	GTEC	MSAE	NZPL	APFA	COPC	ABFA	SNUL	CHXX	FRCV	FRCN
		Mean	41.853	19.525	17.258	1.223	1.082	0.464	0.404	0.282	0.241	0.181	0.163
		Percent	100.0%	46.7%	41.2%	2.9%	2.6%	1.1%	1.0%	0.7%	0.6%	0.4%	0.4%
IR01 0-0.1m	31	Species	TOTAL	MSAE	APFA	NZPL	CHXX	FRCR	GSHR	TRHS	CXER	GFSB	COPC
		Mean	20.022	15.012	2.834	1.349	0.190	0.132	0.108	0.091	0.057	0.052	0.039
		Percent	100.0%	75.0%	14.2%	6.7%	0.9%	0.7%	0.5%	0.5%	0.3%	0.3%	0.2%
IR01 0.5-1m	76	Species	TOTAL	APFA	MSAE	GTEC	FRCR	MLGR	CXER	NZPL	CJHR	CHXX	ABFA
		Mean	1.672	1.038	0.188	0.097	0.073	0.071	0.064	0.029	0.018	0.017	0.012
		Percent	100.0%	62.1%	11.3%	5.8%	4.3%	4.2%	3.8%	1.7%	1.1%	1.0%	0.7%
IR01 8m-Int	35*	Species	TOTAL	APFA	FRCR	MLGR	MSAE	RPGB	GTEC	CXER	NZPL	EPTR	STHN
		Mean	1.186	0.439	0.154	0.149	0.132	0.098	0.053	0.039	0.023	0.013	0.012
		Percent	100.0%	37.1%	13.0%	12.5%	11.2%	8.3%	4.5%	3.3%	2.0%	1.1%	1.0%
KRBI	120	Species	TOTAL	MSAE	APFA	COPC	MLGR	GSHR	FRCR	SNUL	FRCN	GFSB	DTVL
		Mean	1.781	0.393	0.287	0.240	0.127	0.091	0.087	0.077	0.065	0.045	0.039
		Percent	100.0%	22.1%	16.1%	13.5%	7.2%	5.1%	4.9%	4.3%	3.6%	2.5%	2.2%

* No depth-integrated samples were collected at CR01 and IR01 in 2006 because PacifiCorp did not sample that year. 0-10m depth-integrated samples from 2005 are included with the “0-8m Int” data in the table.

** Shoreline stations (CRCC, CRMC, IRCC, IRJW) not sampled in 2010. In other years, shoreline stations not sampled throughout the entire June-Oct. period, but rather a shorter period that varied by year and station.

Table 4. Key to four-letter species coded used in Table 3.

Species Code	Species Name	Major Taxonomic Group
ABFA	Anabaena flos-aquae	Cyanophyta
ABXX	Anabaena sp	Cyanophyta
APFA	Aphanizomenon flos-aquae	Cyanophyta
AUGR	Aulacoseira granulata	Diatoms
CCMG	Cyclotella meneghiniana	Diatoms
CHXX	Chlamydomonas sp	Chlorophyta
CJHR	Ceratium hirundinella	Pyrrophyta
COPC	Cocconeis placentula	Diatoms
CUMC	Coelastrum microporum	Chlorophyta
CXER	Cryptomonas erosa	Cryptophyta
DTVL	Diatoma vulgare	Diatoms
EPTR	Epithemia turgida	Diatoms
FRCM	Fragilaria capucina mesolepta	Diatoms
FRCN	Fragilaria construens	Diatoms
FRCR	Fragilaria crotonensis	Diatoms
FRCV	Fragilaria construens venter	Diatoms
GDXX	Glenodinium sp	Pyrrophyta
GFSB	Gomphonema subclavatum	Diatoms
GSHR	Gomphoneis herculeana	Diatoms
GTEC	Gloeotrichia echinulata	Cyanophyta
MLGR	Melosira granulata	Diatoms
MLVR	Melosira varians	Diatoms
MSAE	Microcystis aeruginosa	Cyanophyta
NVTP	Navicula tripunctata	Diatoms
NZDS	Nitzschia dissipata	Diatoms
NZFR	Nitzschia frustulum	Diatoms
NZPL	Nitzschia palea	Diatoms
RDMN	Rhodomonas minuta	Cryptophyta
RHCU	Rhoicosphenia curvata	Diatoms
RPGB	Rhopalodia gibba	Diatoms
SNUL	Synedra ulna	Diatoms
SPXX	Spirogyra sp	Chlorophyta
STAM	Stephanodiscus astraea minutula	Diatoms
STHN	Stephanodiscus hantzschii	Diatoms
TRHS	Trachelomonas hispida	Euglenophyta

CR01

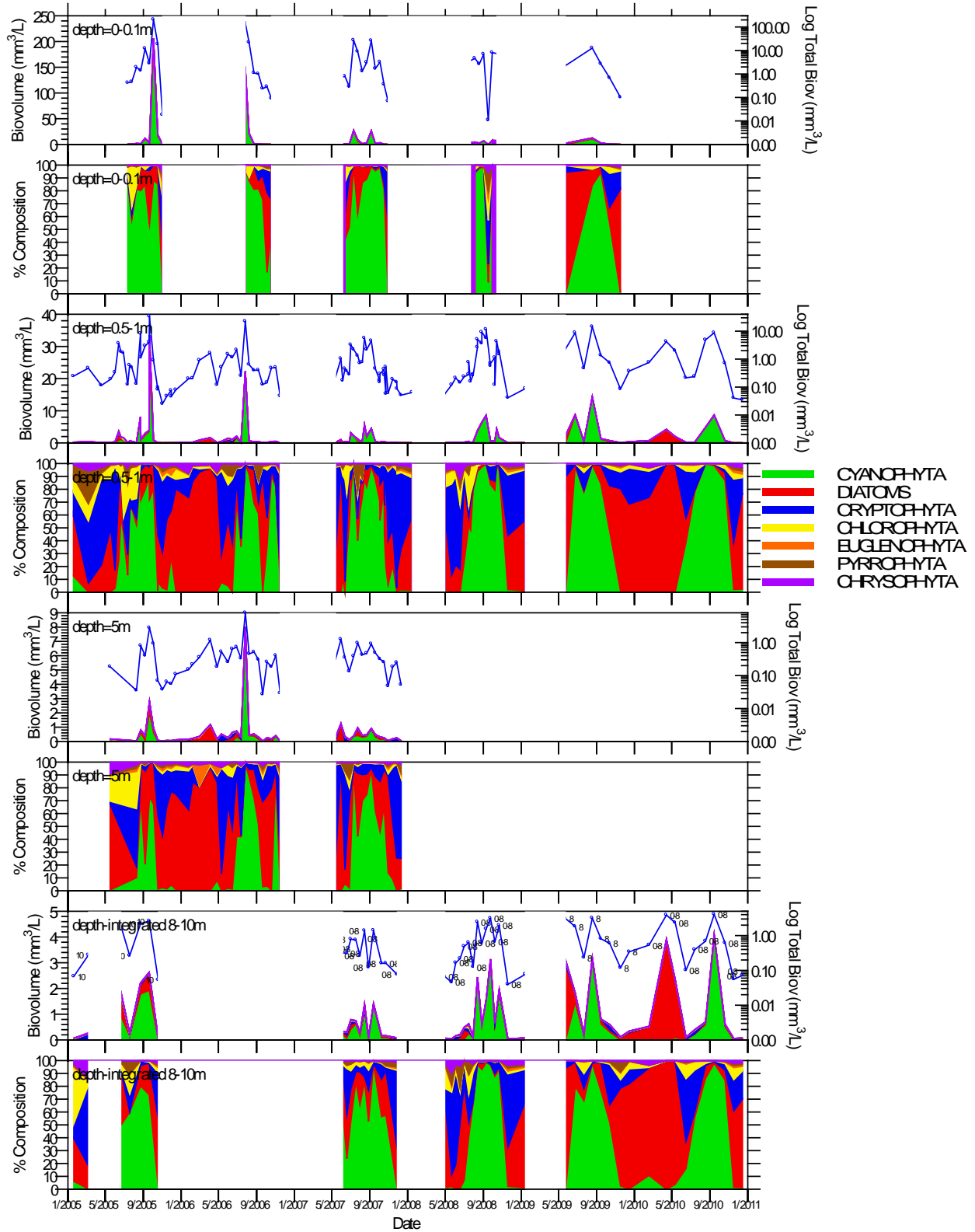


Figure 24. Biovolume and percent biovolume of major phytoplankton taxonomic groups at measured depths for reservoir station CR01, 2005-2010. Notes: 1) the total biovolume (blue line) is shown with a log scale on the right axis, and 2) labels for depth 8-10m depth-integrated panel denote the depth over which the sample was collected.

IR01

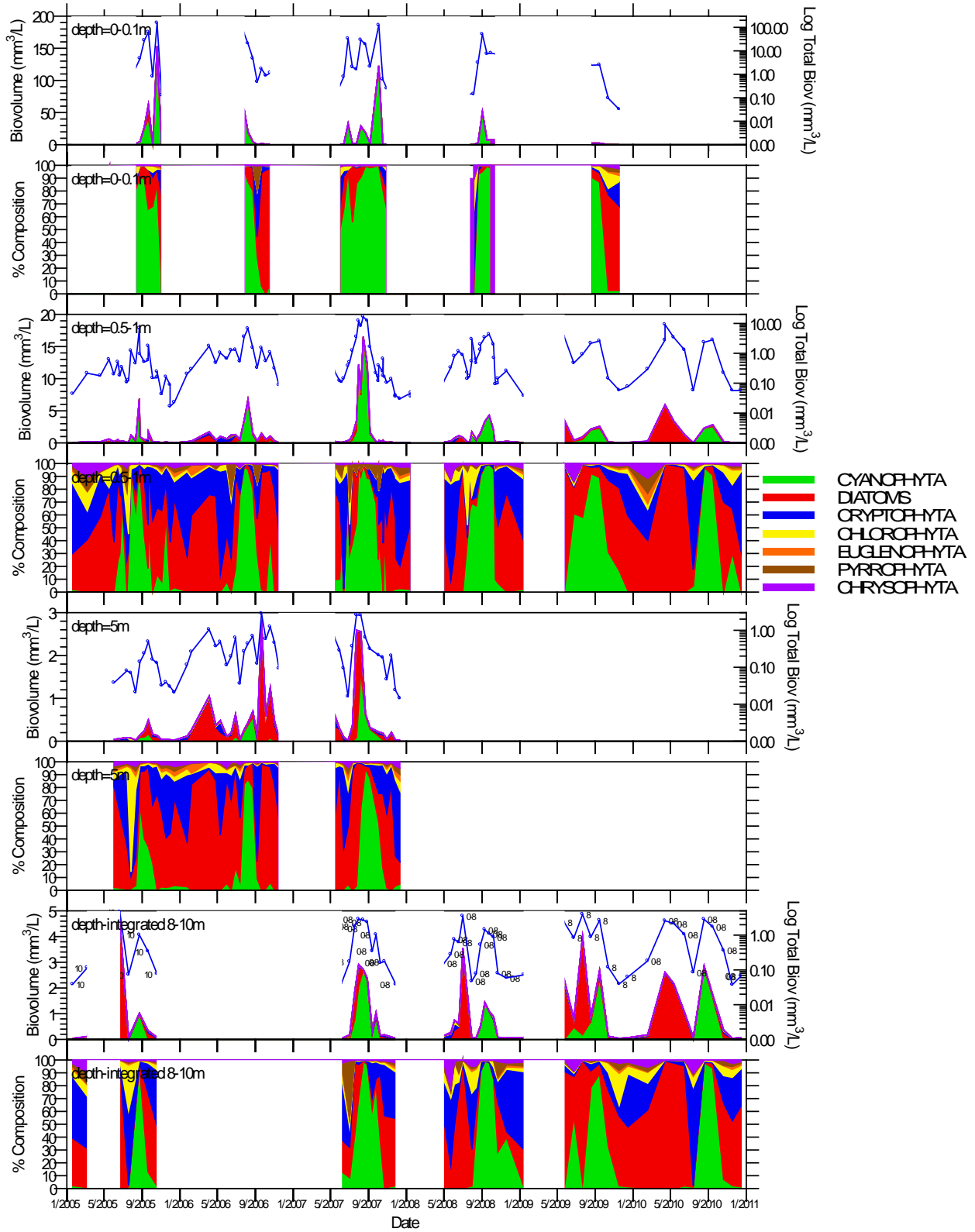


Figure 25. Biovolume and percent biovolume of major phytoplankton taxonomic groups at measured depths for reservoir station IR01, 2005-2010. Notes: 1) the total biovolume (blue line) is shown with a log scale on the right axis, and 2) labels for depth 8-10m depth-integrated panel denote the depth over which the sample was collected.

These data clearly show that overall biovolume as well as biovolume and percent composition of cyanophyte species can remain high (relative to inflow quantities) even at reservoir depths significantly below the surface. This trend is confirmed by chlorophyll data which also showed elevated values at depths $\geq 5\text{m}$ (Figure 26). Peak values at 5 m during the July-September period were greater than many times higher than inflow values at KRAC (see Figure 21). For CR01 (and IR01 to a lesser extent), values exceeded $10\ \mu\text{g/L}$ for much of August-September in 2005-2007 (the only years in which 5 m samples were collected). Depths $\geq 13\text{ m}$ were sampled in only some years (portions of 2005 and 2008-2010) but available data typically showed very low chlorophyll throughout the stratified period season, with the notable exception of June-July 2008 at both CR01 and IR01 when chlorophyll exceeded $15\ \mu\text{g/L}$ for several consecutive sample periods. In addition, higher chlorophyll values were detected at $\geq 13\text{ m}$ during April 2010 during a diatom bloom.

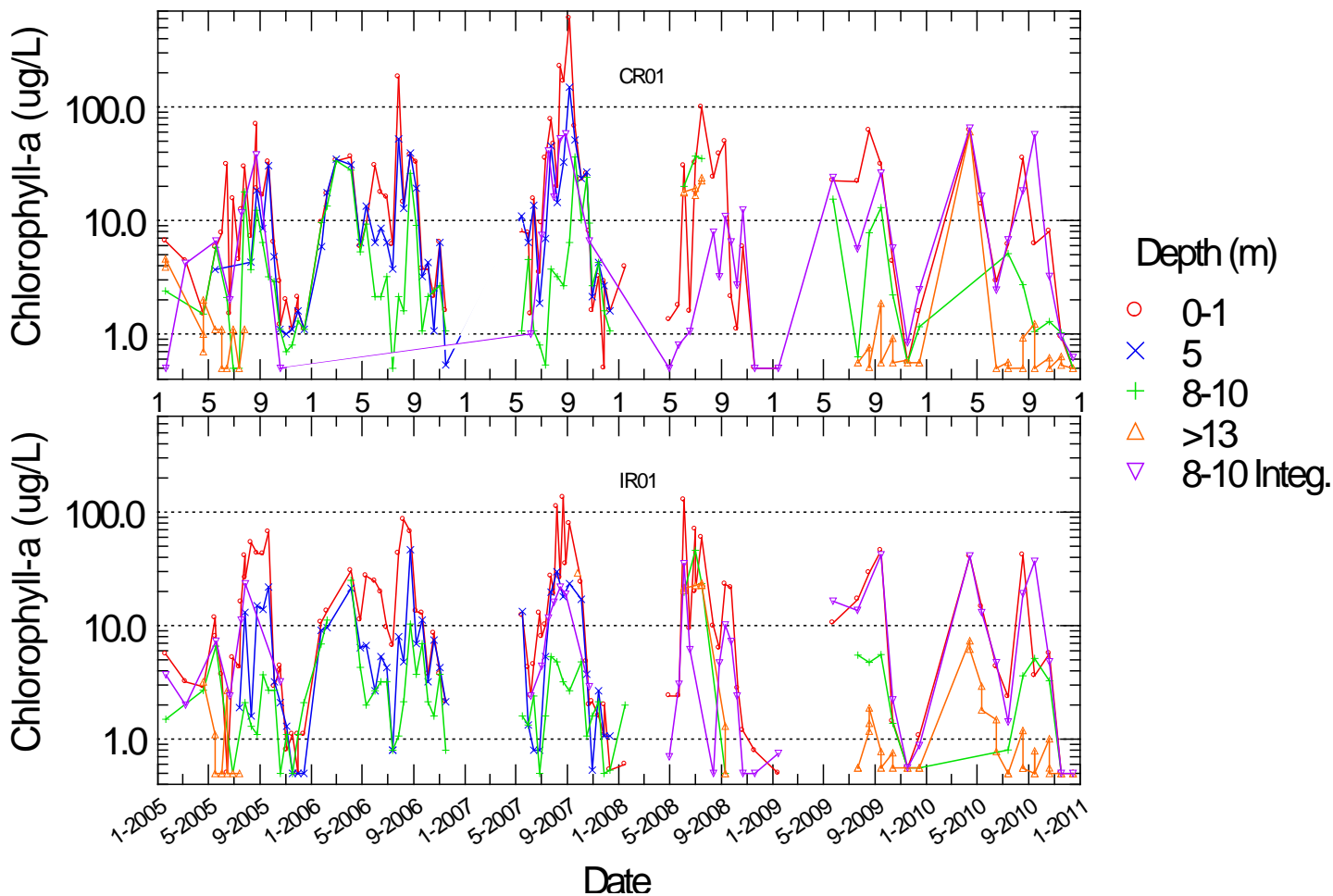


Figure 26. Chlorophyll *a* at measured depths for reservoir stations CR01 and IR01, 2005-2010. To reduce y-axis and improve legibility, all values less than 0.5 are set to 0.5.

Seasonal trends for dominant species/genera are shown for the main reservoir stations CR01 and IR01 (Figure 27-Figure 28). The intent of this section is not to provide detailed information on individual species, but rather to determine those species that comprise the major taxonomic groups described in the above figures.

The dominant June-October 0-0.1 m and 0.5-1 m species in Copco Reservoir were typically *Aphanizomenon flos-aquae* (APFA) and *Microcystis aeruginosa* (MSAE), with MSAE showing both greater biomass and composition at the surface depth except in 2008 (Figure 27). Prior to the period of major cyanophyte dominance that usually began in June or July, early season composition was dominated by *Cryptomonas* (Cryptophyta) and the diatoms *Stephanodiscus* and *Asterionella formosa* at the 0.5-1 m depth. *Cryptomonas*, along with diatoms such as *Stephanodiscus*, *Nitzschia*, and *Melosira*, increased in importance during the fall months. Although relative biovolume was much lower, APFA and MSAE were still present and constituted relatively high percentages of the composition at the 5 m depths.

At IR01, MSAE was generally less prevalent relative to CR01 at all depths (Figure 28). Exceptions where MSAE was greater at IR01 than CR01 included higher peak biomass in 2007 and 2008 in surface samples, and higher percent composition at all depths in 2005. Peak APFA biomass was generally lower at all depths in IR01 than CR01, except in 2007. Other differences between IR01 and CR01 include the bloom of the cyanophyte *Gloeotrichia echinulata* (GTEC) during mid-July to early September in 2005 only, primarily at the 0.5-1m depth. Seasonal pattern in Iron Gate included spring-early summer dominance by *Cryptomonas* and diatoms (e.g., *Stephanodiscus*, *Melosira* and *Fragilaria*), summer dominance by the Cyanophyta (e.g., *Aphanizomenon*, *Microcystis*, *Anabaena*, and *Gloeotrichia*) near the surface and *Nitzschia* at deeper depths, and fall dominance by *Cryptomonas* and the diatoms *Asterionella formosa*, *Melosira*, and *Fragilaria* (Figure 28). These figures also confirm that relevant (i.e., with respect to toxic and eutrophic species) blue-green algal species are not only relegated to surface depths.

CR01

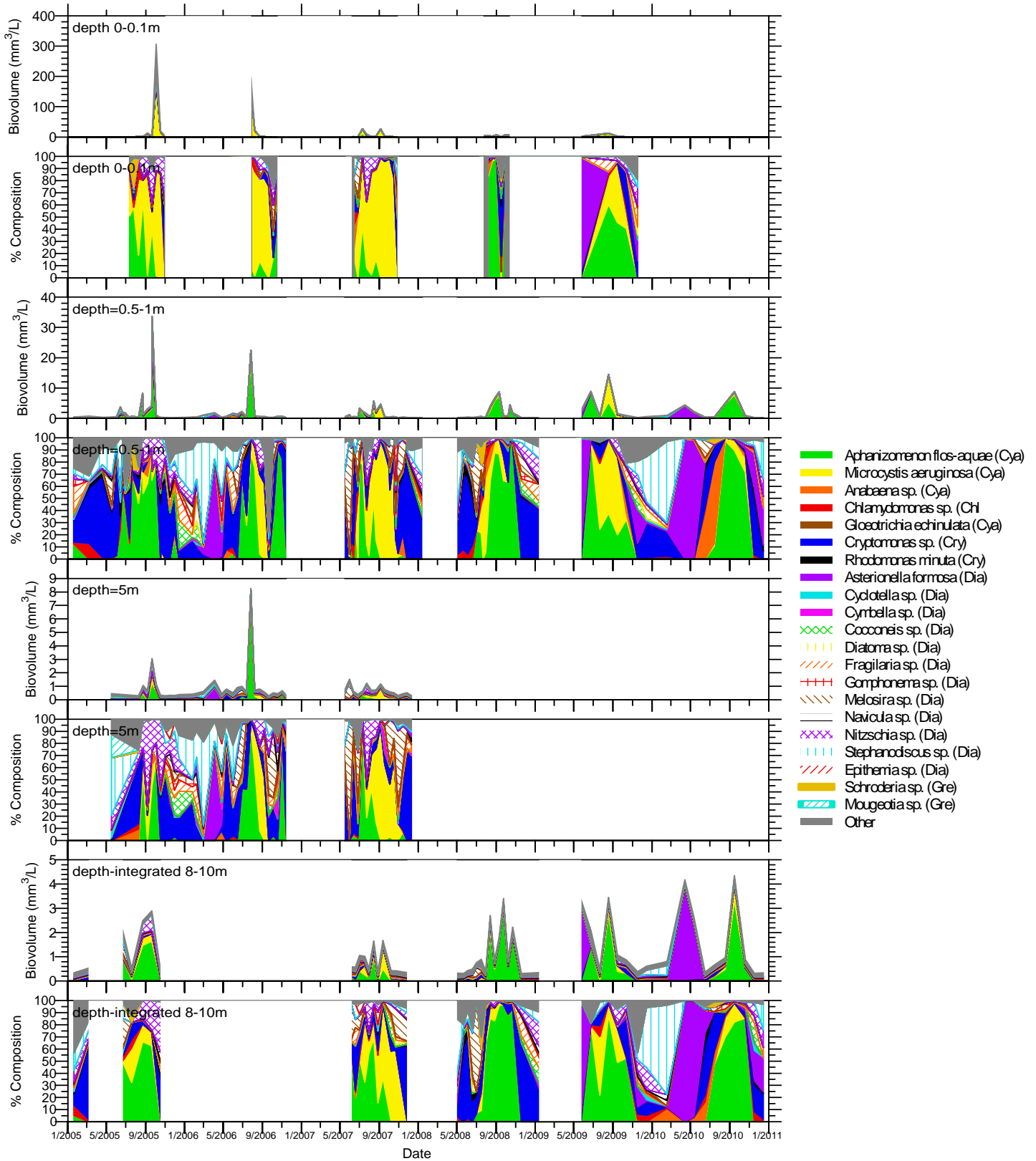


Figure 27. Biovolume and percent biovolume of dominant species of phytoplankton at measured depths for reservoir station CR01, 2005-2010.

IR01

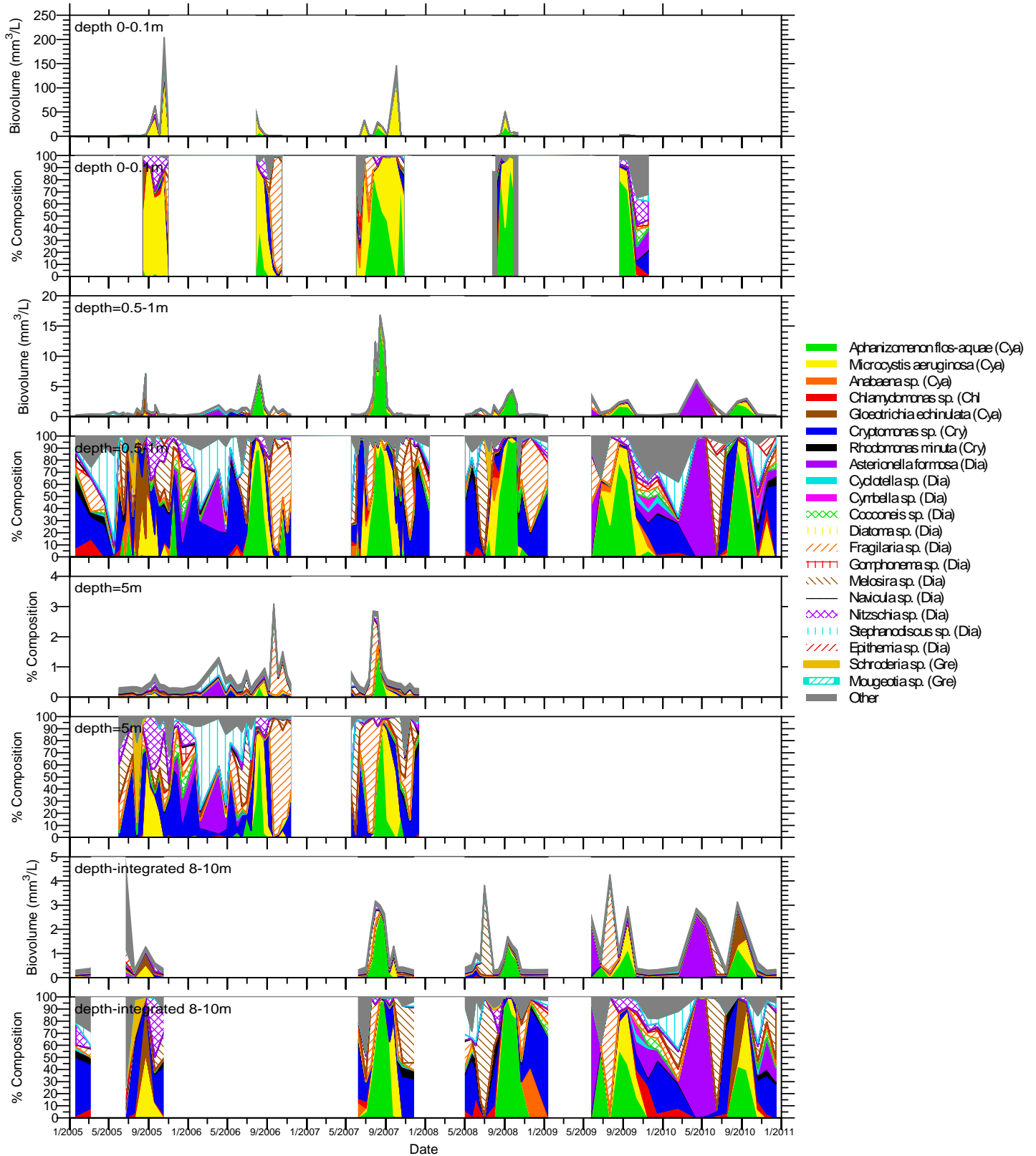


Figure 28. Biovolume and percent biovolume of dominant species of phytoplankton at measured depths for reservoir station IR01, 2005-2010.

3.4.2.2 River Stations: Major Taxonomic Groups and Species/Generic Composition

Seasonal trends of major taxonomic groups for the three river stations (KRAC, KRAI, and KRBI) are shown in Figure 29. In contrast to the reservoirs, aside from occasional cyanophyte peaks, KRAC was dominated by diatoms (Figure 29; top panel). Downstream at KRAI and at KRBI the Cyanophyta increased in importance on a seasonal basis, at times accounting for >50% of the composition. As mentioned above, these values were lower than the in-reservoir upper water column values because water released from the reservoirs is drawn from lower in the water column; as noted previously, release depths are 7 to 9.8 m below the surface in Copco and 4 – 6.4 m in Iron Gate. Seasonal composition trends at these below reservoir stations tended to follow those of reservoir stations directly upstream.

In contrast to the reservoirs, KRAC was dominated by a variety of periphytic or attached diatom genera typical of riverine systems (e.g., *Cocconeis*, *Gomphonema*, and *Navicula*) and other more planktonic diatoms (e.g., *Stephanodiscus* and *Fragilaria*) for the majority of the season, although APFA was frequently present with occasional high levels (Figure 30; top panel). Other commonly observed taxa included *Cryptomonas* and the diatoms *Nitzschia*, *Asterionella formosa*, *Epithemia*, *Gomphonema*, and *Melosira*. Downstream to KRAI and at KRBI, APFA and MSAE increased in importance on a seasonal basis, at times accounting for ~90% of the composition. In addition, the planktonic diatoms *Fragilaria* and *Melosira* increase in dominance below Iron Gate at KRBI. As expected based on trends shown above, seasonal composition at these below reservoir stations tended to follow those of reservoir stations directly upstream. For example, similar to the reservoirs which showed MSAE to be generally more prevalent in Copco than in Iron Gate; these results also show the same trend of increased MSAE below Copco relative to Iron Gate.

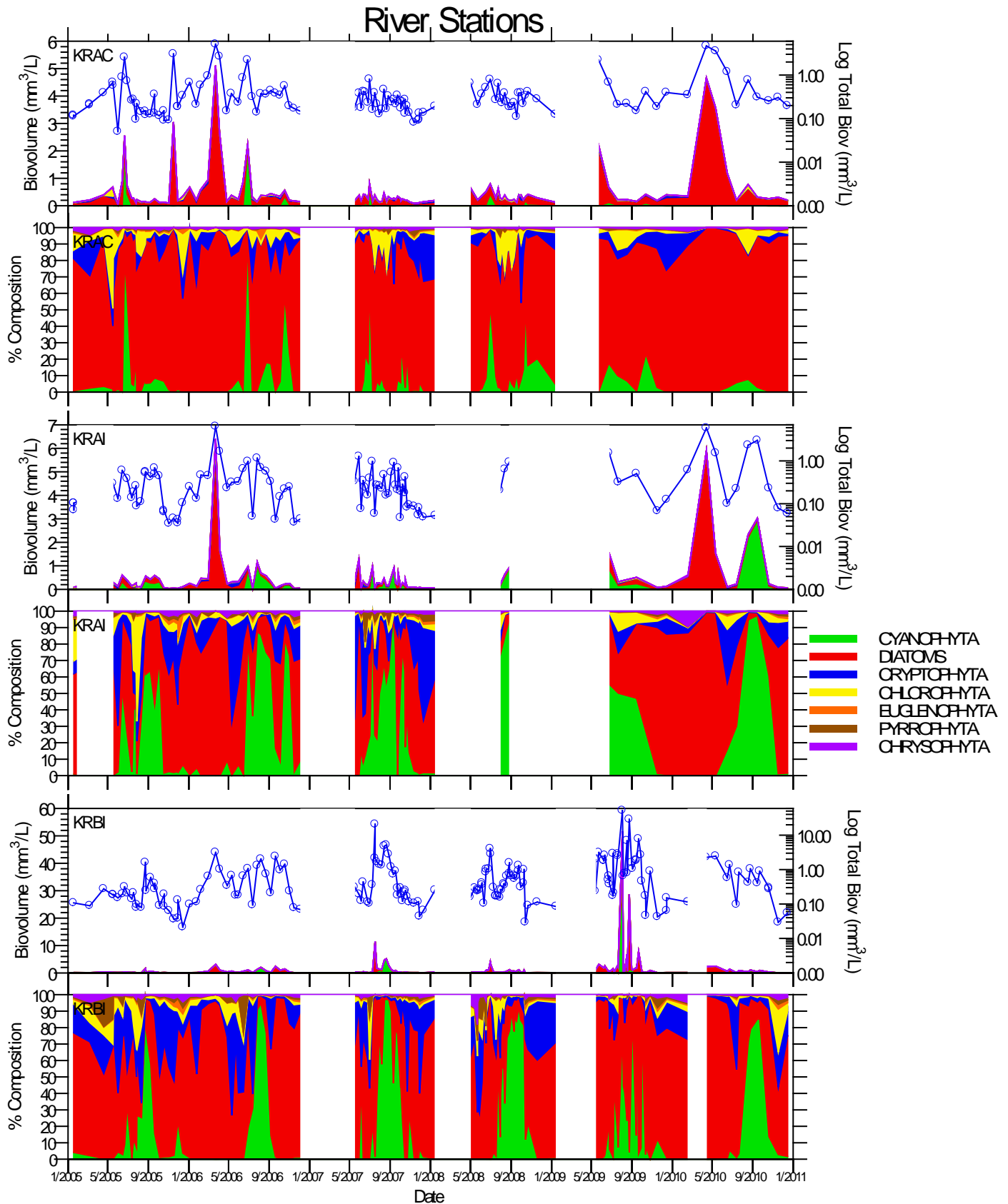


Figure 29. Biovolume and percent biovolume of major phytoplankton taxonomic groups at Klamath River stations KRAC, KRAI, and KRBI, 2005-2010. Note: the total biovolume (blue line) is shown with a log scale on the right axis.

River Stations

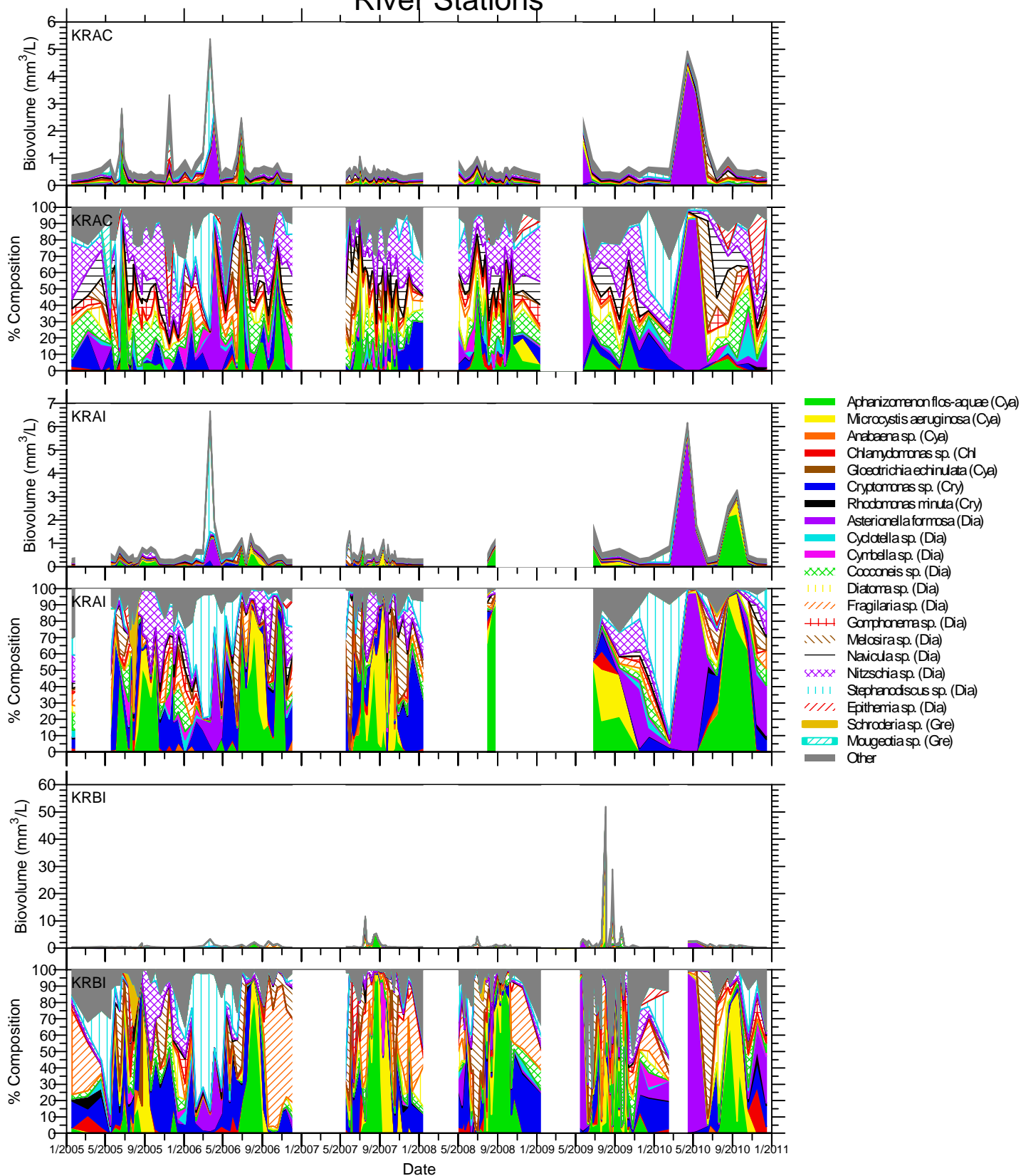


Figure 30. Biovolume and percent biovolume of dominant species of phytoplankton at Klamath River stations KRAC, KRAI, and KRBI, 2005-2010.

3.4.3 Toxic Species and a Comparison of Shoreline Stations and Open-Water Stations

Four shoreline stations were monitored to assess toxic algae for public health purposes. The length of time in which samples were collected at shoreline stations (CRMC, CRCC, IRJW, and IRCC) varied across years and sites; however, August and September were consistently sampled at all four shoreline stations as well as the surface (0-0.1 m depth) of the open water reservoir stations and a comparison of these data (Figure 31 and Figure 32) indicates some trends between stations and depths. Shoreline stations had generally similar taxonomic composition (i.e. dominated by the cyanophytes *Aphanizomenon flos-aquae* (APFA) and *Microcystis aeruginosa* (MSAE) during the summer months) as the surface (0-0.1m) samples at the open water stations (IR01 and CR01) (Figure 31), but peak biomass was much higher (Figure 32). The differences in peak biomass are in part due to differences in sampling methodology. Shoreline samples were collected for public health purposes and always targeted the worst-case scenario scums. Surface samples at open water stations are ambient, not targeted, conditions. Peak biomass of cyanophytes was much higher at Copco shoreline stations CRMC and CRCC than at Iron Gate shoreline stations IRJW and IRCC (Figure 32); that same pattern was also evident but to a lesser degree for percent composition of cyanophytes (Figure 31).

Microcystis percent composition was higher at the 0.1m depth than 0.5-1m depth, especially at sites in Copco Reservoir. Conversely, APFA percent composition was lower at the 0.1m depth than the 0.5-1m depth. Additionally, APFA percent composition was much higher at both depths at the open-water stations than at the shoreline stations. Finally, Iron Gate shoreline stations IRJW and IRCC had a much lower percent composition of APFA (and hence total Cyanophyta) and much higher percent composition of diatoms, than did other sites and depths. There were also some inter-annual trends in percent composition, with MSAE being lower in 2008 than other years. Supplemental plots showing a complete time series of biovolume and percent biovolume at shoreline stations is available in Appendix E.

MSAE was much more prevalent at KRBI than at KRAC and concentrations were higher (Figure 33). MSAE was detected in only 3 of 123 samples for all dates at KRAC, with no detections in the June-September period (detections: 10/3/2007 , 10/4/2007, and 11/19/2008).

Anabaena (identified by the laboratory as *Anabaena flos-aquae* or *Anabaena* sp.) is another toxic species detected in the reservoirs during the study period; however, it was much less common than MSAE. For example, MSAE had the highest or second-highest mean biovolume for June-October periods 2005-2010 of any species at the 0-0.1m and 0.5-1m depths for all shoreline and open-water stations in Iron Gate and Copco Reservoirs, while *Anabaena* was in the top 10 species at only three sites/depths: shoreline stations CRCC (#6), CRMC (#3), the 0.5-1m depth for IR01 (#10) (Table 3).

Median Biovolume of Cyanophytes and Other Major Phytoplankton Taxa, Aug-Sept

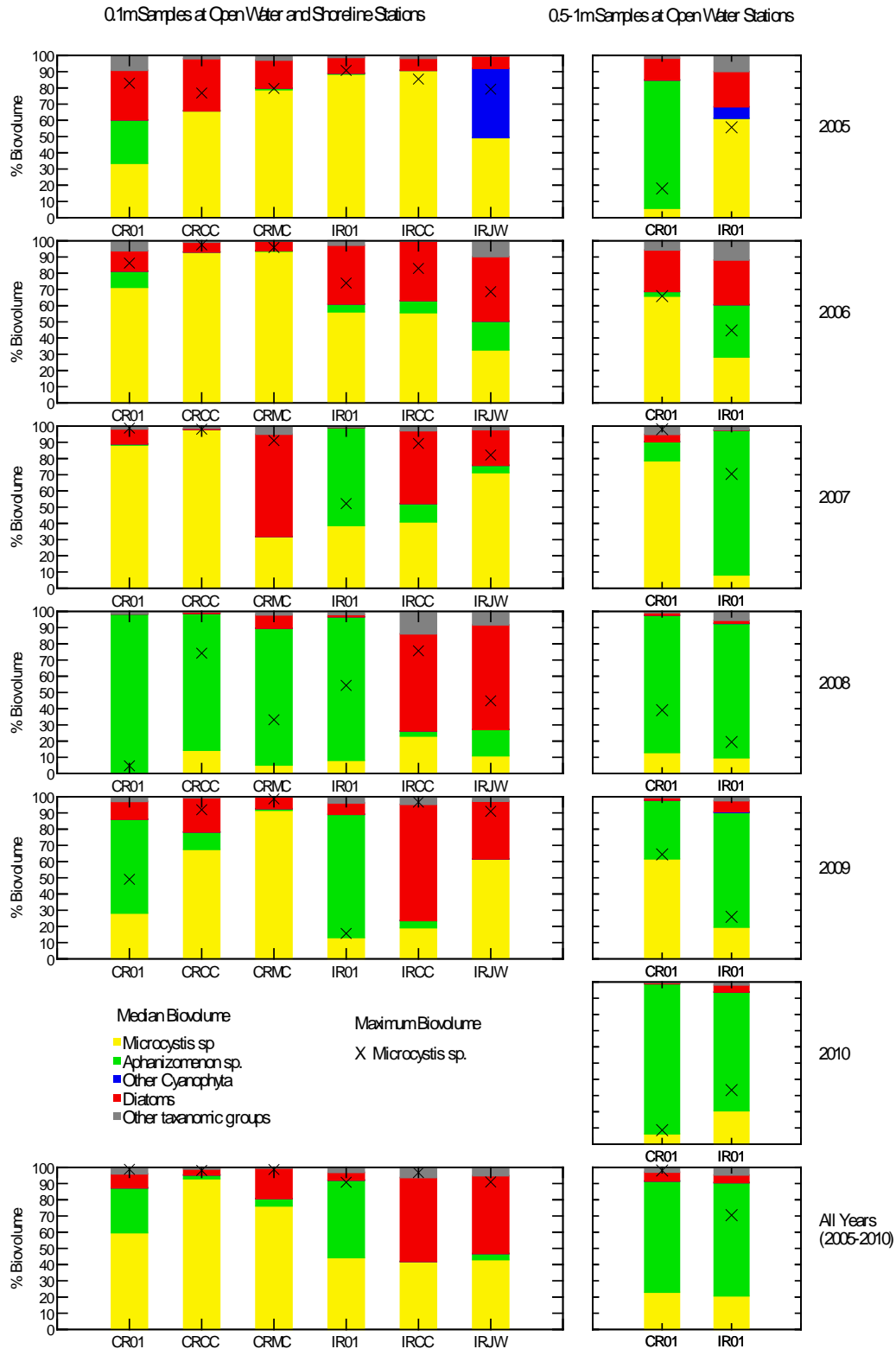


Figure 31. Median percent biovolume of *Microcystis* (MSAE), *Aphanizomenon* (APFA), diatoms, other Cyanophyta, and other taxonomic groups for August and September 2005-2010 surface (0.1 m depth) (left panel) samples at shoreline stations (CRMC, CRCC, IRCC, and IRJW) and open water stations (CR01 and IR01), as well as the 0.5-1m depth for open-water stations (right panel). The highest individual sample percent biovolume *Microcystis* is also shown for each station and time period (x symbol).

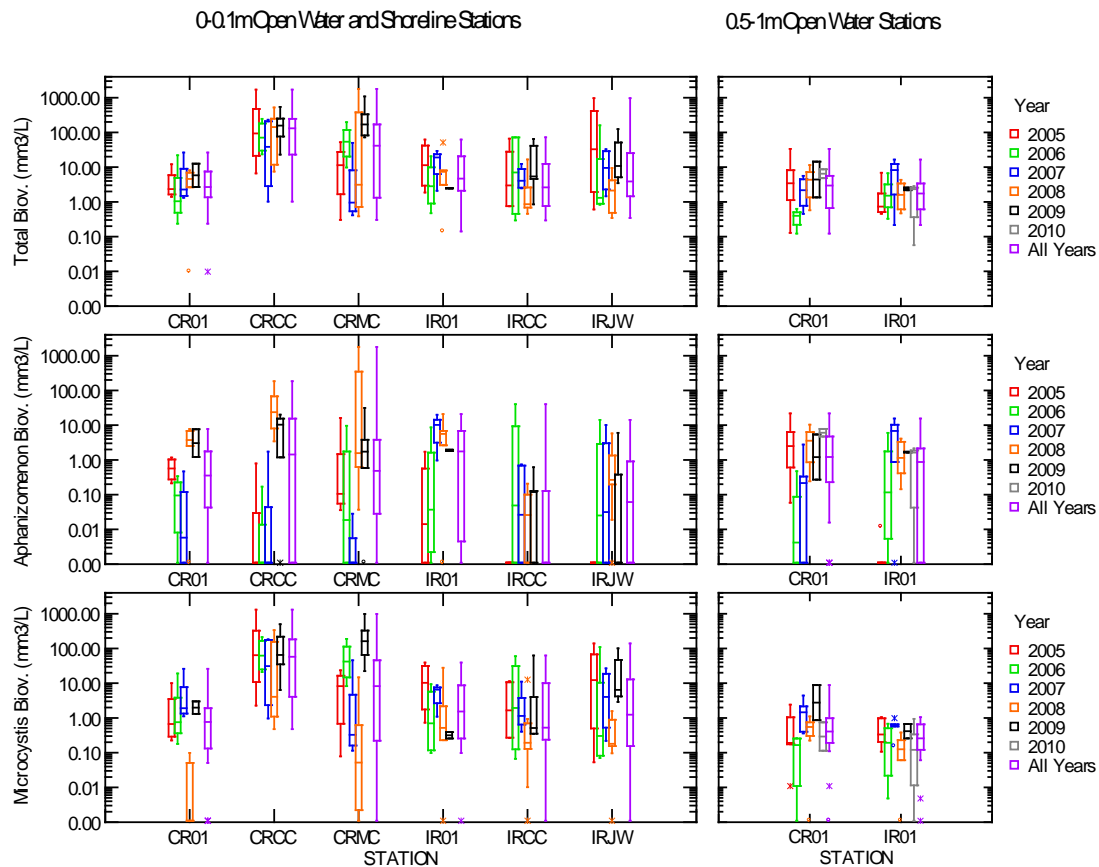


Figure 32. Total biovolume, *Microcystis aeruginosa* (MSAE) biovolume, and *Aphanizomenon flos-aquae* (APFA) biovolume for August and September 2005-2010 surface (0.1 m depth) (left panel) samples at shoreline stations (CRMC, CRCC, IRCC, and IRJW) and open water stations (CR01 and IR01), as well as the 0.5-1m depth for open-water stations (right panel).

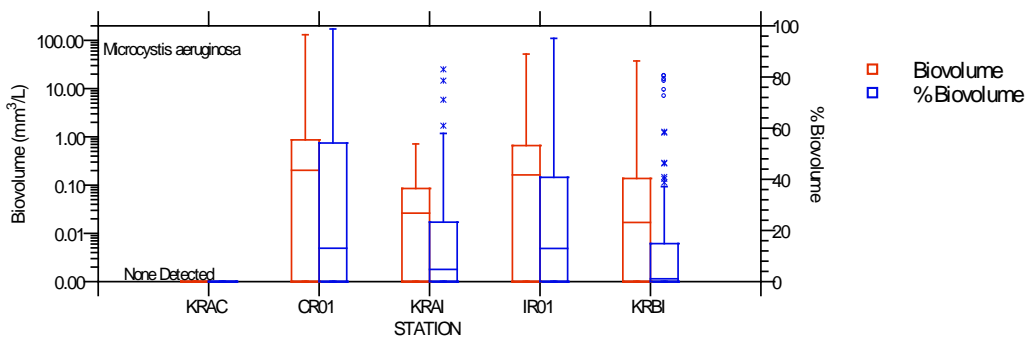


Figure 33. Biovolume and percent composition of *Microcystis aeruginosa* (MSAE), 0-1m samples, June-Sept. 2005-2010.

3.4.4 Seasonal Cyanophyta Dynamics and Relationships to Other Variables

Because the 0.5-1.0 meter depth was the only depth consistently sampled each year 2005-2010, it provides the best overall comparison for the entire study period. A fairly consistent pattern in seasonal Cyanophyta dynamics at both CR01 and IR01 is that MSAE biomass temporally lags APFA biomass (N-fixer biovolume is primarily comprised of APFA) (Figure 34 and Figure 35). This applies most strongly to the start of the seasonal increase, but also to the peak and to a lesser extent the decline in the fall. The major exception to this trend was in 2008 when the MSAE bloom declined early and APFA not only persisted but accounted for the majority of biomass (e.g., see Figure 27 and Figure 28 above). In addition, a second peak of APFA sometimes occurred in the fall after MSAE subsided.

Nutrients and Phytoplankton Seasonality in Copco Reservoir 2005-2010

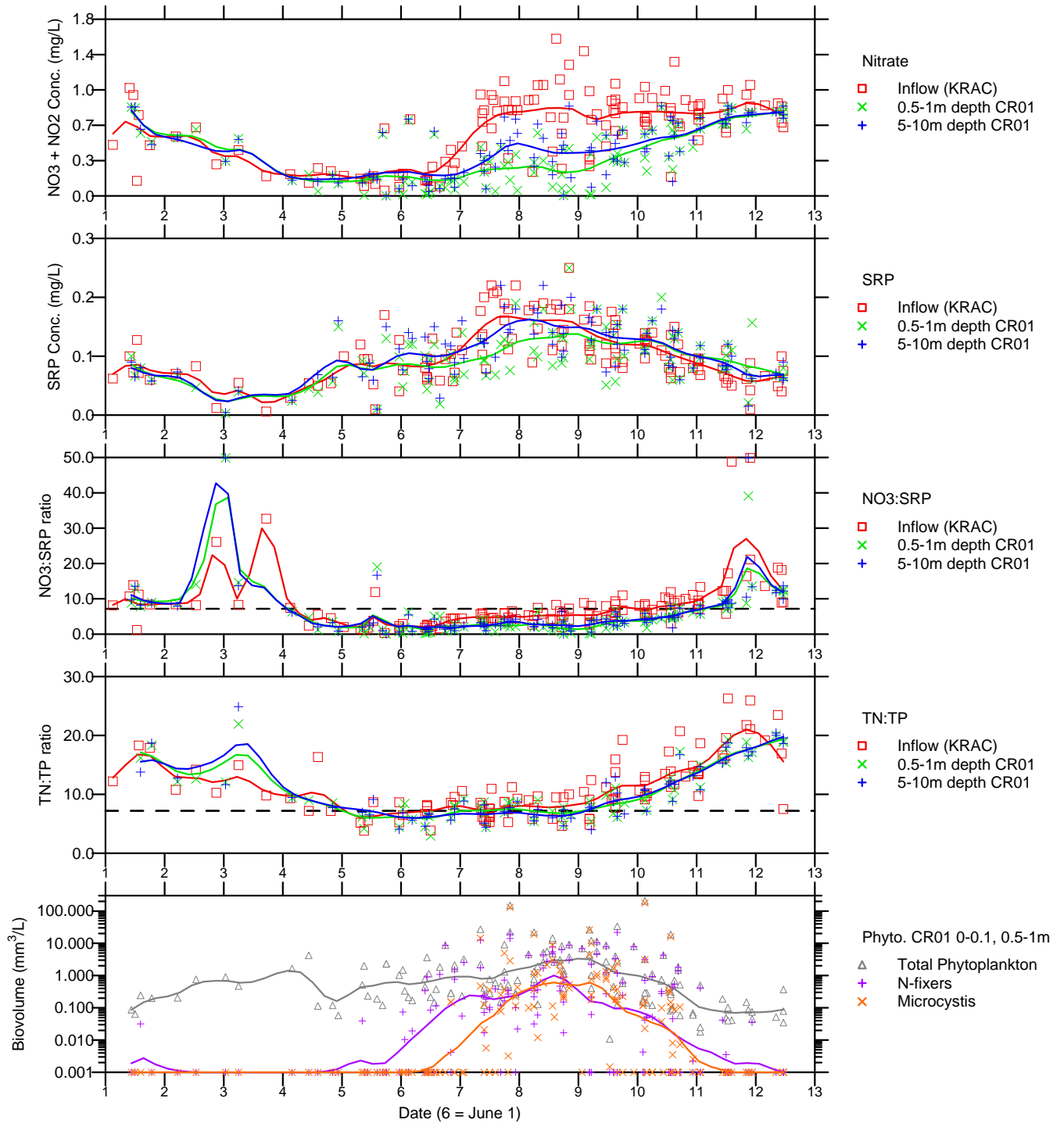


Figure 34. Seasonal trends for nutrient and phytoplankton parameters in the inflow and surface of Copco Reservoir 2005-2010. Parameters include NO₃+NO₂ concentration, SRP concentration, NO₃:SRP ratio, TN:TP ratio, and biovolume of total phytoplankton, nitrogen fixing phytoplankton, and *Microcystis*.

Nutrients and Phytoplankton Seasonality in Iron Gate Reservoir 2005-2010

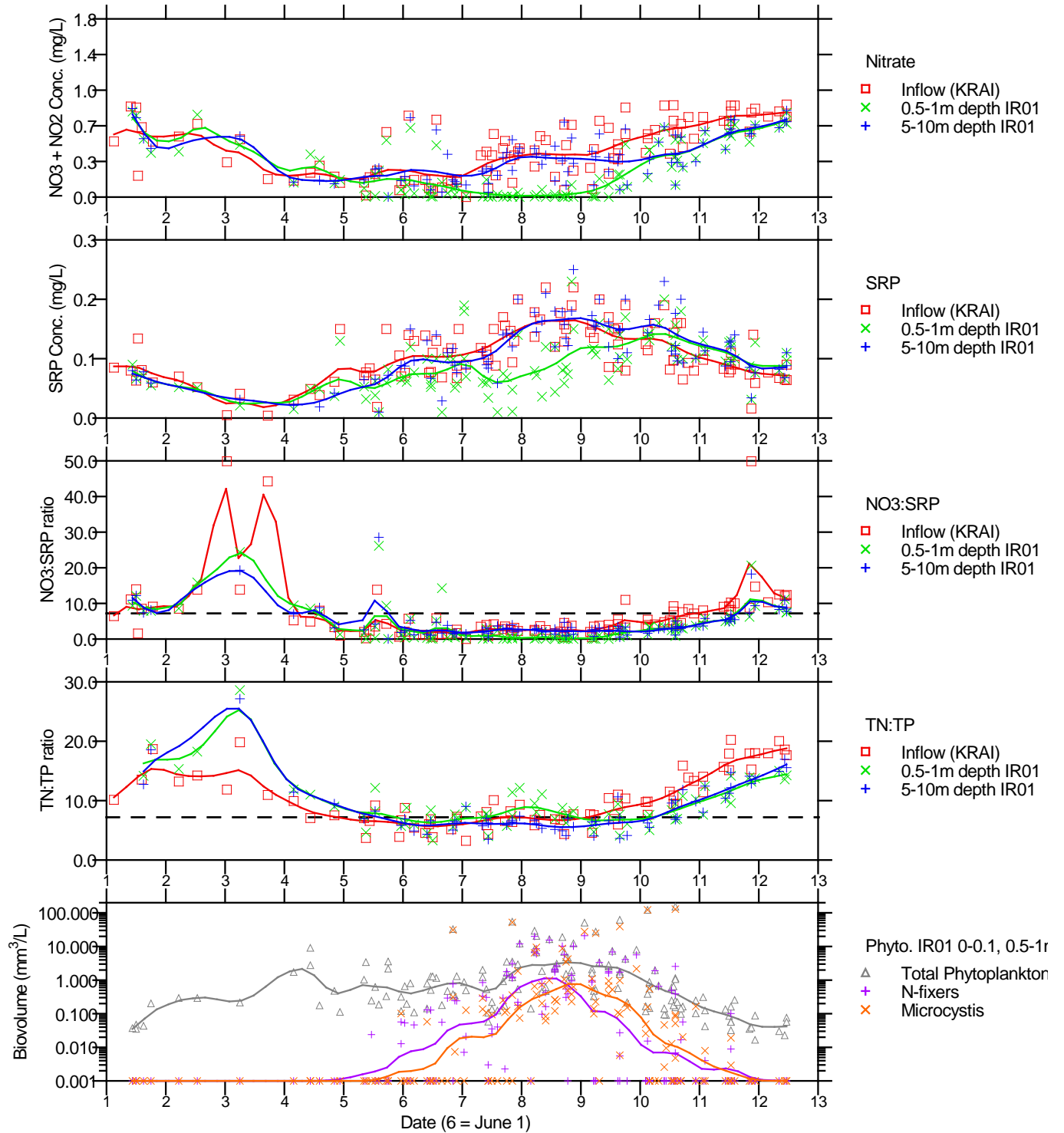


Figure 35. Seasonal trends for nutrient and phytoplankton parameters in the inflow and surface of Iron Gate Reservoir 2005-2010. Parameters include NO₃+NO₂ concentration, SRP concentration, NO₃:SRP ratio, TN:TP ratio, and biovolume of total phytoplankton, nitrogen-fixing phytoplankton, and *Microcystis*.

As shown above in both reservoirs, early season (May-June) biovolume and percent biovolume of APFA increases prior to that of MSAE (Figure 27 and Figure 28; also shown in the river stations below each reservoir in Figure 30). The overall trend indicates that the increase in N-fixer biomass and dominance (comprised mainly of APFA) occurred when inflow nitrate was at seasonal low concentrations, and that MSAE biovolume only began to increase when inflow nitrate increased beginning in about late-June for Copco and early-July for Iron Gate (Figure 34 and Figure 35).

Although inter-annual variability in the timing of both inflow nitrate and onset of MSAE was high (Appendix G), with the exception of 2008 when nitrate did not undergo the typical seasonal depression in late-spring, N-fixers increased during the period of depressed nitrate, and the onset and increase in MSAE consistently lagged that of increased inflow nitrate. Such a trend fits with expected dominance of such nitrogen-fixers as APFA vs. MSAE given that APFA has the ability to fix atmospheric nitrogen while MSAE does not and must have an adequate nitrogen source (such as nitrate or ammonia) present in the water column. In general this trend was even more apparent for percent biovolume than it was for absolute biovolume (Appendix G), indicating that once a certain nitrate threshold was reached initiation of MSAE growth occurred, but after that point absolute biovolume was controlled by other factors.

These trends were explored further by plotting monthly means of the N-fixers and MSAE vs. various nutrient parameters. Due to both the threshold effect of nutrient parameters and high inter-annual variability in the timing of the onset and peak APFA and MSAE biomass and relative dominance¹¹, the somewhat arbitrary monthly cut-off used to compute means made it such with only 6 years of data it was difficult to establish patterns (e.g., often there was the hint of a trend but then one year was a significant outlier). Moreover, additional variability can be induced by a change in sampling frequency from biweekly in 2005-2008 to monthly in 2009 and 2010. It is possible to employ more sophisticated multivariate techniques or to focus more on the timing rather than monthly mean algal or nutrient parameters, but that is beyond the scope of this data compilation effort.

In addition to the nutrient parameters in Figure 34 and Figure 35, TP and TN were also evaluated as independent variables (TIN, TIN:SRP ratio, and NH₄ were not evaluated due to issues with the ammonia detection limit). Dependent variables consisted of chlorophyll-a, N-fixer absolute and relative biovolume, and MSAE absolute and relative biovolume. We generally focused on June and July because these are the months when initiation of blue-green algal blooms typically occurs as well as the transition from N-fixers to MSAE. It is important to note that only apparent relationships are discussed below, and that relationships were not discerned for other combinations of parameters or months. For example, variability in June was such that no relationships were determined for either Copco or Iron Gate for any of the combinations, including those for inflow and in-reservoir nutrients.

In general relationships were more apparent for in-reservoir scatter plots than they were for inflow scatter plots (Figure 36 through Figure 38). For TP there was a tendency towards a positive relationship between TP and Chlorophyll for July (Copco only), August (Iron Gate only) and September (Figure 36). Positive relationships were also observed between TP and MSAE biovolume in July (for Copco only) and August (Iron Gate only); between TP and N-fixer biovolume in August (Iron Gate only), and

¹¹ As indicated, the relative availability of a nutrient may control dominance of one species over another, particularly when N-fixers vs. non N-fixers are competing, but the absolute biomass may be impacted by many other factors (e.g., water temperature, mixing, and light), and once a certain concentration threshold is reached that particular nutrient may no longer be limiting. These factors can cause the stronger observed effect to be on timing and dominance rather than absolute biomass.

between TP and MSAE relative biovolume in September (both reservoirs)¹². These relationships indicate the role of TP in controlling both total algal biomass as well as biomass of N-fixers and MSAE. However, one of the stronger apparent relationships that existed in both reservoirs was between TP and relative MSAE biomass in September, indicating the potential importance of phosphorus in dictating relative MSAE biomass.

In-reservoir trends for July, the period of typical MSAE onset, included positive relationships between both SRP and NO₃ and relative MSAE biovolume in Copco Reservoir, and conversely a negative relationship between these parameters and relative N-fixer biomass in Copco Reservoir (Figure 37 and Figure 38). For Iron Gate Reservoir these relationships were less apparent, although the direction of the trend lines (positive for SRP and relative MSAE biovolume and negative for SRP and relative N-fixer biovolume) were similar to Copco Reservoir. No relationships were observed between these parameters and absolute biomass in July.

Despite the observation that MSAE development occurred subsequent to the increase in inflow NO₃ (Appendix G), attempts to determine trends in inflow nutrients and algal parameters in July only showed a relationship between NO₃ and MSAE relative biovolume in Iron gate (Figure 38). As noted above, the lack of more consistent relationships between inflow nitrate and MSAE is due to the lag between increasing inflow concentration and the onset in the reservoirs. However, similar to the in-reservoir trends, a positive relationship between inflow (KRAC and KRAI) SRP and relative MSAE biovolume in Copco and Iron Gate was observed (Figure 37). Also similar to the July in-reservoir negative relationship between SRP and N-fixer relative biovolume, KRAC SRP was also inversely related to relative N-Fixer biovolume (Figure 37).

Although as noted above these investigations are preliminary, they indicate that both NO₃ and SRP are important drivers of MSAE dominance in Copco and Iron Gate reservoirs. Both higher NO₃ and higher SRP were associated with increased July dominance of MSAE in Copco Reservoir, indicating that not only was NO₃ necessary for the non-nitrogen fixing MSAE to increase in importance but that increased SRP was further associated with increased MSAE dominance. In-reservoir control of MSAE biomass by both nitrogen and phosphorus was noted by Moisander et al. 2009), who showed frequent co-limitation by these nutrients.

Relationships with inflow SRP also indicate that relative supply of SRP to the reservoirs may explain year-to-year dominance patterns of MSAE and N-fixing algae. As expected based on lag-time between increasing inflow NO₃ and the onset of MSAE apparent in the graphical analysis, the scatter plots did not show a trend between inflow NO₃ and MSAE. However, as noted above the presence of NO₃ was a prerequisite for the transition from N-fixers to MSAE.

This phenomenon likely explains the increased presence of MSAE in Copco and Iron Gate reservoirs, relative to Upper Klamath Lake upstream. In Upper Klamath Lake, the nitrogen-fixing APFA dominates the May through October growing season while inflow nitrogen sources remain low throughout that entire time period (Kann 2010), with low levels of MSAE only occurring later in the season (although never dominating) when internally generated nitrogen sources become available.

¹² Whether an apparent trend could be identified in Figures 35-37 was not based only on the direction of the distance weighted least squares (DWLS) fitted curve, but also whether the curve was robust with respect to removal of one or more points. Thus, scatter plots where one or both systems showed apparent trends are highlighted in Figure 36 through Figure 38. For example, although both Copco and Iron Gate appear to show a positive trend between TP and Chl in July (Figure 36), only Iron Gate was robust to the criteria used (removal of 2007 for Copco clearly obviates the relationship). Further statistical testing of the observed relationships could be performed but is beyond the scope of this preliminary analysis.

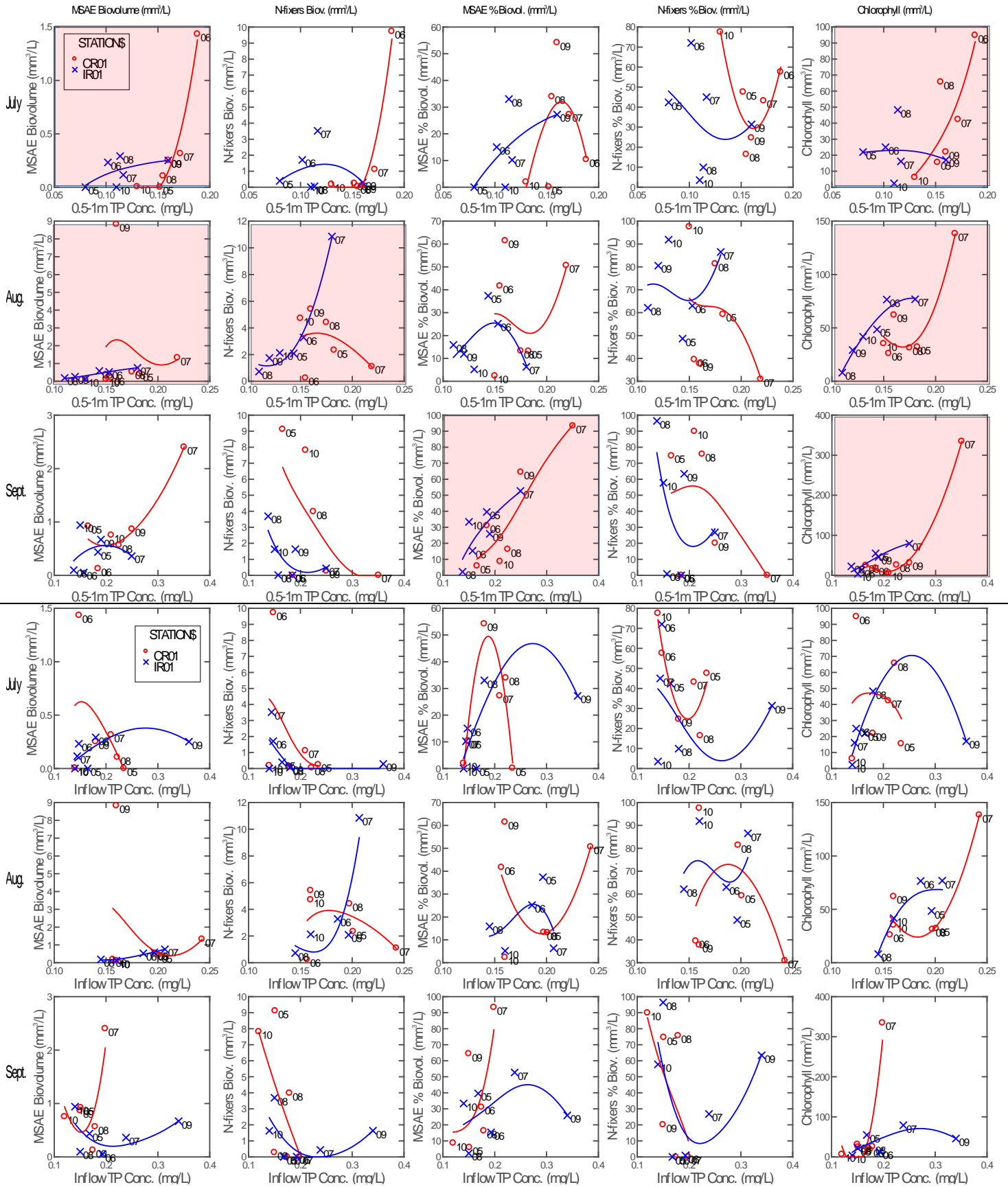


Figure 36. Relationships between TP concentration and algal response variables for Copco (red) and Iron Gate Reservoirs (blue), arranged in rows (months July-Sept) and columns (response variables). Each point is monthly mean, labeled by year (05=2005). X-axis: upper 3 rows are TP conc. of 0.5-1m reservoir samples, lower 3 rows are TP conc. of reservoir inflow. Y-axis: biovolume and % biovolume of MSAE and N-fixing species (left 4 columns) and chlorophyll (right column).

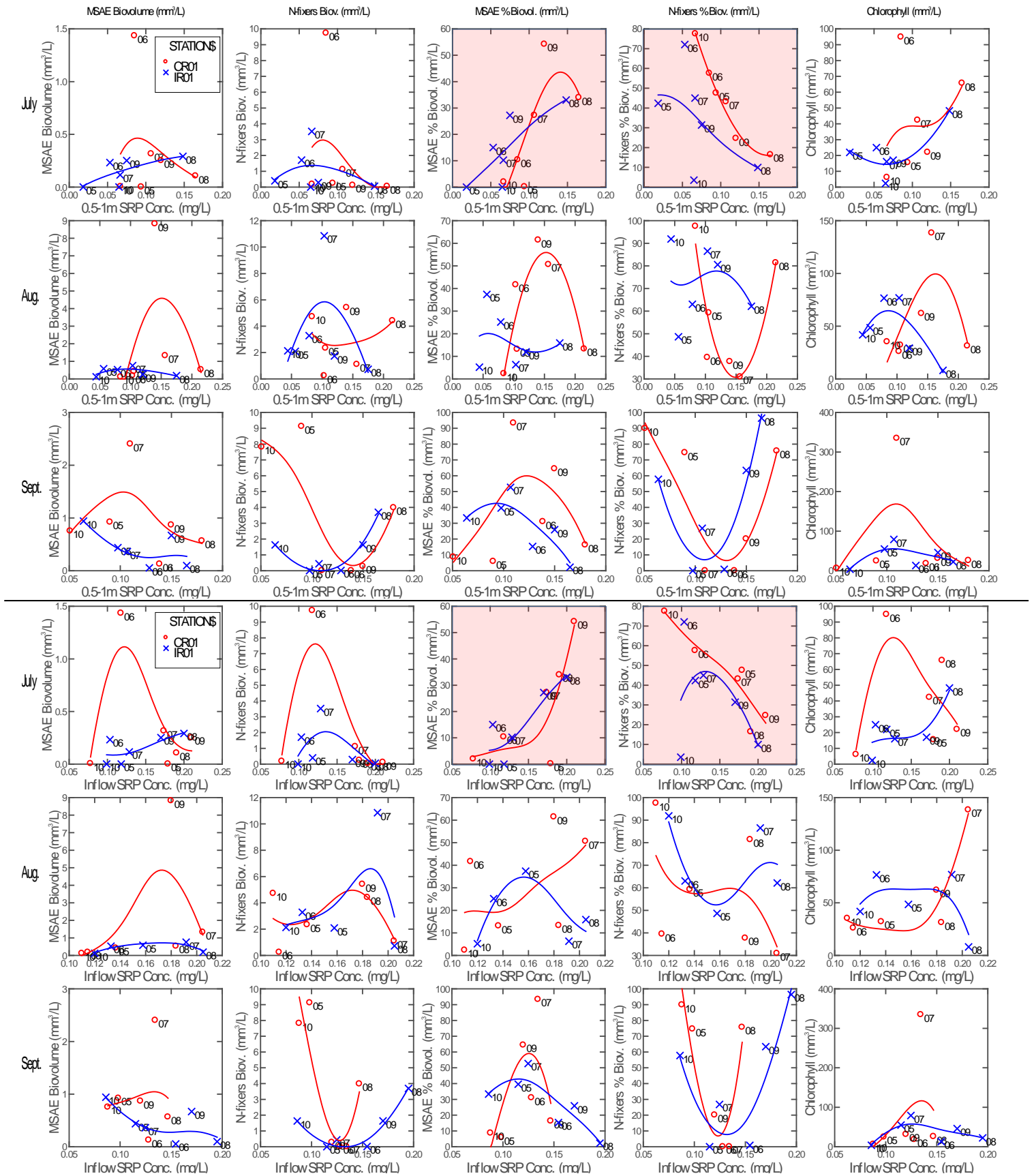


Figure 37. Relationships between SRP concentration and algal response variables for Copco (red) and Iron Gate Reservoirs (blue), arranged in rows (months July-Sept) and columns (response variables). Each point is monthly mean, labeled by year (05=2005). X-axis: upper 3 rows are SRP conc. of 0.5-1m reservoir samples, lower 3 rows are SRP conc. of reservoir inflow. Y-axis: biovolume and % biovolume of MSAE and N-fixing species (left 4 columns) and chlorophyll (right column).

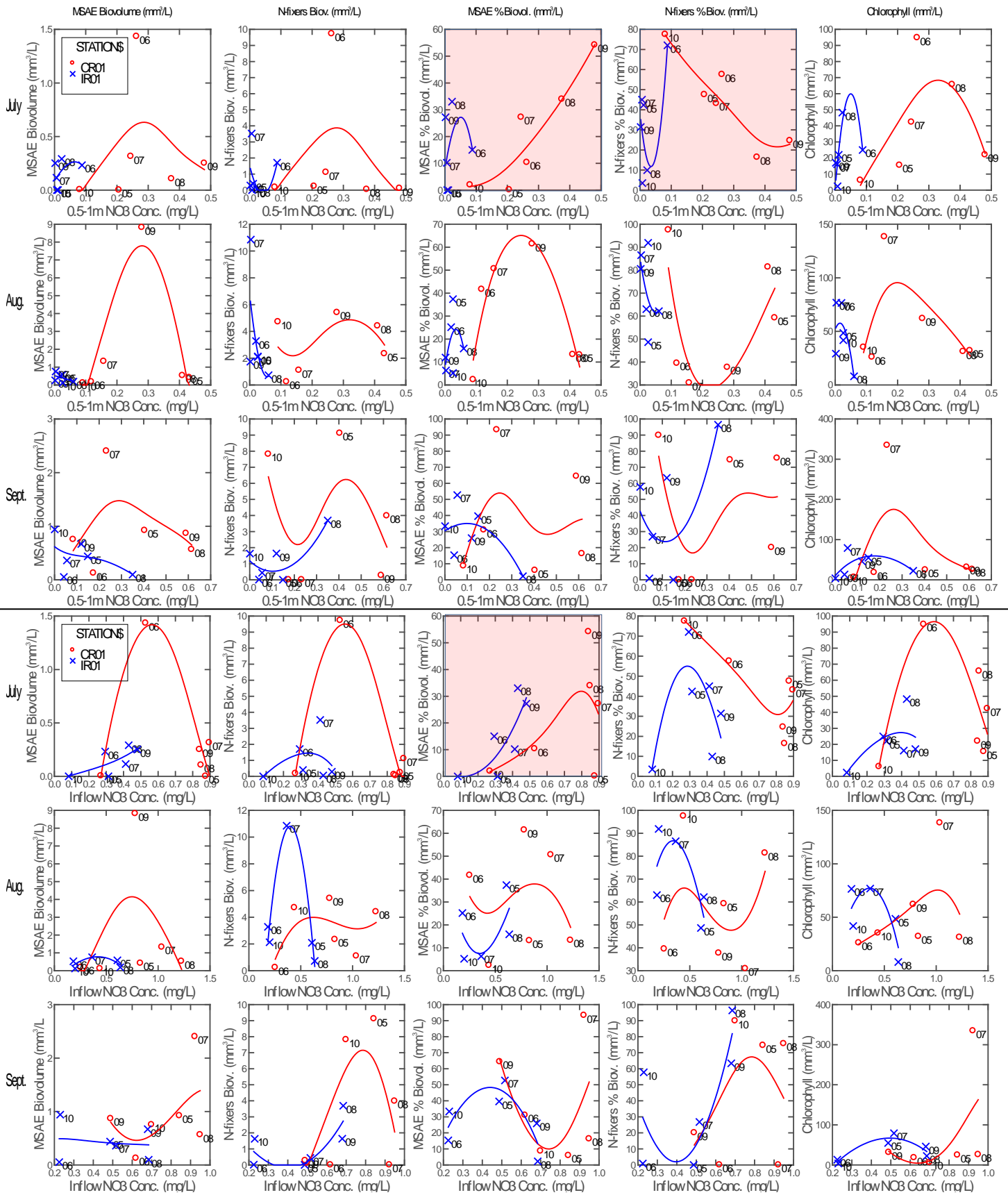


Figure 38. Relationships between NO₃ concentration and algal response variables for Copco (red) and Iron Gate Reservoirs (blue), arranged in rows (months July-Sept) and columns (response variables). Each point is monthly mean, labeled by year (05=2005). X-axis: upper 3 rows are NO₃ conc. of 0.5-1m reservoir samples, lower 3 rows are NO₃ conc. of reservoir inflow. Y-axis: biovolume and % biovolume of MSAE and N-fixing species (left 4 columns) and chlorophyll (right column).

3.4.5 Nitrogen Fixing Species and Heterocyst Ratios

As noted above, several nitrogen-fixing blue-green algal species, including *Aphanizomenon flos-aquae* (APFA), *Anabaena* sp., and *Gloeotrichia echinulata* are present in the Klamath River reservoir system. Such species can play an important role in introducing nitrogen into aquatic systems, as well as achieve dominance under nitrogen limiting conditions. Because heterocysts (specialized cyanobacterial cells that function as the site of nitrogen fixation) can indicate active N-fixation, their relative abundance has been used to evaluate potential fixation trends. Heterocysts were not enumerated in the PacifiCorp samples, and thus we limit our analysis here to just the Karuk Tribe's 2005-2008 samples¹³.

The ratio of number of heterocysts to number of vegetative cells shows that very few (two samples in four years) heterocysts were detected at KRAC relative to the other stations and that there was a longitudinal trend of increasing heterocyst ratio from KRAC to KRAI to KRBI for both APFA and *Anabaena flos-aquae* (ABFA) (Figure 39). June-September summaries indicate that APFA heterocyst ratios were higher at IR01 than CR01 (Figure 39), consistent with lower nitrogen concentrations at IR01 (Figure 13, Figure 15). Conversely, ABFA heterocyst ratios were higher at CR01 than IR01. For both species, the heterocyst ratios were lower at reservoir outlets (KRAI and KRBI) relative to the in-reservoir stations immediately upstream (CR01 and IR01). As shown above, the biovolume of these species was low at depths where water is withdrawn from Iron Gate. Heterocyst ratios of both species showed similar inter-annual patterns for June-September with ratios being highest in 2007, lowest in 2005, and intermediate in 2006 and 2008 (Figure 40), a pattern that does not correspond to differences with nitrogen concentrations or N:P ratios between years.

Seasonally, APFA heterocyst ratios increased in June (coinciding with the general period of lower inflow nitrate concentrations; see Figure 34 and Figure 35, above), peaked in July and August, and declined in September and October (Figure 41). This pattern reveals that although the timing of increased nitrogen fixation (as well as the timing of the initial period of dominance by APFA) tends to occur prior to the increase in inflow nitrate concentration, that after that point a decoupling between heterocyst ratio and either inflow or in-reservoir nitrate concentration occurs. Peak heterocyst ratios at IR01 and CR01 were similar to those previously observed in Upper Klamath Lake (Kann 1998).

¹³ Heterocyst were counted in all the Karuk Tribe's samples, so heterocyst data is available for all stations in 2005-2007, but in 2008 the Karuk Tribe only sampled KRAC, KRBI, and a limited number of surface samples at CR01 and IR01 (PacifiCorp conducted most of the sampling in 2008-2010).

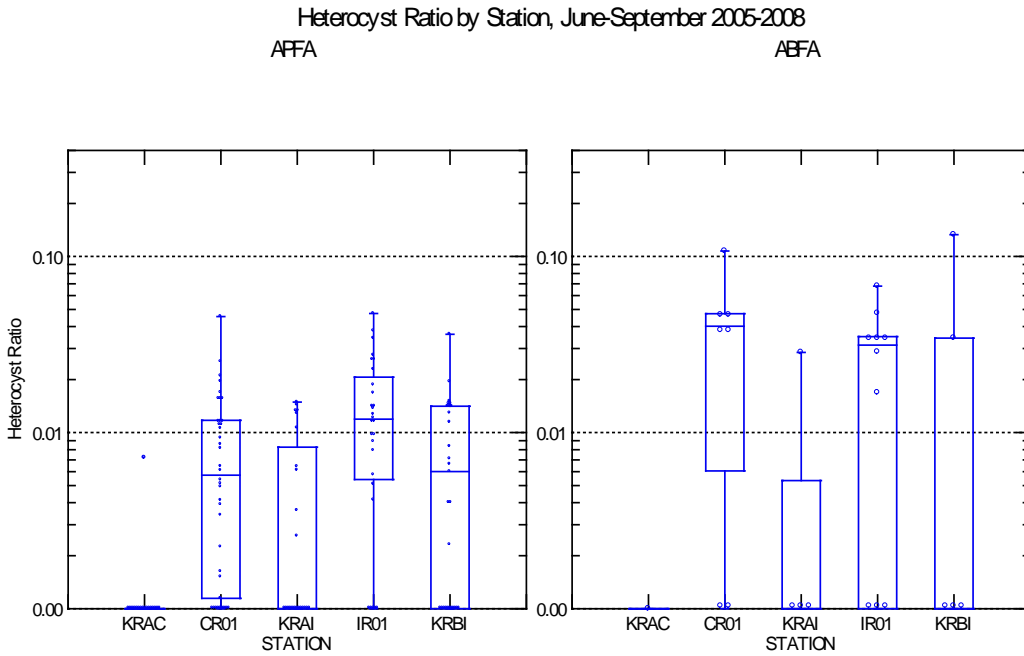


Figure 39. Summary by station of the ratio of number of heterocysts to vegetative cells for *Aphanizomenon flos-aquae* (APFA) and *Anabaena flos-aquae* (ABFA) at Klamath River and reservoir stations KRAC, CR01, KRAI, IR01, and KRBI, 2005-2008.

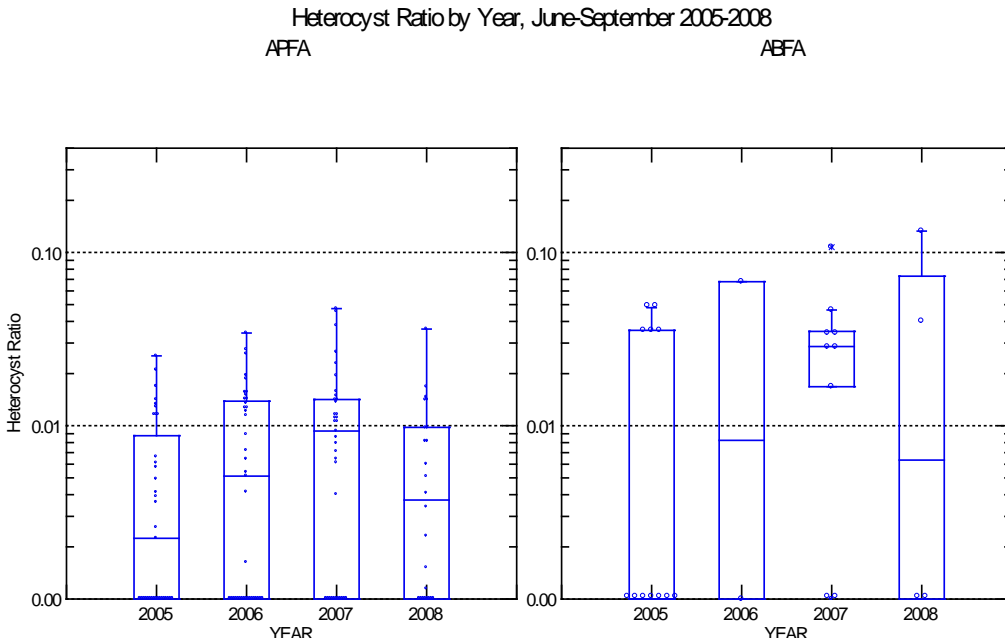


Figure 40. Summary by year of the ratio of number of heterocysts to vegetative cells for *Aphanizomenon flos-aquae* (APFA) and *Anabaena flos-aquae* (ABFA) at Klamath River and reservoir stations KRAC, CR01, KRAI, IR01, and KRBI, 2005-2008.

Ratio of Heterocyst Cells to Vegetative Cells 2005-2008

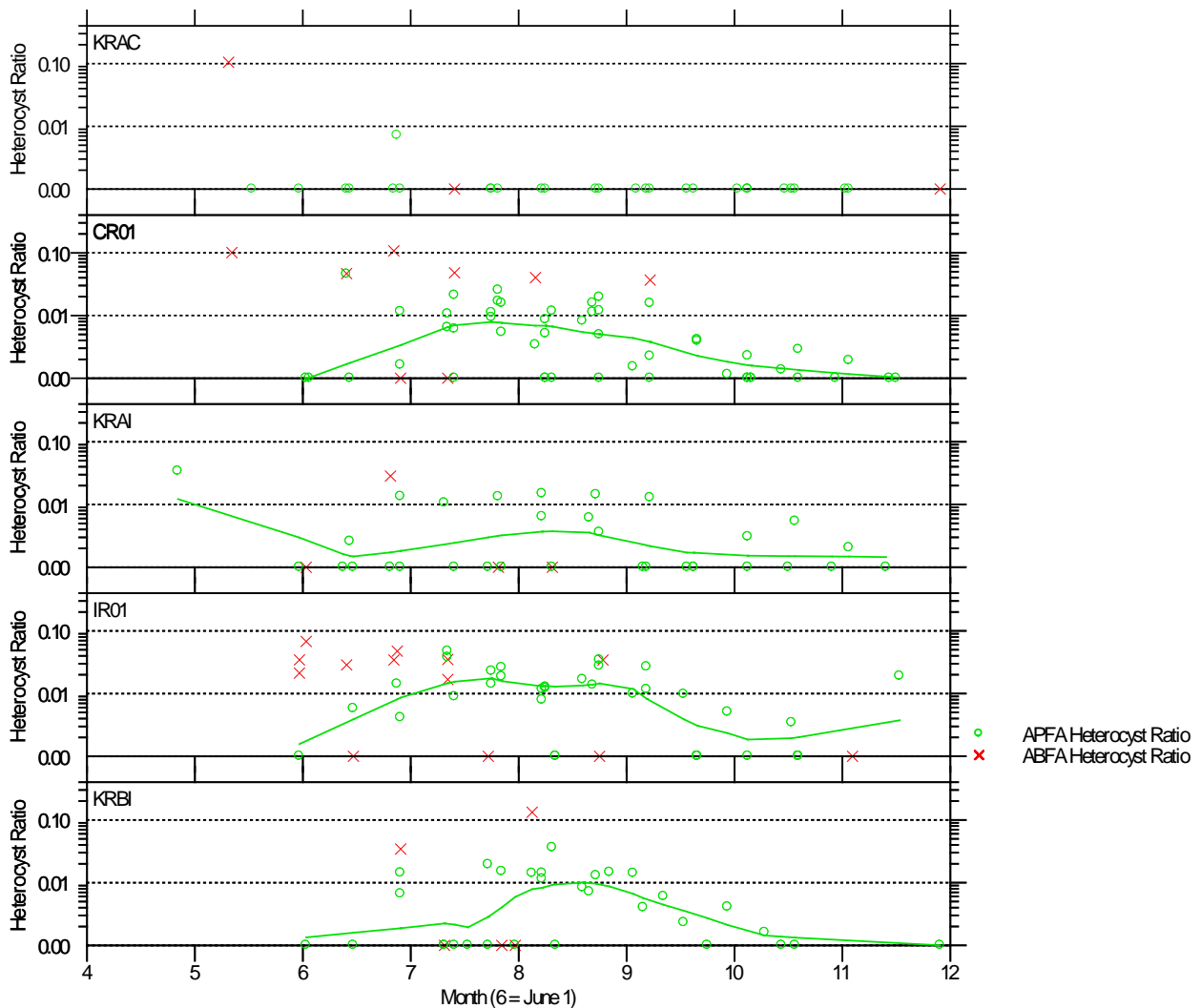


Figure 41. Time series of the ratio of number of heterocysts to vegetative cells for *Aphanizomenon flos-aquae* (APFA) and *Anabaena flos-aquae* (ABFA) at Klamath River and reservoir stations KRAC, CR01, KRAI, IR01, and KRBI, 2005-2008.

Further longitudinal examination of trends in cyanobacteria and nitrogen fixing species shows that for 2005-2010, biovolume and percent composition of N-fixing species increased in Copco stations and at KRAI (relative to KRAC), increased again in Iron Gate (although not as much as in Copco), and then were higher at KRBI below Iron Gate (Figure 42).

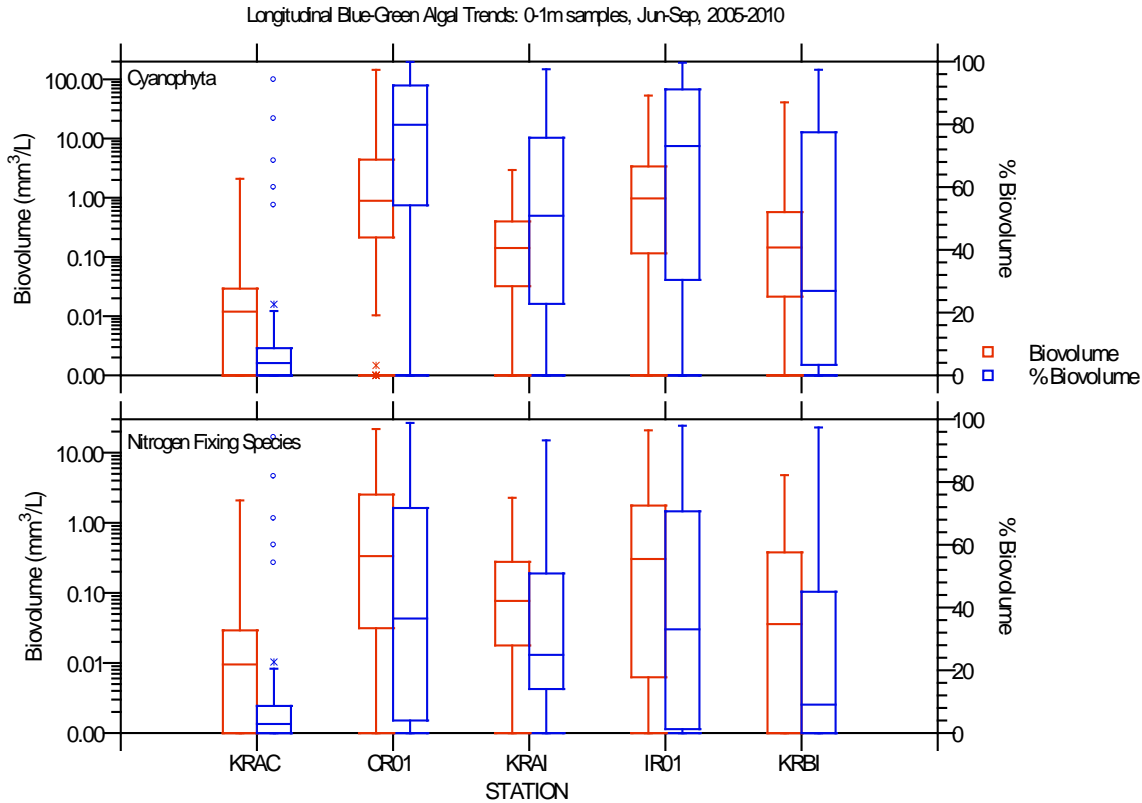


Figure 42. Biovolume and percent composition of the Cyanophyta (top panel) and nitrogen-fixing species (bottom panel) for 0-1m samples, June-September 2005-2010.

3.4.6 Chlorophyll to Algal Biovolume Relationship

As expected, there was a statistically significant relationship between chlorophyll-a and total algal biovolume ($p < 0.001$, $r^2 = 0.515$). Factors that could cause scatter in the relationship include: 1) the chlorophyll content of different phytoplankton species and varying seasonal relationships, 2) phytoplankton laboratory issues such as sub-sample volume, counting resolution for algal unit density (i.e., total number of units counted), sub-sampling resolution for number of cells per algal unit (for colony-forming species only), cell sizes used to calculate biovolume¹⁴, and 3) chlorophyll laboratory issues including utilization of data from two different laboratories. To investigate part of #3, we ran the regressions separately for the Karuk and PacifiCorp data, resulting in only slight improvement in the r^2 value ($r^2 = 0.564$ for Karuk samples and $r^2 = 0.520$ PacifiCorp samples).

Given varying chlorophyll-a content for given phytoplankton species, as well as physiological changes in algal growth state over a season, such moderate r^2 values are not unexpected. For example, decoupling between the timing of chlorophyll and biovolume maxima, changes in cell pigment content with cell size, and spatial or successional trends in species dominance have been shown to affect variability in chlorophyll to biovolume relationships (Felip and Catalan 2000). In addition others have shown that at higher chlorophyll values ($> 20 \mu\text{g/L}$), such as those observed in Copco and Iron Gate reservoirs, that linear relationships with biovolume were less apparent (LaBaugh 1995).

¹⁴ The laboratory that processed the phytoplankton samples used a constant (i.e. over the entire study) long-term average cell size for each species, rather than measuring/calculating an average cell size for each sampling date.

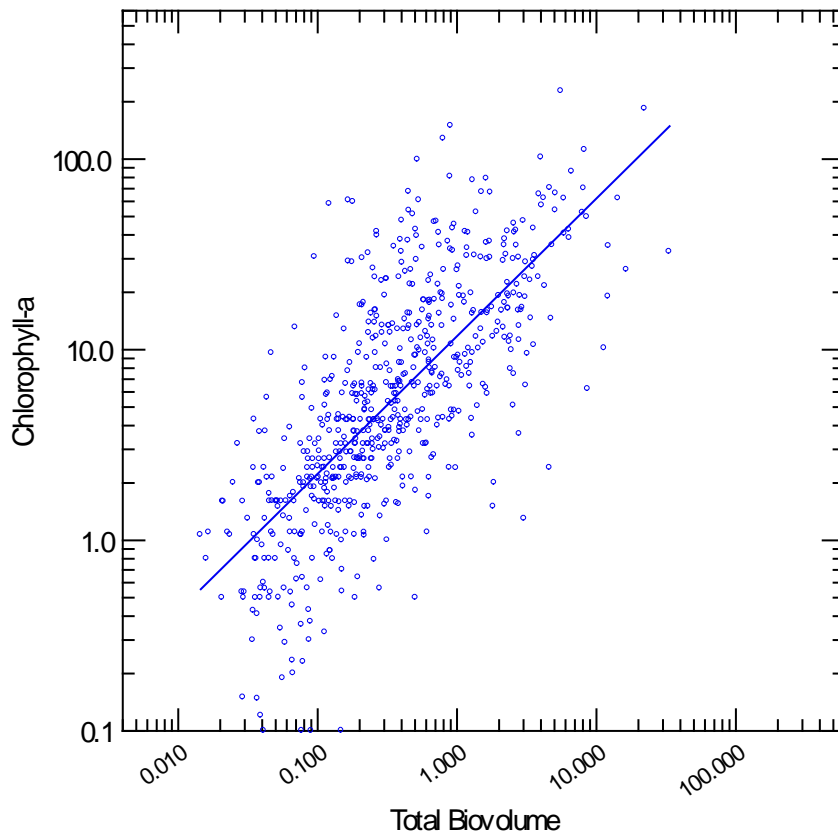


Figure 43. Chlorophyll-*a* vs. total algal biovolume for individual samples (or daily averages if there was more than one sample per day) for all dates, stations, depths, 2005-2010.

4 CONCLUSIONS

The study described herein examined longitudinal, temporal, and depth trends in phytoplankton and physical and chemical water quality in Copco and Iron Gate reservoirs from January 2005 to December 2010.

Both reservoirs thermally stratified during the warm summer months, with the deeper waters (hypolimnion) in both reservoirs exhibiting low levels of dissolved oxygen as well as high concentrations of NH₃ and SRP. The upper water column layers (epilimnion) in both reservoirs hosted large blooms of phytoplankton (as evidenced by chlorophyll *a*) and had elevated pH. Concentrations of total nitrogen (TN) were consistently lower at Klamath River below Iron Gate than Klamath River above Copco. Relative to the Klamath River above Copco, total phosphorus (TP) concentrations at the Klamath River below Iron Gate were generally equal or lower from January through August or September (varies by year). This is likely due to 1) nutrient storage in the water column and sediments of the reservoirs, 2) penstock intakes that draw water from intermediate depths where concentrations are lower, and 3) possible atmospheric losses through denitrification (for nitrogen only). Higher TP concentrations were generally observed below Iron Gate than above Copco for the August/September (varies by year) through November period, likely reflecting a combination of internal loading from sediments as well as hydraulic residence time (the reservoirs' volume results in a temporal lag in the arrival of the seasonal maximum TP concentrations at Iron Gate relative to above Copco).

The longitudinal effects of reservoirs on phytoplankton at Iron Gate Dam (i.e. relative to above Copco) is higher chlorophyll and total phytoplankton biovolume from June-October (blue green blooms), due to in-reservoir blooms of blue-green algae. Conversely, chlorophyll and algal biovolume were lower below Iron Gate than above Copco from November through April, reflecting the settling of diatoms from upstream; however, there were relatively few samples collected in November-April, so additional data should be collected to confirm this apparent trend. Both relative and absolute biovolume of blue-green algae, predominantly *Aphanizomenon flos-aquae* (APFA) and *Microcystis aeruginosa* (MSAE), were substantially higher below each of the reservoirs than they were in the Klamath River above the reservoirs.

Prolific blue-green algal blooms occurred in Iron Gate and Copco reservoirs each summer, primarily composed of ABFA and MSAE. A seasonal progression to the blooms was evident, with APFA blooms beginning sooner, followed by MSAE. One apparent contributor to the seasonal dynamics was that SRP increased earlier in the spring than nitrate, favoring early season blooms of N-fixing species (APFA). Later in the season there is a transition to non-N-fixing MSAE. With variation, MSAE was generally higher at surface (0.1m), while APFA higher at 0.5-1m, 5m depth.

Peak blooms (as measured by either chlorophyll or total algal biovolume) were generally larger in Copco than Iron Gate (with exceptions). MSAE was generally lower in Iron Gate than in Copco (for both open-water and shoreline stations), which could be due to more N availability in Copco.

Time-series graphs and scatter plots between inflowing and in-reservoir nutrient concentrations and phytoplankton parameters indicate that both NO₃ and SRP are important drivers of MSAE dominance in Copco and Iron Gate reservoirs. Both higher NO₃ and higher SRP were associated with increased July dominance of MSAE in Copco Reservoir, indicating that not only was NO₃ necessary for the non-nitrogen fixing MSAE to increase in importance but that increased SRP was

further associated with increased MSAE dominance. Relationships with inflow SRP also indicate that relative supply of SRP to the reservoirs may explain year-to-year dominance patterns of MSAE and N-fixing algae. As expected based on lag-time between increasing inflow NO_3 and the onset of MSAE apparent in the graphical analysis, the scatter plots did not show a trend between inflow NO_3 and MSAE. However, as noted above the presence of NO_3 was a prerequisite for the transition from N-fixers to MSAE. This phenomenon likely explains the increased presence of MSAE in Copco and Iron Gate reservoirs, relative to Upper Klamath Lake upstream. In Upper Klamath Lake, the nitrogen-fixing APFA dominates the May through October growing season while inflow nitrogen sources remain low throughout that entire time period (Kann 2010), with low levels of MSAE only occurring later in the season (although never dominating) when internally generated nitrogen sources become available.

For APFA, the ratio of heterocysts to vegetative cells was higher in Iron Gate than in Copco, consistent with lower nitrate concentrations at depths <10m; however, heterocyst ratios did not correspond to differences in nitrogen concentrations or N:P ratios between years.

An obstacle to a more complete analysis of the dataset is that it is difficult to assess algal response to seasonal changes in nutrients and meteorological conditions with monthly data (which is what is available for 2009-2010). In addition, consistent comparisons over the entire time period 2005-2010 were difficult due to inconsistent sampling of depths between the various years. Despite the limitations of the available data, multivariate statistical analyses could potentially provide further insight regarding factors affecting bloom dynamics.

5 LITERATURE CITED

- Arcata Fish and Wildlife Office (ARFO). 2005. Protocol for Collection of Nutrient Grab Samples. Arcata Fish and Wildlife Office, Arcata, CA. Available online at: <http://www.cfwow.r1.fws.gov/fisheries/reports/wq/2004_grab_protocol_pzedits_nea_comments.pdf> Accessed 2005 1 April.
- Armstrong, N.E. and Ward, G.E. 2005. Review of the AFWO Klamath River Grab Sample Water Quality Database. University of Texas, Austin, TX.
- Asarian, E. J. Kann, and W. Walker, 2009. Multi-year Nutrient Budget Dynamics for Iron Gate and Copco Reservoirs, California. Prepared by Riverbend Sciences, Kier Associates, Aquatic Ecosystem Sciences, and William Walker for the Karuk Tribe Department of Natural Resources, Orleans, CA. 55pp + appendices.
- Asarian, E. J. Kann, and W. Walker. 2010. Klamath River Nutrient Loading and Retention Dynamics in Free-Flowing Reaches, 2005-2008. Final Technical Report to the Yurok Tribe Environmental Program, Klamath, CA. 59pp + appendices.
- Felip. M. and J. Catalan. 2000. The relationship between phytoplankton biovolume and chlorophyll in a deep oligotrophic lake: decoupling in their spatial and temporal maxima. *Journal of Plankton Research* 22: 91–105.

- Kann, J., L. Bowater and S. Corum. 2010. Middle Klamath River Toxic Cyanobacteria Trends, 2009. Aquatic Ecosystem Sciences LLC. and Karuk Tribe Department of Natural Resources. 25 pp. http://www.klamathwaterquality.com/documents/kann_et_al_2010_Karuk_Public_Health_Cyano_2009_Report_6-30-10.pdf> Accessed 2011 24 September.
- Kann, J. and S. Corum. 2006. Summary of 2005 Toxic Microcystis aeruginosa Trends in Copco and Iron Gate Reservoirs on the Klamath River, CA. Prepared For: Karuk Tribe Department of Natural Resources, P.O. Box 282 Orleans, CA, 95556, by Kann, J; Corum, Susan; March, 2006. [http://www.klamathwaterquality.com/documents/kann_Corum_2006_karuk_MSAE_200603_28-5041\(14979421\).pdf](http://www.klamathwaterquality.com/documents/kann_Corum_2006_karuk_MSAE_200603_28-5041(14979421).pdf)
- Kann, J. and S. Corum. 2007. Summary of 2006 Toxic Microcystis aeruginosa Trends in Copco and Iron Gate Reservoirs on the Klamath River, CA. Prepared For: Karuk Tribe Department of Natural Resources, P.O. Box 282 Orleans, CA, 95556, by Kann, J; Corum, Susan; June, 2007. 23 pp. [http://www.klamathwaterquality.com/documents/kann_corum_2007_20070816-5016\(17802347\).pdf](http://www.klamathwaterquality.com/documents/kann_corum_2007_20070816-5016(17802347).pdf)
- Kann, J. and S. Corum. 2009. Toxigenic Microcystis aeruginosa bloom dynamics and cell density/chlorophyll a relationships with microcystin toxin in the Klamath River, 2005-2008. Aquatic Ecosystem Sciences LLC. and Karuk Tribe Department of Natural Resources, Orleans, CA. 46 pp. http://www.klamathwaterquality.com/documents/2009/2008_Karuk_Toxic_Cyanobacteria_summary.pdf
- Karuk Tribe. 2007. Water Quality Assessment Report 2007. Karuk Tribe Department of Natural Resources, Orleans, CA. 64 p. <http://karuk.us/dnr/pdf/wqdocuments/2007WQReport_Final.pdf> Accessed 2009 21 December.
- Karuk Tribe. 2008. Water Quality Assessment Report 2008. Karuk Tribe Department of Natural Resources, Orleans, CA. 75 p. <http://www.klamathwaterquality.com/documents/2009/2008_WQReport_Karuk.pdf> Accessed 2009 21 December.
- LaBaugh, J.W. 1995. Relation of algal biovolume to chlorophyll a in selected lakes and wetlands in the north-central United States. Can. J. of Fish. and Aquat Sci. 2:416-424.
- Moisander, P.H., Ochiai, M., and A. Lincoff. 2009. Nutrient limitation of Microcystis aeruginosa in northern California Klamath River reservoirs. Harmful Algae 8(6), 889-897.
- North Coast Regional Water Quality Control Board (NCRWQCB). 2010. Final Staff Report for the Klamath River Total Maximum Daily Loads (TMDL) Addressing Temperature, Dissolved Oxygen, Nutrient, and Microcystin Impairments in California; the Proposed Site Specific Dissolved Oxygen Objectives for the Klamath River in California; and the Klamath River and Lost River Implementation Plans. North Coast Regional Water Quality Control Board, Santa Rosa, CA.

- Raymond, R. 2008a. Results of 2007 Phytoplankton Sampling in the Klamath River and Klamath Hydroelectric Project (FERC 2082). Prepared for PacifiCorp Energy by E&S Environmental Chemistry, Inc., Corvallis, Oregon. 48pp.
http://www.pacificorp.com/content/dam/pacificorp/doc/Energy_Sources/Hydro/Hydro_Licensing/Klamath_River/Results_of_2007_Phytoplankton_Sampling_in_the_Klamath_River_and_Klamath_Hydroelectric_Project.pdf
- Raymond, R. 2008b. Water Quality Conditions During 2007 in the Vicinity of the Klamath Hydroelectric Project. Prepared for PacifiCorp Energy by E&S Environmental Chemistry, Inc., Corvallis, Oregon. 34pp + appendices.
http://www.pacificorp.com/content/dam/pacificorp/doc/Energy_Sources/Hydro/Hydro_Licensing/Klamath_River/Water_Quality_Conditions_During_2007_in_the_Vicinity_of_the_Klamath_Hydroelectric_Project.pdf
- Raymond, R. 2009a. Phytoplankton Species and Abundance Observed During 2008 in the Vicinity of the Klamath Hydroelectric Project . Prepared for PacifiCorp Energy by E&S Environmental Chemistry, Inc., Corvallis, Oregon. 67pp.
http://www.pacificorp.com/content/dam/pacificorp/doc/Energy_Sources/Hydro/Hydro_Licensing/Klamath_River/2008PhytoRpt.pdf
- Raymond, R. 2009b. Water Quality Conditions During 2008 in the Vicinity of the Klamath Hydroelectric Project. Prepared for PacifiCorp Energy by E&S Environmental Chemistry, Inc., Corvallis, Oregon. 66pp.
http://www.pacificorp.com/content/dam/pacificorp/doc/Energy_Sources/Hydro/Hydro_Licensing/Klamath_River/Water_Quality_Conditions_During_2008_in_the_Vicinity_of_the_Klamath_Hydroelectric_Project.pdf
- Raymond, R. 2010a. Phytoplankton Species and Abundance Observed During 2009 in the Vicinity of the Klamath Hydroelectric Project . Prepared for PacifiCorp Energy by E&S Environmental Chemistry, Inc., Corvallis, Oregon. 50pp.
http://www.pacificorp.com/content/dam/pacificorp/doc/Energy_Sources/Hydro/Hydro_Licensing/Klamath_River/2009PPLKReportFinal.pdf
- Raymond, R. 2010b. Water Quality Conditions During 2009 in the Vicinity of the Klamath Hydroelectric Project. Prepared for PacifiCorp Energy by E&S Environmental Chemistry, Inc., Corvallis, Oregon. 74pp.
- Watercourse Engineering, Inc., 2011. Klamath River Baseline Water Quality Sampling, 2009 Annual Report. Prepared for the KHSa Water Quality Monitoring Group. Watercourse Engineering, Inc., Davis, CA. 42pp.